AD-A144 773 REAL TIME SENSING AND CONTROL OF OUT-OF-PLANE DISTORTION DUE TO LINE HEAT..(U) MASSACHUSETTS INST OF TECH CAMBRIDGE DEPT OF OCEAN ENGINEERIN.. R C JOHNSON

1/2

UNCLASSIFIED JUN 84 N66314-70-A-0073 F/G 11/6 NL

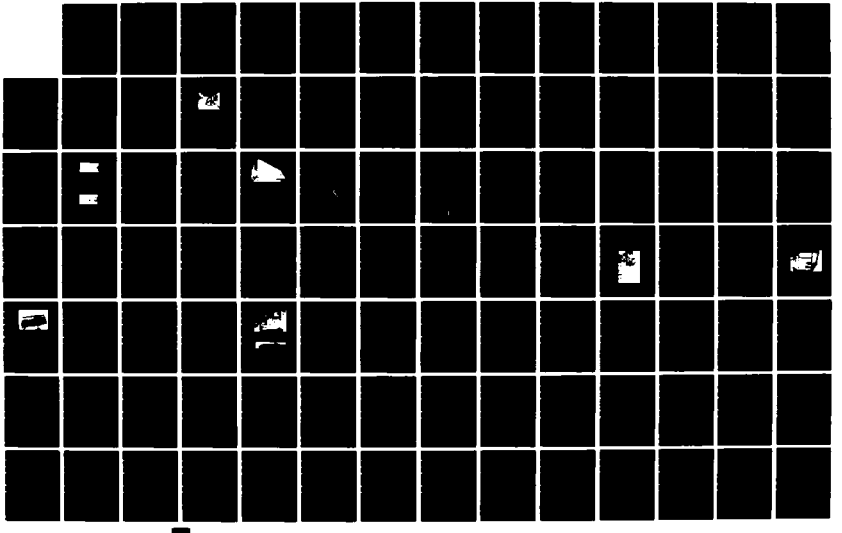

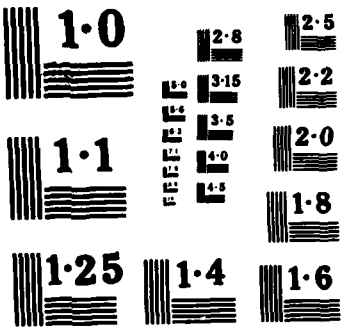
1·0
1·1
1·25
2·8
3·15
3·5
4·0
4·5
1·4
2·5
2·2
2·0
1·8
1·6

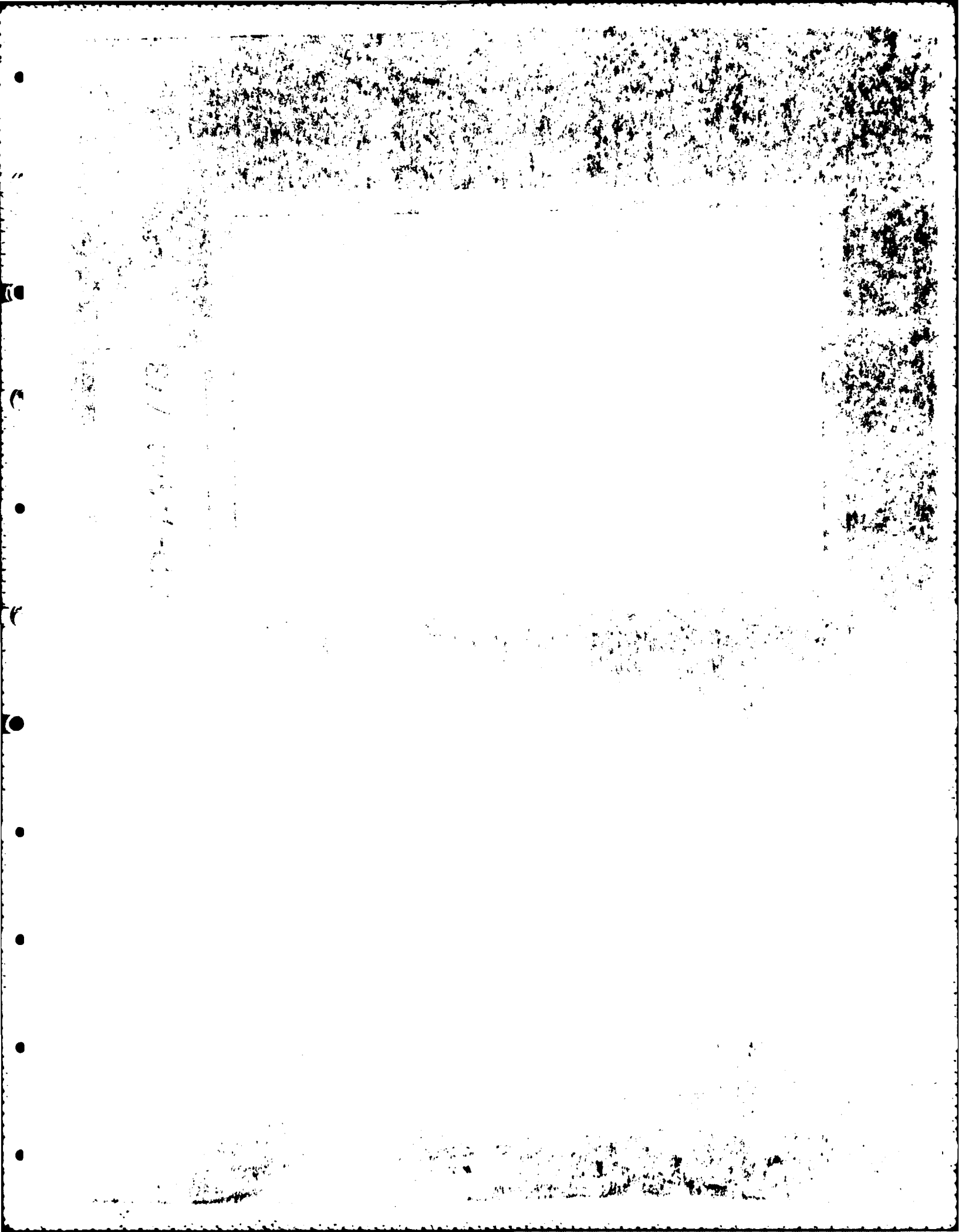

N66314-70-A-0073

REAL TIME SENSING AND CONTROL OF OUT-OF-PLANE DISTORTION DUE TO LINE HEATING BY LASER

by

ROBERT CHARLES JOHNSON

B.S. Elec. Eng., N.C. State University
(1976)

SUBMITTED TO THE DEPARTMENT OF
OCEAN ENGINEERING
IN PARTIAL FULFILLMENT OF THE REQUIREMENTS
FOR THE DEGREES OF

MASTER OF SCIENCE IN NAVAL ARCHITECTURE AND MARINE ENGINEERING

and

MASTER OF SCIENCE IN MECHANICAL ENGINEERING

at the

MASSACHUSETTS INSTITUTE OF TECHNOLOGY
May, 1984

Signature of Author Robert Charles Johnson
Department of Ocean Engineering
May 11, 1984

Certified by Koichi Masubuchi
Professor Koichi Masubuchi
Thesis Supervisor

Accepted by A. Douglas Carmichael
Professor A. Douglas Carmichael, Chairman
Departmental Graduate Committee

REAL TIME SENSING AND CONTROL OF OUT-OF-PLANE DISTORTION DUE TO LINE HEATING BY LASER

by

ROBERT CHARLES JOHNSON

Submitted to the Department of Ocean Engineering on May 11, 1984 in partial fulfillment of the requirements for the Degrees of Master of Science in Naval Architecture and Marine Engineering and Master of Science in Mechanical Engineering.

ABSTRACT

Experiments were conducted using a U.T.C. 15 kw CO_2 laser. The laser was used as a heat source to perform line heating on HY-80 and AISI 1018 specimens. The resulting angular distortion, as a function of heat input, speed, and number of passes, was measured. This out-of-plane distortion is measured using an interferometer which uses a 5 mW Helium-Neon laser as a light source. As the interference fringes appear on the specimen surface, they are recorded by a video camera and stored on a video cassette recorder to provide real time distortion information. HY-80 averaged 0.8° per pass while AISI 1018 averaged 1.1° per pass.

Strain and temperature data were taken to be used as baseline data. The results are presented in the form of temperature and strain plotted against time. A heat transfer/temperature analysis was performed using ADINAT; results of experimental and analytical temperatures are plotted for comparison.

ACKNOWLEDGMENTS

I wish to thank the United States Navy for sponsoring my studies at M.I.T.

I also thank Professor Koichi Masubuchi for his assistance and many helpful suggestions throughout the course of this investigation. The assistance of Walter Cook in using the interferometer and making distortion measurements is also appreciated. The help given by Paul Denny at the Naval Research Lab and Greg Haidemenopoulos for his help with the heat transfer/temperature analysis is appreciated.

Finally, I thank my wife, Jenny, for her untiring support during my time at M.I.T., and for her efficient typing of this thesis.

Dedicated to my family

Jenny, Robert, and David

TABLE OF CONTENTS

LIST OF FIGURES

List of Figures (Continued)

List of Figures (Continued)

List of Figures (Continued)

LIST OF TABLES

CHAPTER ONE

FORWARD

A. Introduction

Flame heating techniques, which normally involve heating by an oxyacetylene torch followed by air cooling or water spraying, are widely used in shipbuilding for forming and straightening metal structures. The basic mechanism involved in these techniques is to produce plastic strain (permanent deformation) by applying heat to a particular part. The heat produces thermal stresses which are controlled by the heating-and-cooling cycle to produce strains in adequate amounts and of an appropriate distribution.

Looking at an ideal case, it is possible to bend a flat plate into a cylindrical form. This could be accomplished by using a large, powerful heating pad capable of heating the entire top surface of the plate uniformly while keeping the bottom surface cool. However, a tricky heating system is needed; it must be able to produce shrinkage in one direction but no dimensional change in the transverse direction.

An important fact here is that the amount of temperature difference between the top and the bottom surfaces of the steel plate does not need to be too large to cause bending. Figure 1.1 shows how a heating and cooling

cycle causes residual stresses in a rigid frame system composed of three bars [1]. Shown here are changes of stress in the middle bar. In the case of a frame system made of low-carbon steel, the stress in the middle bar reaches the yield stress when the bar is heated to approximately 300° F. When the middle bar is heated to above 600° F, the residual stresses that remain are as high as the yield stress. This example suggests that a temperature difference of only several hundred degress between the top and bottom surfaces is needed to bend the plate.

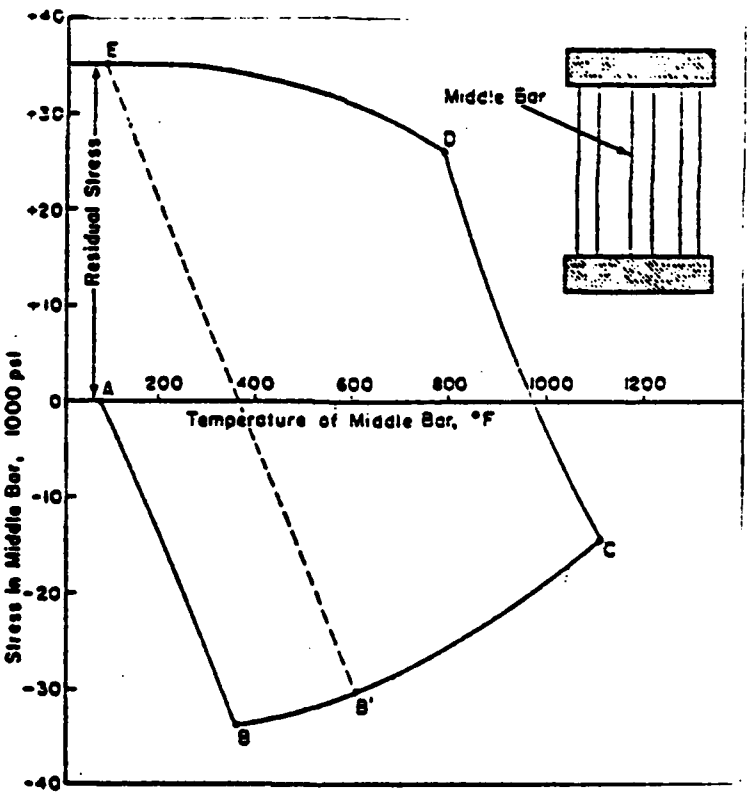

FIGURE 1.1: Stress-temperature for middle bar of a three-bar frame

The above cases are ideal. In reality, problems are encountered in the construction of a large, powerful heating pad due to its high cost. Also, in current shipyard construction, an oxyacetylene torch, far smaller and less powerful than the ideal heating pad, is used to heat the plate. The heat supplied by the torch dissipates into the plate which acts like a large heat sink. Therefore, regions of the plate directly below the torch tend to be heated to excessive temperatures before some portions below the surface are heated to temperatures necessary to form the plate.

Although the flame heating techniques are widely used in shipyards today [2], the techniques have some problems. First, the current techniques are more of an art than a science. They are done primarily by skilled workers with many years of experience. Unfortunately these skilled workers are retiring rather rapidly, and few young workers have enough patience to spend many years to master the skill required.

It should be noted that even skilled workers make many mistakes during the flame heating operations. This is to be expected since the work is done through human skills without the help of modern sensing and measuring devices and microprocessors. For instance, the senior welder usually determines where a plate should be heated to achieve a particular bend. If the first application of heat fails, a second guess is made and heat again applied and so on until

the proper bend is achieved. The very fact that only a few skilled workers can do satisfactory jobs of flame forming and heating means that average workers make many wrong judgments as to the correct temperature and location where heat should be applied.

Another significant problem sometimes encountered from the flame heating technique is material degradation resulting from the heating and subsequent cooling process. The extent of this problem depends on the thermal history and characteristics of the material being heated. The material degradation is especially severe in quenched and tempered steels such as HY-80 and HY-100, which obtain their excellent fracture toughness and high strength through quenching *followed by tempering* at approximately 1100° F. Therefore, flame heating techniques are approved for low-carbon steel, but their uses are not permitted for quenched and tempered steels.

In shipbuilding, it is essential to have effective means for forming plates into various shapes, some of which are very complex. Rolling and mechanical pressing can be used, but mechanical pressing requires a large press. At the present time, these are the only means used to form HY steels.

In the shipbuilding industry today there is no automatic means of determining if a plate has been formed with the proper curvature. For that reason the accuracy is checked manually using templates. An example is shown in

Figure 1.2 [3]. Accuracy could be increased and time saved if an automatic means of measuring this curvature or distortion were available.

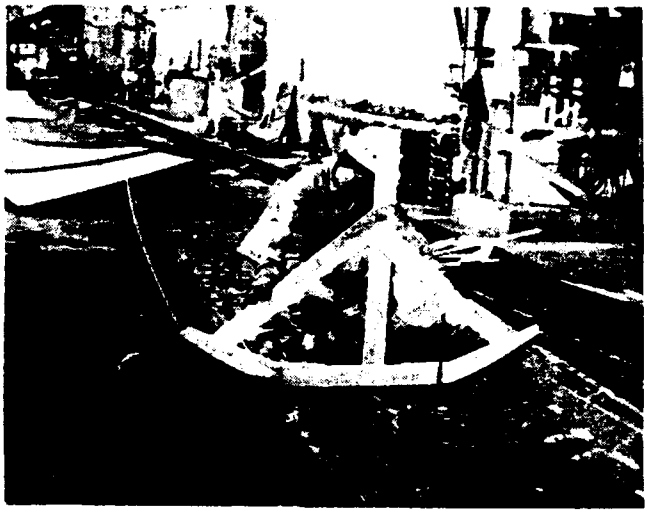

FIGURE 1.2: Checking Curvature with Template

B. Purpose of Study

The purpose of this study was:

(1) to determine the feasibility of laser line heating to form steel plates

(2) to determine the feasibility of using an interferometer to measure real time distortion

(3) to gather temperature and strain data that can be used as a basis to compare or develop a better computer simulation model.

CHAPTER TWO

BACKGROUND

A. Line Heating

A study for plate bending by line heating is documented in the Ishikawajima Engineering Reports in January of 1956. Fundamentals for practical application were published in 1961 based on the use of an oxyacetylene torch [4]. Basic information about the development and use of line heating will be presented to acquaint the reader with its origin and concept.

Line heating, the process of forming shapes by controlled heating and cooling, was developed by the Japanese in order to increase accuracy and reduce the cost associated with shipbuilding. The most significant shipbuilding problem, commonly encountered, is difficulty in joining blocks during hull erection due to inaccuracies, such as in overall block dimensions and misalignment of structural members [3]. During block assembly extra material known as margin is allowed, and certain welding is deferred to ensure that the final assembly of sections can be completed. However, the cost for deferred welding at the building site is at least three times more than the cost for the same welding during block assembly [3].

In order to minimize these problems, the accuracy and control at each stage of production must be increased. This

will reduce the required rework and thereby reduce costs. In addition, out-of-tolerance work will not be arbitrarily passed downstream where it would eventually cause more serious disruptions.

Line heating can help achieve these desired results. It is relatively safe and features nominal facilities investment. It can be used to remove distortion, improve accuracy, and increase production. In short, line heating is a means for converting much of the rework and deferred work normally performed at the erection site into safer, easier, and less work. In addition, this transformed work is more evenly distributed over all preceeding processes for hull construction, including designing and lofting.

The principle of line heating comes from the fact that stress is induced in a steel plate when part of it is heated. When the stress is controlled it is possible to produce plastic strain which results in permanent deformation. Likewise, thermally induced stresses can be used to eliminate distortion. It is therefore possible to achieve a desired curvature by controlling the heating and cooling and thereby regulating the strain.

When a plate is heated along a line, such as with a torch or other heat source, it will bend so as to form a slight knuckle along the line upon cooling as shown in Figure 2.1 [3]. If the heated areas are cooled with water, the bending effect will be more pronounced. The resulting

curvature is the same as if the plate were worked slightly with a press except that some shrinkage occurs.

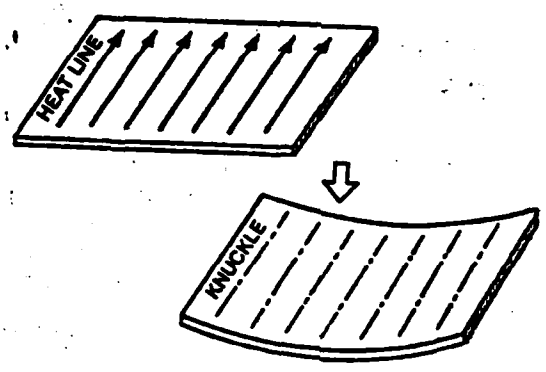

FIGURE 2.1: The curvature achieved by line heating is the same as if the plate was worked slightly with a press except that some shrinkage occurs.

Figure 2.2 [3] shows what actually happens. Local heating causes thermal stress in a small part. Young's Modulus and the Elastic Limit of this part both decrease as the temperature increases. As the heat source travels, the adjacent material remains cool enough to resist the thermally created stress. Because of the constraint, the heated surface swells beyond its Elastic Limit and some deformation remains after it cools. During the cooling process, the heated surface contracts more than the other side. This results in angular distortion or bending and a small amount of shrinkage.

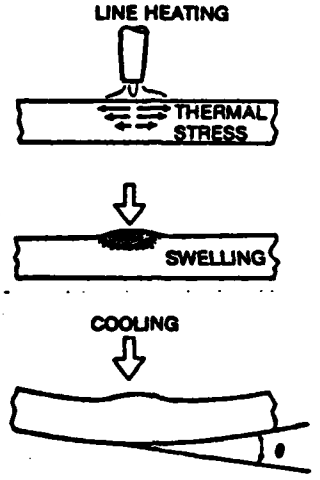

FIGURE 2.2: Local heating creates thermal stress in a very small region. Torch travel is in a direction toward the observer.

B. Laser

A laser heating system has basic features which make it more suitable than an oxyacetylene torch for line heating [5-11]. Some of these features will be presented along with some problem areas.

First, the high-power lasers available today are much more powerful than an oxyacetylene torch; 15 kw CO_2 lasers are very common. Second, the power density of a laser can be adjusted from a highly concentrated beam to one that is diffused over a relatively wide area. Third, the laser heat source can be moved at a wide range of speeds up to 100 inches per minute. This is much faster than the manual travel of an oxyacetylene torch which might be around 5 inches per minute.

The high power CO_2 laser emits energy at a wavelength of 10.6 um. This can be a problem since all metals are relatively poor absorbers of energy at this wavelength. Surface finish is one of the reasons: at the 10.6 um wavelength, most machined surfaces appear specular. Figure 2.3 shows the change in absorptivity of a given metal as a function of its surface temperature [5]. Since it is desirable to have no surface melting, it is evident from Figure 2.3 that most of the incident energy is reflected and lost.

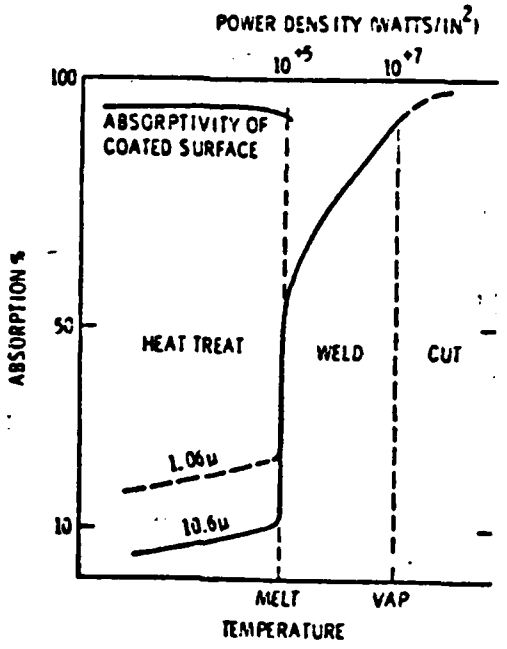

FIGURE 2.3: Simplified model of laser metal processing in terms of absorbed energy, surface temperature of the metal and incident power density.

The application of energy absorbing surface coatings can be used to increase the absorptivity of the metal so that good coupling of energy can take place. Manganese phosphate is very effective for this purpose, but painting also works and is much cheaper.

The anticipated advantages of the laser heat source as compared to the oxyacetylene torch are as follows:

(1) Since the laser heating can be limited to small areas near the surface, the laser can be very effective for forming plates, perhaps without using water quenching;

(2) Material degradations could be limited to small areas near the surface; and

(3) Since the laser technique is completely automated, consistent results can be obtained and duplicated.

C. Distortion

During heating and cooling in a flame heating or welding cycle, thermal strains occur in the metal near where the heat is applied. The strains produced during heating are accompanied by plastic upsetting. The stresses resulting from these strains combine and react to produce internal forces that cause the bending, buckling, and rotation shown in Figure 2.4 [1]. These displacements are called distortion. This paper is concerned only with Figure 2.4 (b), (e), and (f) since these are out-of-plane distortions.

Distortion is usually thought of in a negative way, as something that should either be prevented or removed. This is not necessarily true. A simple name for distortion is bending. This paper is concerned with obtaining as much controlled distortion as possible with a minimal amount of material degradation.

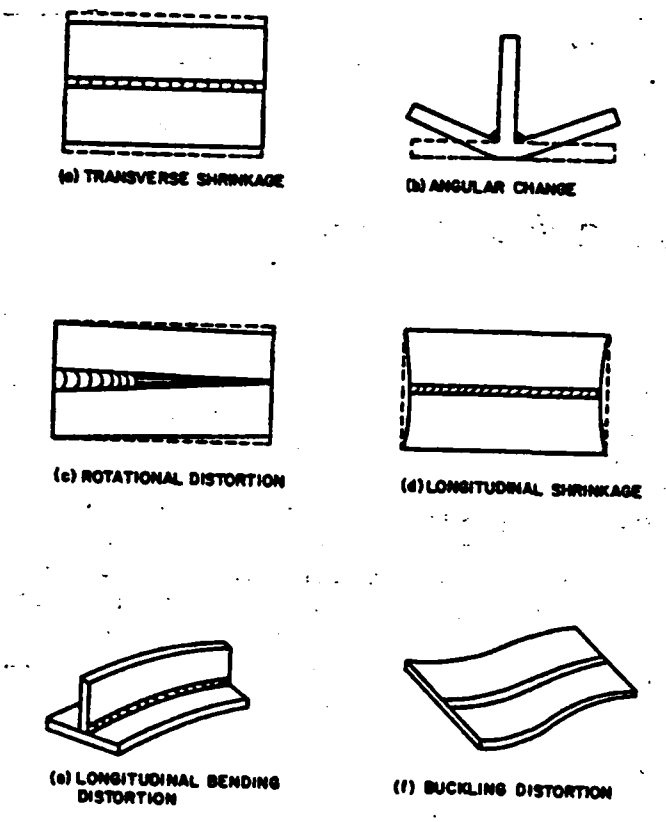

FIGURE 2.4: Various types of distortion

D. Interferometer

Interferometry provides a high-resolution, non-contact measurement of surface irregularities and bends that result from welding and heat forming of metal plates. Both before-and-after, and real-time measurements are possible. Real-time measurements can be made via a computer with video camera input.

An optical interferometer works on the principle of producing interference fringes on a surface. They appear as a pattern of alternating bright and dark lines. The shape of the pattern can give quantitative information on the contour of the surface. Figure 2.5 shows an example of a fringe pattern on a specimen before and after welding [12]. Note the fringe pattern in the after welding picture. The fringes are no longer straight, but curved; this curvature indicates that some distortion has taken place.

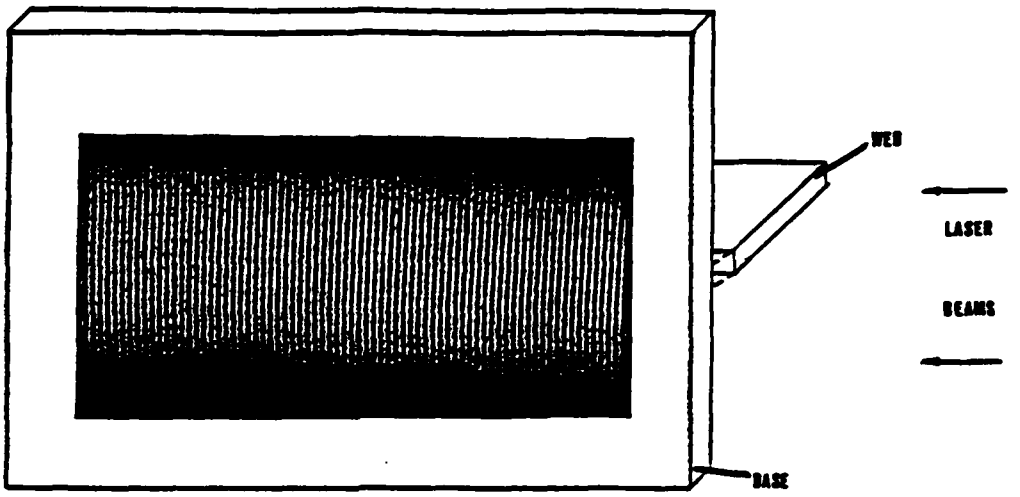

BEFORE WELDING

PLANAR INTERFERENCE FRINGES INDICATE A FLAT BASE PLATE.

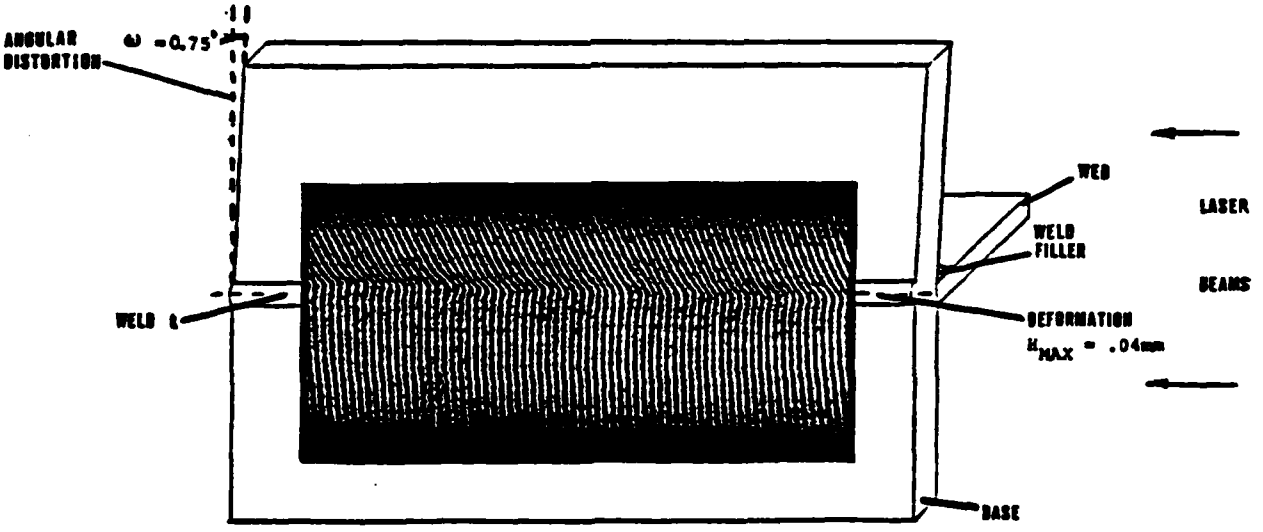

AFTER WELDING

THIS INTERFERENCE FRINGE PATTERN INDICATES A BEND OF ANGLE ω, WITH A RIDGE OF HEIGHT H, ALONG WELD CENTERLINE.

FIGURE 2.5: Interference Fringe Pattern

The interferometer is not a recent discovery. Various types of interferometers have been developed since the mid-1800's to measure small distances, velocity, and refraction index. The general type of optical interferometer consists of a single monochromatic light source, a wavefront or beam splitter, one or more mirrors, and a target surface on which the fringes are viewed. Each bright or dark fringe is produced by a pair of light rays traveling from the source to the surface. By the action of the wavefront splitter and mirrors, the rays of each pair are arranged to travel by different paths, which may be of unequal lengths. The rays recombine on the surface so as to either constructively or destructively interfere with one another, depending on their phase relationship, which in turn, depends on the path length difference. A path length difference of zero or an integral multiple of wavelengths results in constructive interference, and a bright fringe is produced. A path length difference of an odd multiple of half wavelengths results in destructive interference, and a dark fringe is produced.

Various specific optical configurations exist for interferometers depending on their application. The interferometer used in this research was developed by Walter Cook as a graduate student for Professor Koichi Masubuchi. It is a portable instrument and can be used to measure surface contour changes on a smooth surface down to 0.01 mm and bend angles down to 0.1 degree.

Certain constraints do exist, however. The ambient light level must not obscure the interference fringes, and the specimen surface must be smooth to achieve the best resolution. Also, metallic specimen surfaces must be diffused with a thin layer of spray paint in order to see the fringe spacing on the specimen surface.

A picture of the interferometer is shown in Figure 2.6 along with a schematic diagram of the interferometer optics in Figure 2.7 [12]. The monochromatic light source is a 5 mW Helium-Neon laser with output at 632.8 nM. The laser beam strikes a 14 mm focal length concave mirror that is used as a beam diverger. The beam is passed through a focus, then diverges into a cone to cover the split mirror with light. The split mirror is a 3-inch diameter, 30-inch focal length spherical telescope mirror which has been cut in half. The halves have been tilted forward by about 0.1 degree each by placing thin metal shims under the edges. A lever adjustment permits placement of the mirror halves precisely in the same plane to produce vertical fringes on the specimen.

To obtain a suitably large specimen fringe spacing, the beam overlap angle must be small; it is about 0.4 degrees in this interferometer. This requires that the specimen, which should be placed in the maximum width of the zone, must be far from the split mirror.

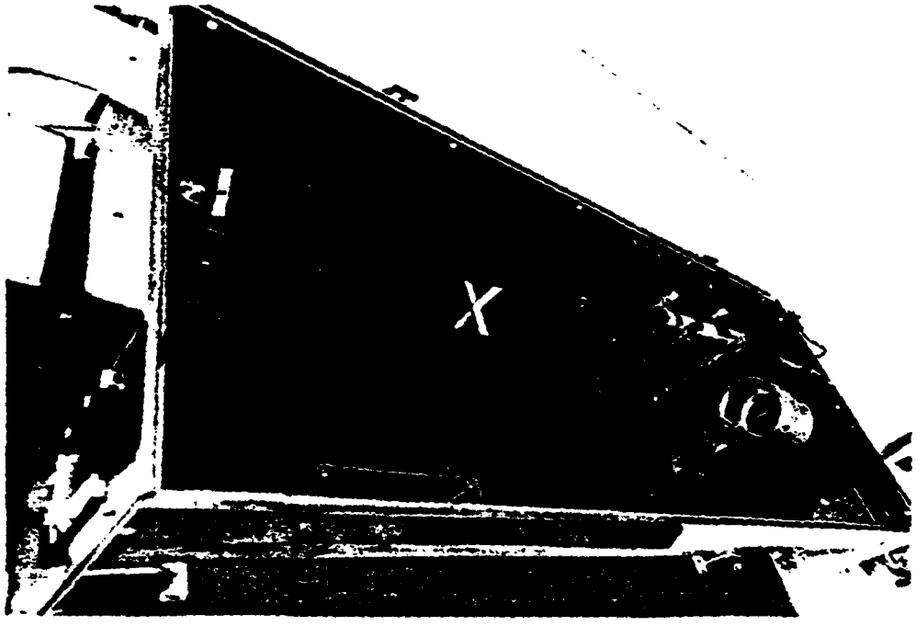

FIGURE 2.6: Interferometer

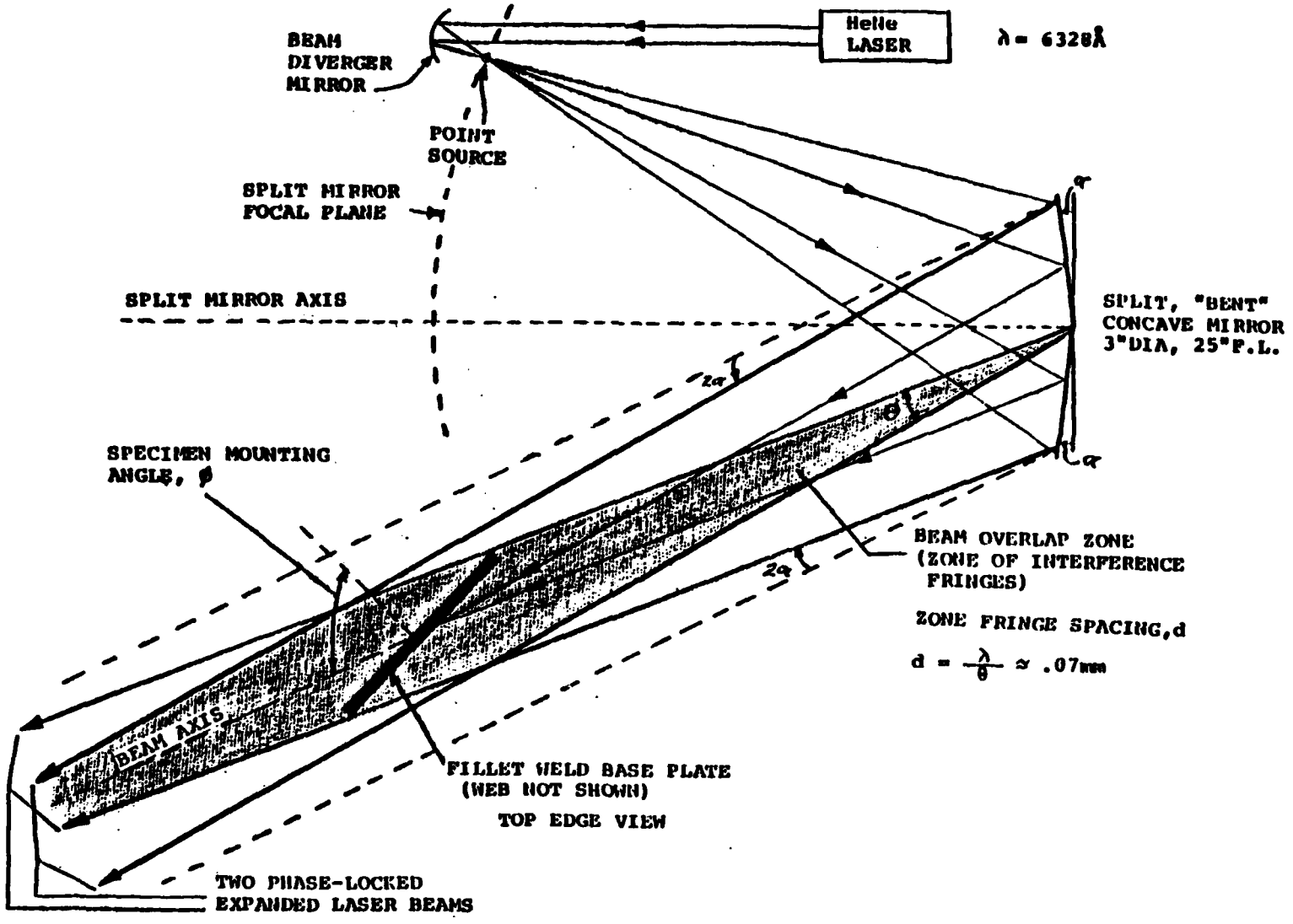

FIGURE 2.7: Interferometer Optics

In the experiments conducted, the lateral bend in the specimen was measured in the same manner as shown in Figure 2.8 [12]. To compute the angular distortion, proceed as follows. On the upper portion of the specimen above the bend, locate a specific fringe on the surface. Mark the point with a sharp pencil. Moving directly upward from the pencil mark, locate the point where the next fringe contacts the line, and mark this point. This distance between the two points is "L" and shhould be substituted in the formula given in Figure 2.8. Since "h" is essentially a constant, "L" is the only variable that must be measured to determine the amount of distortion.

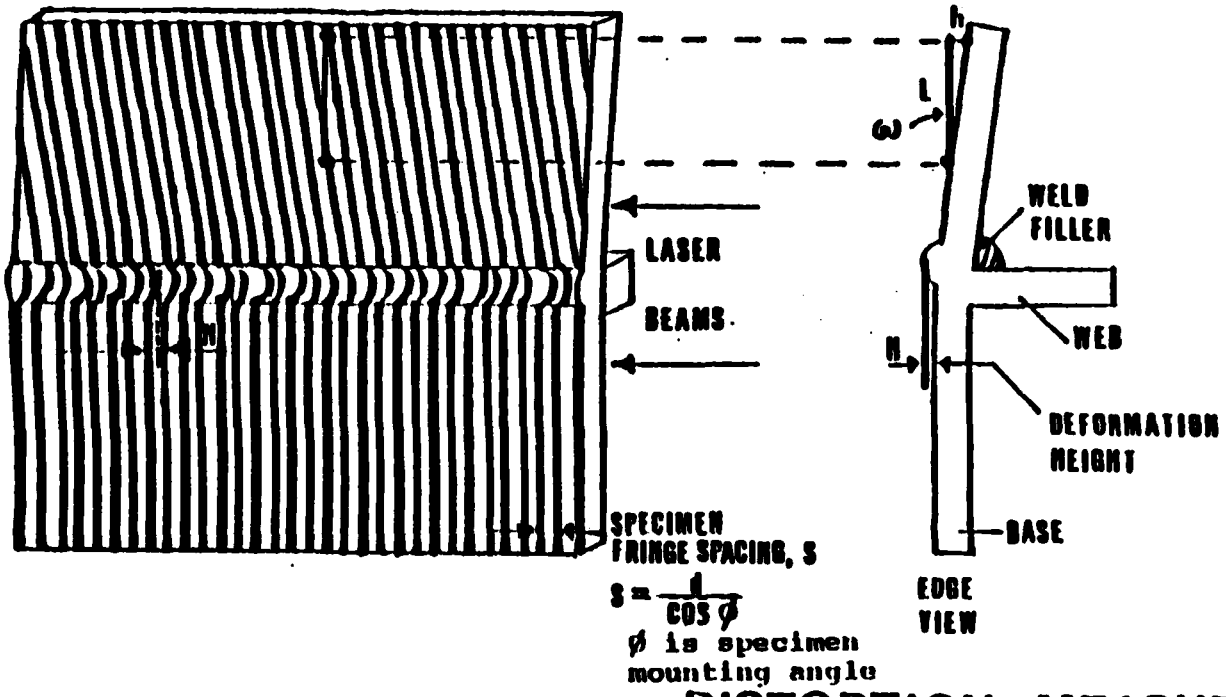

ANGULAR DISTORTION: ω

$$\omega = \tan^{-1} \frac{h}{L}$$

where h = fringe spacing, d for $\phi > 80°$

DEFORMATION HEIGHT: H

$$H = d \times N$$

where: N is no. of fringes
d is fringe spacing for $\phi > 80°$

DISTORTION MEASUREMENT

FIGURE 2.8

E. Previous Work

The laser is an exciting and powerful tool. Much research and experimentation has been conducted on how to use the laser in a variety of ways, but very little work has been done in using a laser to form steel plates. An extensive literature survey turned up only one article. Before reviewing this article, however, it will be worthwhile to examine the mechanism of plate bending by line heating using an oxyactylene torch. This is a good place to start since the basic mechanisms using the oxyacetylene torch and those using a laser beam are essentially the same. These mechanisms have been studied by Satoh and others of Osaka University, by Johnson and others of M.I.T., and jointly by Iwamura of Kawasaki Heavy Industries and Rybicki of Battelle Laboratories [13-19]. The angular change due to welding is also similar and has been studied by Watanabbe and Satoh.

The experimental set-up used by Satoh and others [13] and some of their results are briefly described below to give an idea about what experiental set-ups are needed and what results should be expected. Figure 2.9 (a) shows the experimental set-up used. Steel strips 60 mm wide were heated by an oxyacetylene torch along a line on the top surface. Figure 2.9 (b) shows the definition of the angular change of the plate, θ.

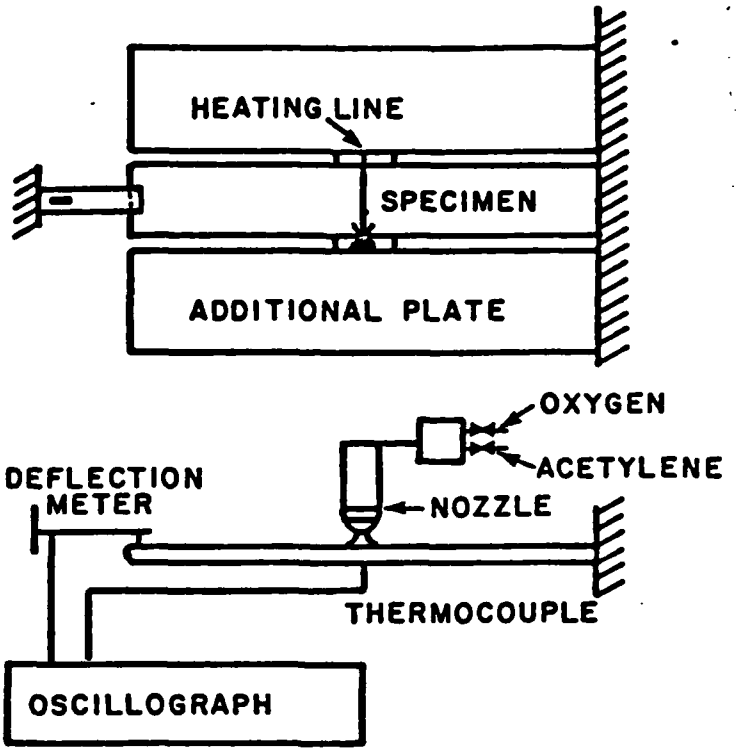

(a) Experimental set-up

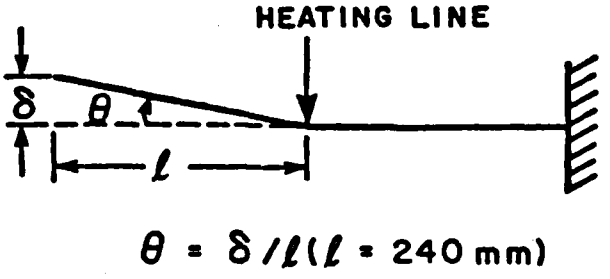

$\theta = \delta / \ell (\ell = 240\,mm)$

(b) Definition of angular change

FIGURE 2.9: Experiments on flame bending performed by Satoh and others

Figures 2.10 (a) and (b) show changes of temperatures and angular distortion on two specimens 15 mm thick, heated at a travel speed of 120 mm/min. After the flame heating, one specimen was air cooled, while the other was sprayed with water on the top surface.

While the plate is being heated, the top surface of the plate expands more than the bottom surface; therefore, the plate first deforms in the negative direction. During this period, regions of the plate near the top surface experience compressive stresses and plastic deformation occurs in some of the regions. When the plate starts to cool, it deforms in the opposite direction. Because of the compressive plastic deformation that occurred during the heating cycle, the plate keeps deforming in that direction passing through a point of no distortion. The final distortion is in the positive direction and remains after the plate returns to its initial temperature.

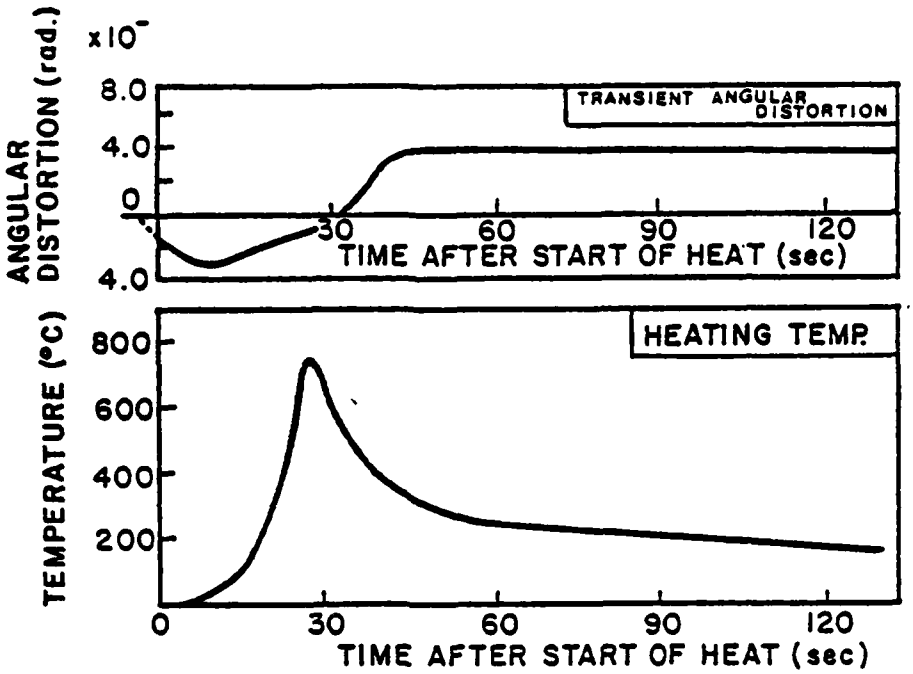

(a) Air cooled specimen

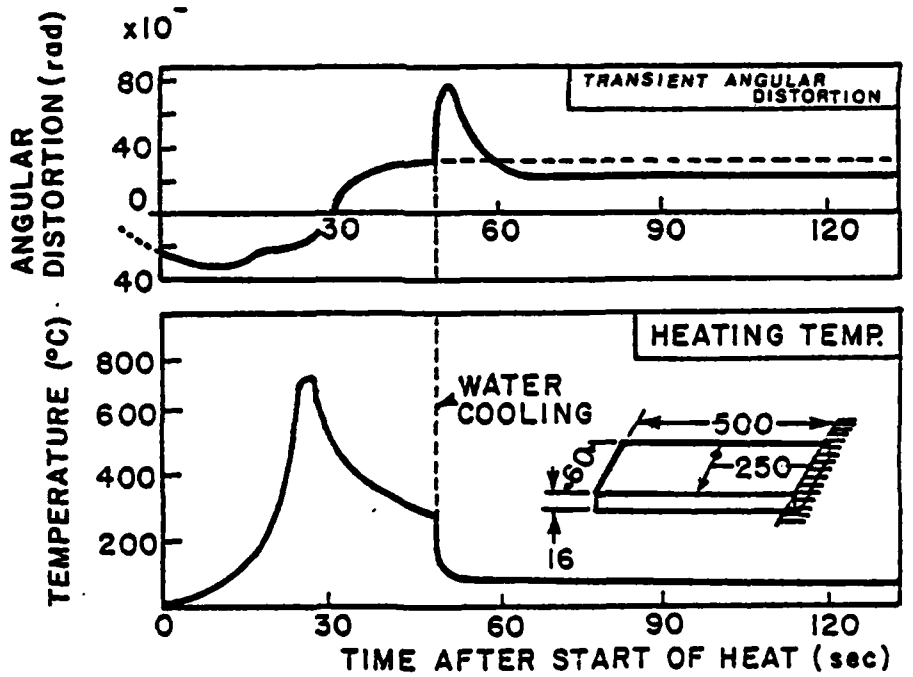

(b) Water cooled specimen

FIGURE 2.10: Changes of temperatures and distortions during and after flame heating. The figures show only temperature changes at a point 1 mm below the heated surface.

Figure 2.11 shows relationships between final distortion and the torch travel speed for plates 8, 16, and 20 mm thick. For a certain thickness there is an optimum torch speed to produce the maximum amount of distortion. When the torch speed is higher than the optimum speed, the amount of distortion decreases. This is due to insufficient heat present throughout the thickness, resulting in a decreased bending moment. When the torch speed is lower than the optimum speed, the amount of distortion is again reduced. This is due to excessive heat present throughout the thickness and results in a decreased bending moment. As the plate thickness increases, the optimum torch travel speed decreases, since deeper heat penetration is required to effectively bend a thicker plate. However, as the plate thickness increases, the maximum amount of distortion, even under the optimum condition, decreases because of the increase in rigidity of the plate.

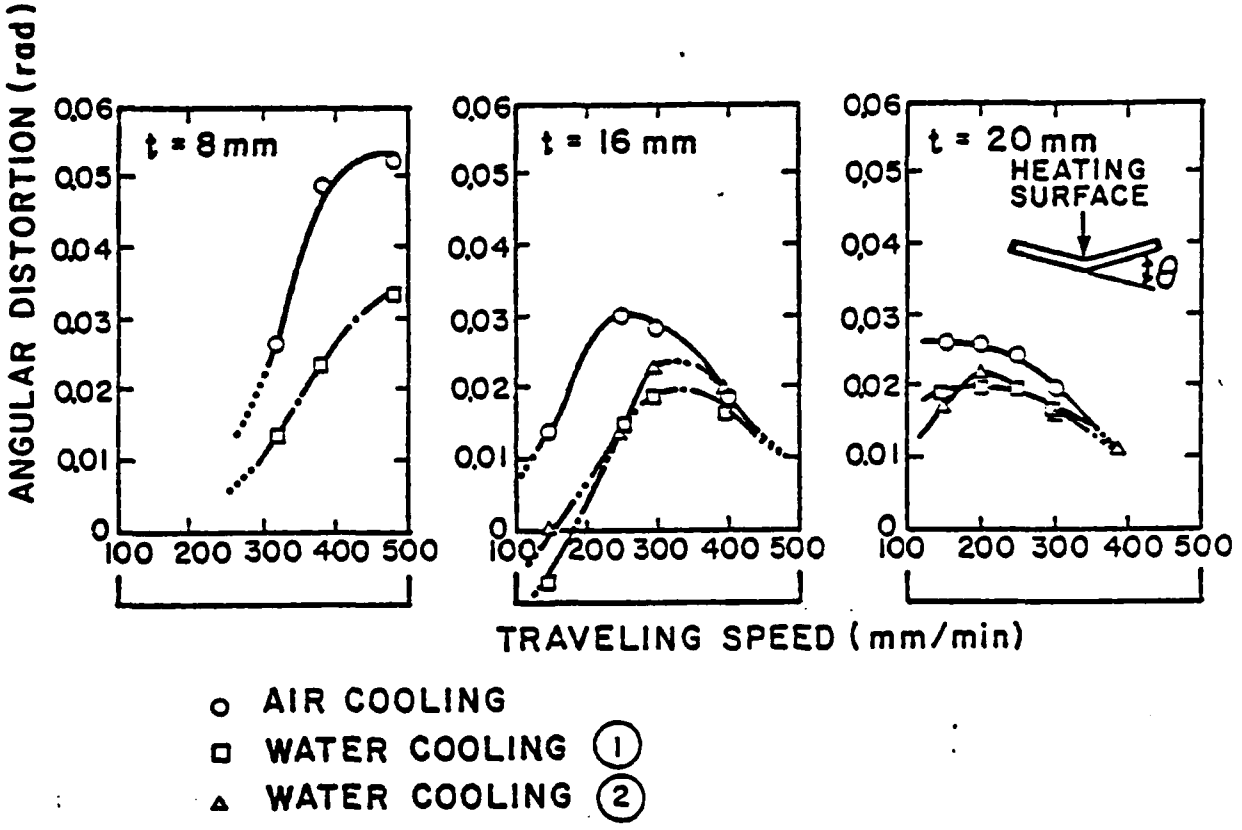

FIGURE 2.11: Effects of travel speed and plate thickness on the final angular distortion

The experimental set-up used by Johnson [14] at M.I.T. is shown in Figures 2.12 and 2.13. He recorded temperature, strain, and distortion data both with and without water cooling. Testing was performed on mild steel, T-1, and Corten specimens. Three passes were made on each plate. His conclusions are presented as follows:

(1) Line flame heating without water cooling is most effective for bending the mild steel.

(2) Line flame heating with water cooling is more efficient as a bending process.

(3) The large values of transverse strain necessitate at least a two dimensional analysis for predicting the effects of flame heating.

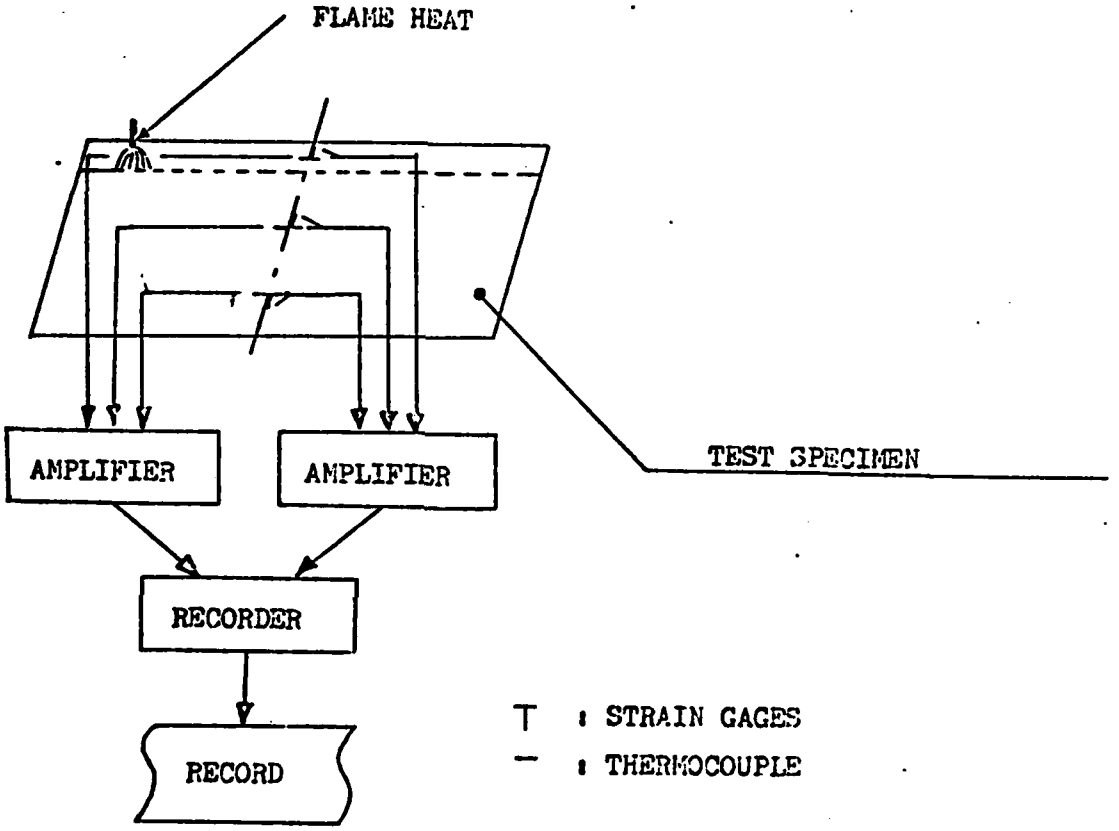

FIGURE 2.12: Experimental Set-Up

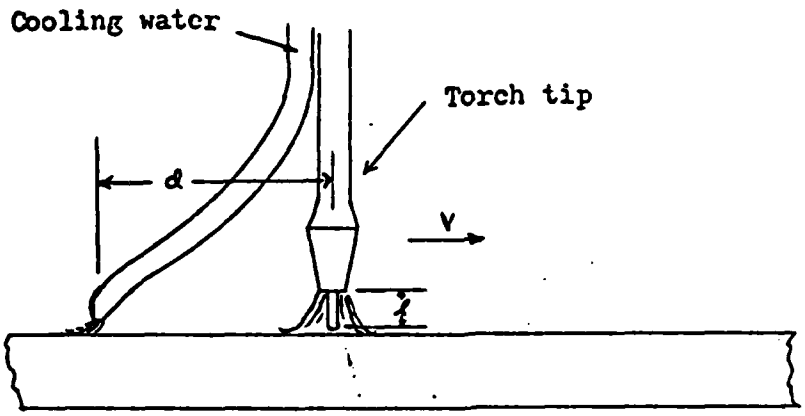

(a) Diagram of torch tip and water cooling attachment

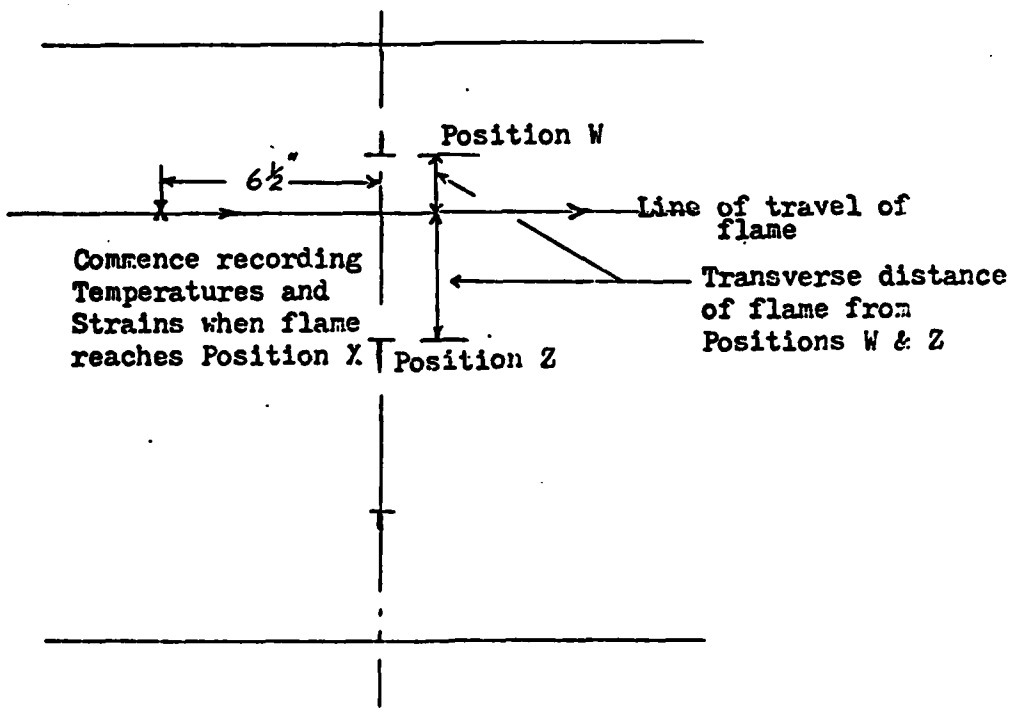

FIGURE 2.13: Diagram of dimensions used to specify location of the flame for each pass

The experimental set-up used by Iwamura and Rybicki [17] is shown in Figure 2.14. The specimens, made of mild steel, were set as shown. A zone was heated with two oxygen-propane torches from both sides at the same time. After it reached the desired temperature, the zone was cooled in air. Throughout the experiment, the remaining area of the specimen was continuously being cooled by the chill plates so as to be maintained at room temperature.

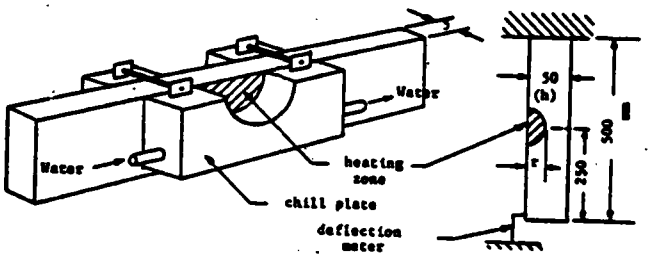

FIGURE 2.14: Experimental apparatus

The angular deformation was obtained by dividing the measured displacement by half the length of the specimen. Figure 2.15 shows several results for transient angular deformation. Figure 2.16 shows the relation between the final angular deformation and maximum temperature for various heated areas. This figure also reinforces other information presented concerning the amount of distortion versus the heat penetration depth.

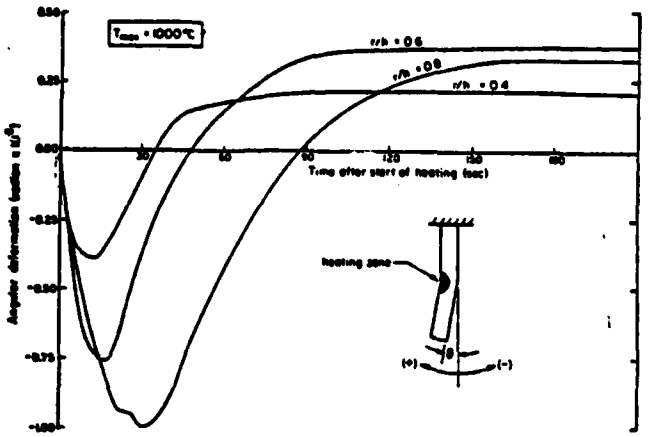

FIGURE 2.15: Transient angular deformation for various heated areas

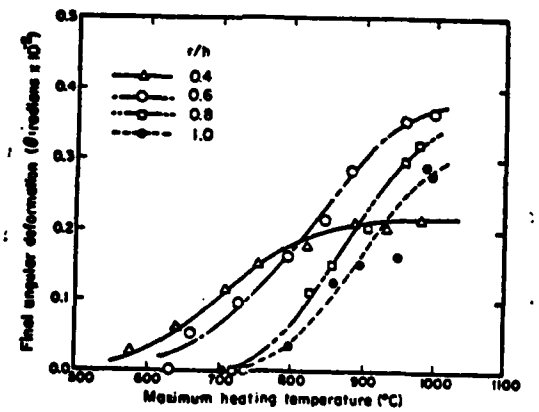

FIGURE 2.16: Relation between the angular deformation and heated temperature for various heated areas

The results shown in Figures 2.10 (a) and (b) are typical for metal movement during welding as well as during flame heating [1]. Watanabe and Satoh [18] studied how welding conditions and other parameters affect values of

angular change in bead-on plate and fillet welds. They found that the angular changes can be expressed as a function of a parameter X which is defined as follows:

$$X = 10^{-3} \frac{I}{h\sqrt{vh}} \qquad \text{where,}$$

I = welding current

v = arc travel speed

h = plate thickness

The angular change for bead-on plate welds is presented in Figure 2.17 and for fillet joints in Figure 2.18. The maximum distortion occurs when the x-value is about 0.24 for the bead-on plate weld and about 0.4 for the fillet weld.

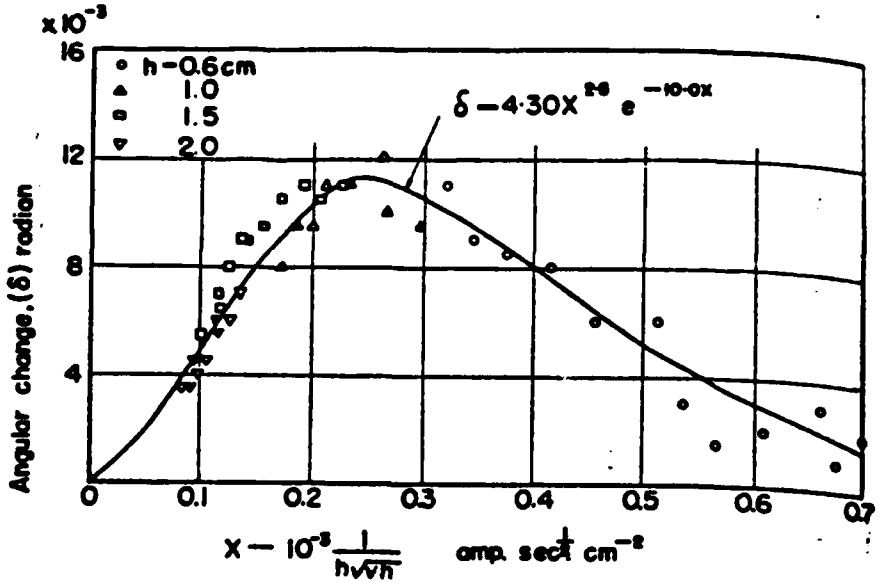

FIGURE 2.17: Effect of welding conditions on the angular change of bead-on plates

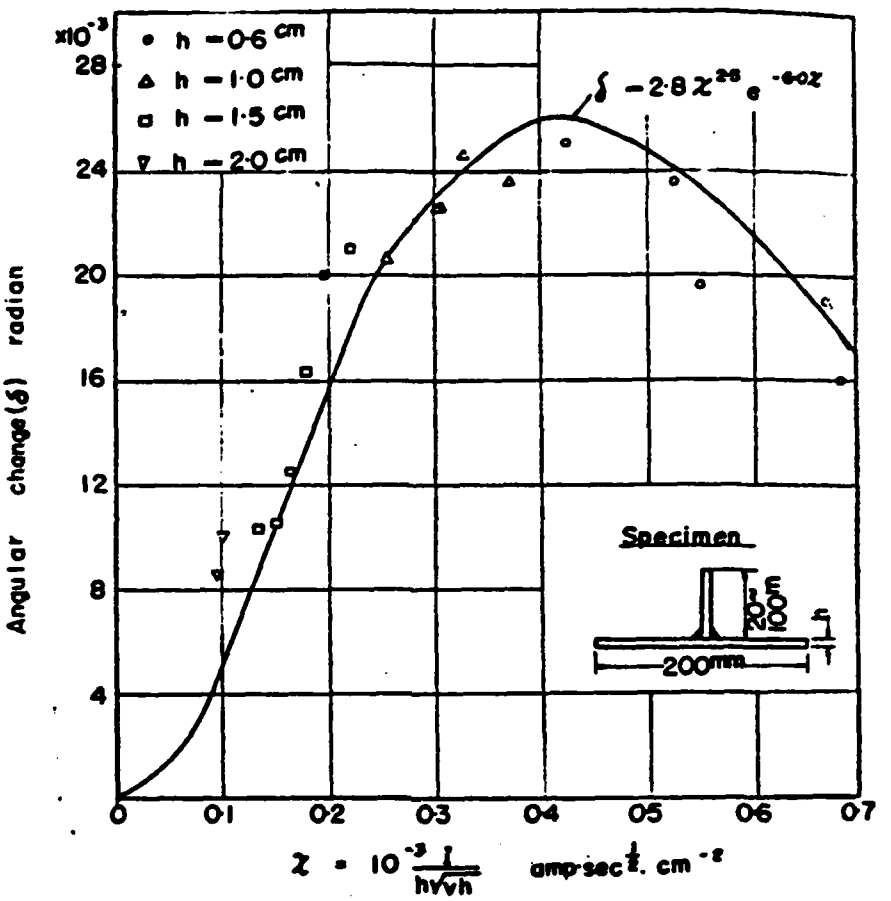

FIGURE 2.18: Effect of welding conditions on the angular change of fillet joint

The one article, previously mentioned, that discusses using a laser to form steel plates was written by The Japan Welding Engineering Society. They formed a technical committee in 1980 to study the feasibility of high power CO_2 laser metal working [19]. This committee examined several areas of interest including practical applications. One practical application examined was the feasibility of precision bending of ship hull structure steel plates. The following paragraph will discuss the set-ups used along with the results obtained.

The committee used a 15 kw CO_2 Avco laser to perform the experiments. Figure 2.19 shows the dimensions of the specimen while Figure 2.20 shows how the angular distortion was measured.

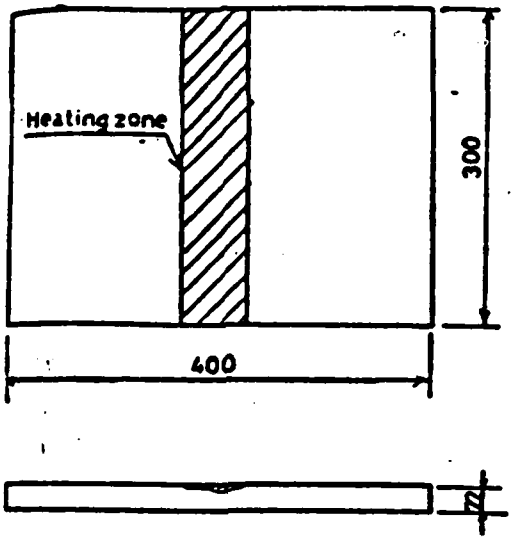

FIGURE 2.19: Dimensions of specimen

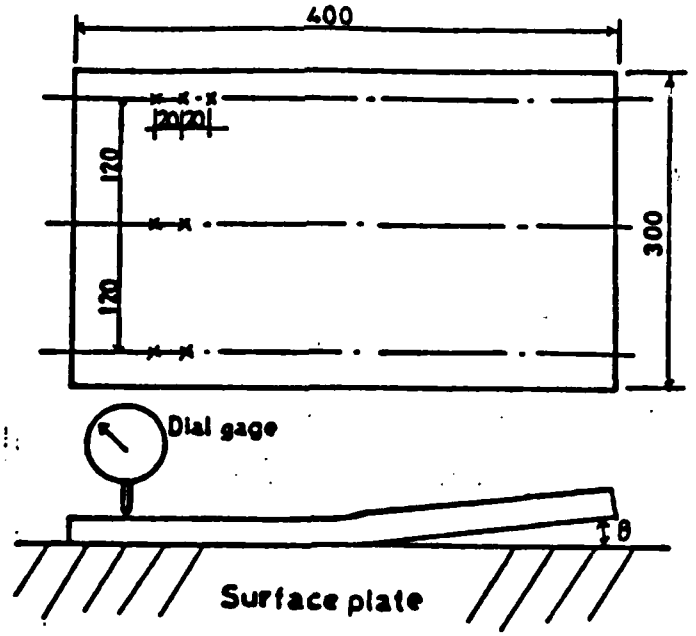

FIGURE 2.20: Method of measuring angular distortion

The effect of beam spot size on angular distortion is shown in Figure 2.21. It also shows where melting took place. This is extremely important since the occurance of melting affects the material degradation.

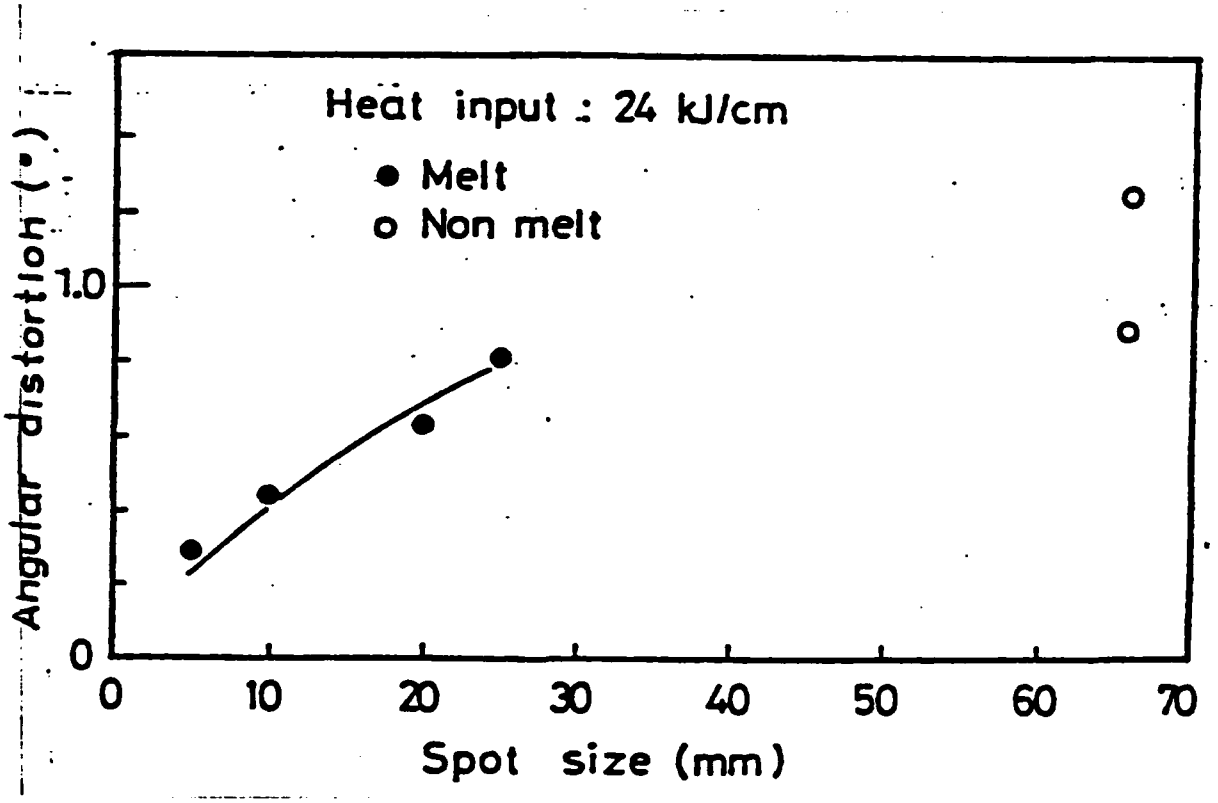

FIGURE 2.21: Effect of beam spot size on angular distortion

Figures 2.22 and 2.23 depict the angular distortion as a function of heat input, speed, and number of passes. As shown in Figure 2.23, distortion of one degree per pass was achieved. The committee reported that laser line heat bending was found to be a feasible application for precision bending of ship hull plates.

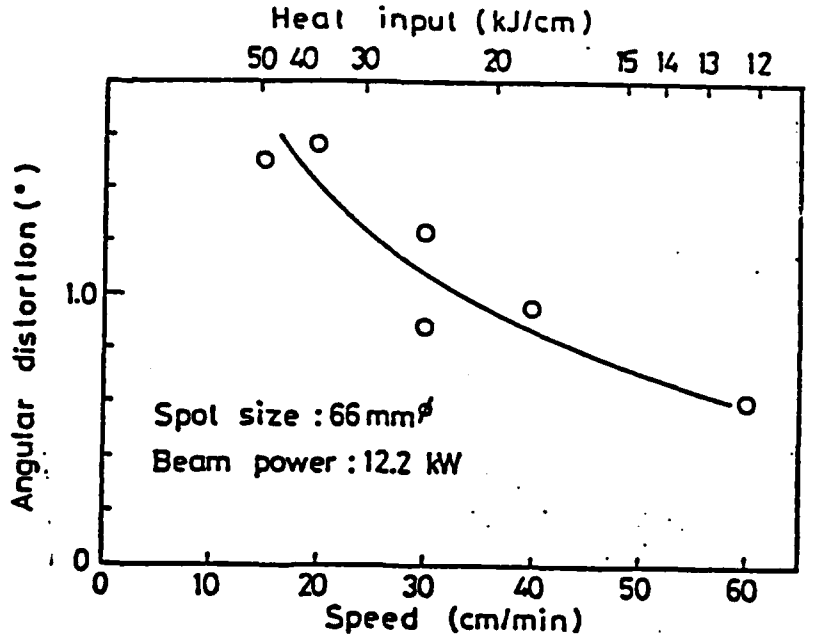

FIGURE 2.22: Effect of speed on angular distortion

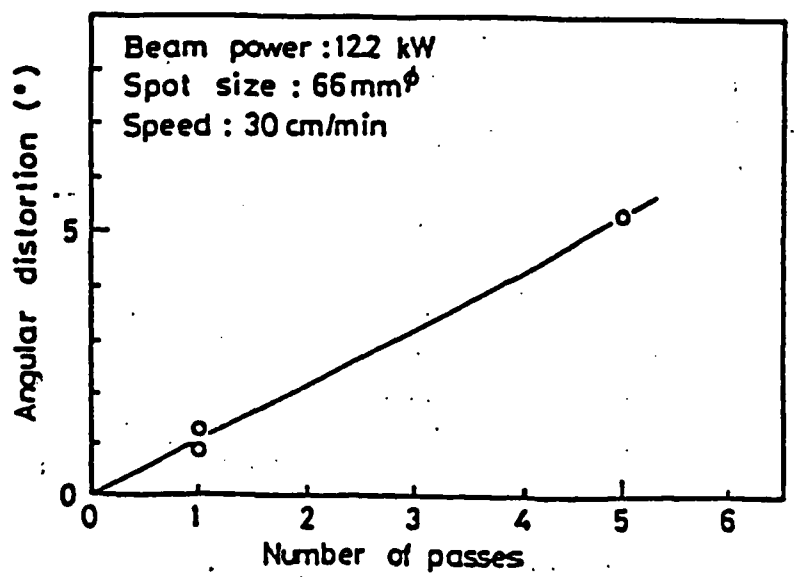

FIGURE 2.23: Effect of multi-pass heating on angular distortion

CHAPTER THREE

EXPERIMENTAL PROCEDURES

A. Scope of Research

Experiments were conducted using an Avco 15 kw CO_2 laser located at the Naval Research Lab (NRL) in Washington, D.C. The laser was used as a heat source to form HY-80 and AISI 1080 carbon steel plates. Emphasis was placed on measuring real-time distortion and on comparing the final distortion achieved between the various plates. Temperature variations were measured by thermocouples while variations in strain were measured by biaxial strain gages. The temperature and strain data will be analized, time permitting, or passed on to others working with Dr. Masubuchi.

B. Description of Specimens

There is a total of seven instrumented plates. Plates #1 through #3 are 6" x 12" HY-80; plates #4 and #5 are 6" x 12" AISI 1018 carbon steel; and plates #6 and #7 are 12" x 12" AISI 1018 carbon steel. All specimens are 1/2 inch thick.

C. Data Collection

The specimens were mounted to a Bridgeport milling machine table using two C-clamps as shown in Figure 3.1. The table's speed is variable and can be preset and automatically controlled by means of switches on the control box. Two speeds, six inches per minute (ipm) and 12 ipm, were used.

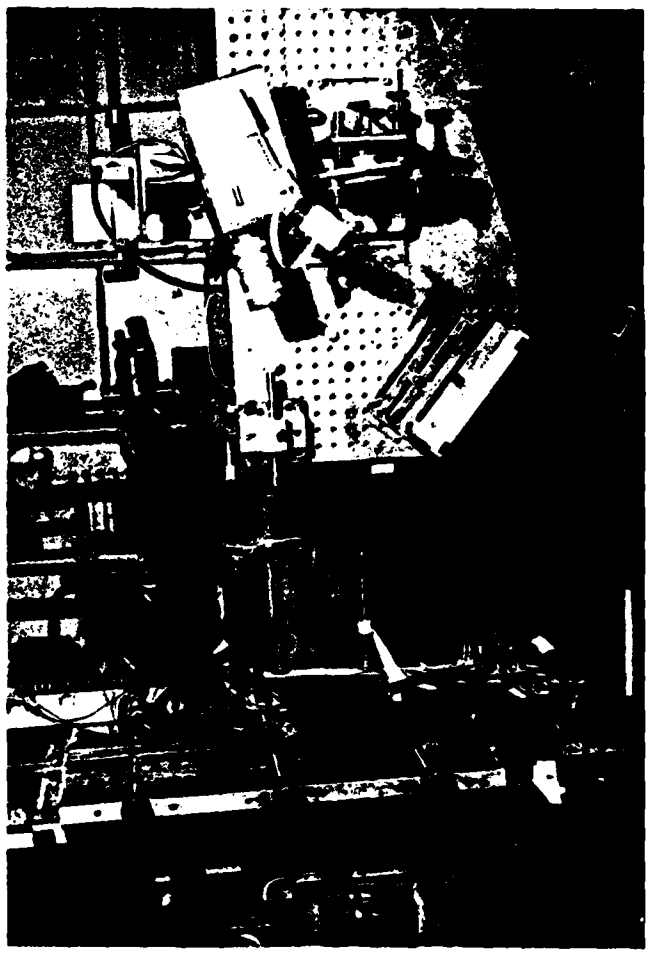

FIGURE 3.1: Experimental Set-Up

The laser is located in an adjoining room, and its power is directed to the specimen located in the test cell through a system of reflecting mirrors. No one is allowed in the test cell when the laser is in use. In fact, the doors to the test cell must be closed and remain closed during laser operation. If the doors are opened, the installed interlock system will automatically secure the laser to ensure personnel safety. There is a window between the laser room and the test cell through which the laser operation can be observed.

The final two mirrors in the laser beam's travel are attached to the upper part of the milling machine which remains stationary. (See Figure 3.1.) The beam is reflected from mirror-to-mirror and then to the specimen as shown in Figure 3.2. This particular set-up is known as "cross four focusing" because the beam path forms the number four. The laser beam remains stationary while the table with the specimen attached moves.

All of the specimens were sprayed with a light coat of Krylon red high-heat paint, good to 1700° F. It was hoped that a light coat of paint would provide sufficient coupling to cause a satisfactory bend. Earlier test runs had demonstrated that a light coat of paint on the test samples would not burn when the laser beam struck the plate. With a heavier coat of paint, however, the paint did burn giving off black-body radiation that prevented a clear image of the fringe spacing from being recorded by the camera.

Unfortunately, there was minimal coupling with the light coat of paint. This necessitated additional paint being added to the plate. To reduce the burning effect, an interference filter designed to transmit only the Helium-Neon laser wavelength of 6328 Å was attached to the camera. This filter was helpful, but the light within that pass band was just too intense to be completely blocked. Since a better filter was not immediately available, the experiments continued using what was at hand.

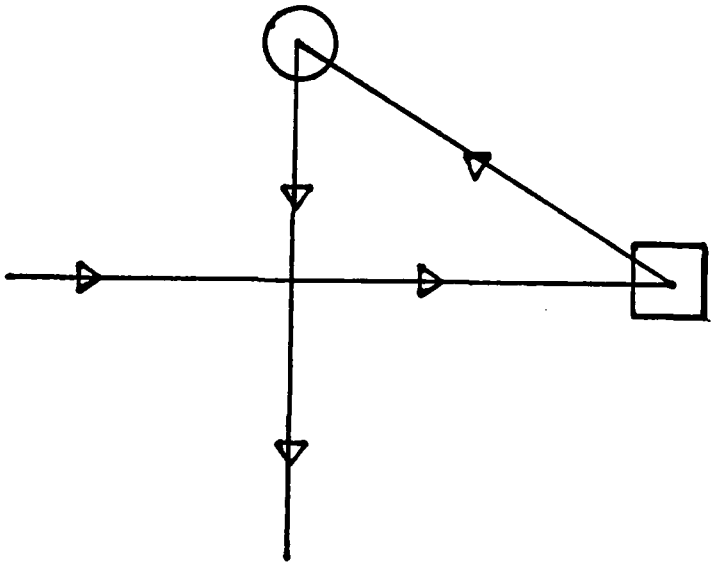

FIGURE 3.2: Cross Four Focusing

Distortion measurements were made using the interferometer as described in Chapter 2. A video camera was used to record an image of the fringe spacings which

were then sent to a video cassette recorder (VCR) for permanent storage. This allows the possibility of real-time measurements, and also makes it easier to make measurements on a monitor after the run is completed rather than on the hot specimen surface. Figure 3.3 shows the equipment set-up while Figure 3.4 shows an example of the fringe spacing on plate # 4.

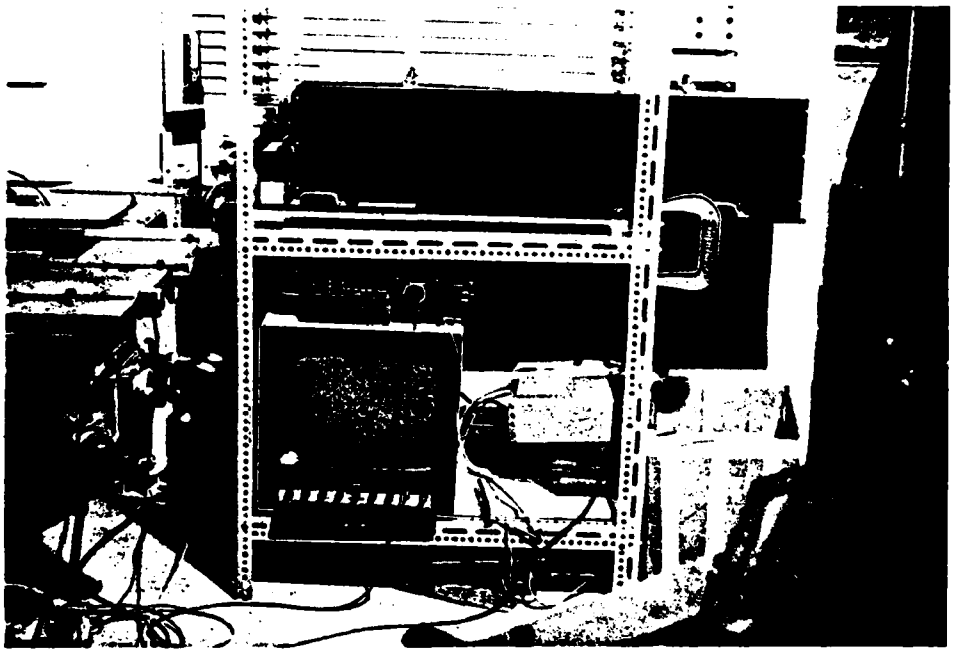

FIGURE 3.3: Equipment Set-Up

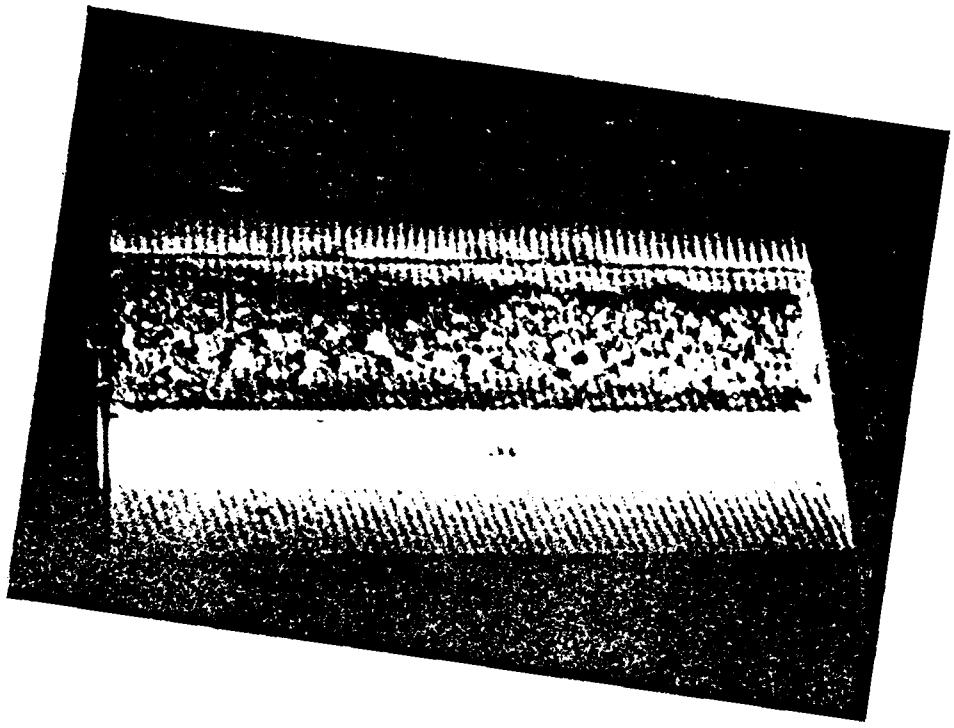

FIGURE 3.4: Fringe Spacing

The strain gages and thermocouples were mounted by Brewer Engineering Laboratories of Marion, Massachusetts as shown in Figure 3.5. Strain gages were connected to a Wheatstone Bridge circuit, balanced and calibrated as indicated schematically in Figure 3.6. Thermocouples were referenced to a 32° F ice-bath and calibrated as indicated in Figure 3.7. The data from the strain gages and thermocouples served as input to the Honeywell Visicorder (Figure 3.8). The output from the Visicorder was on stripcharts with an example shown in Figure 3.9.

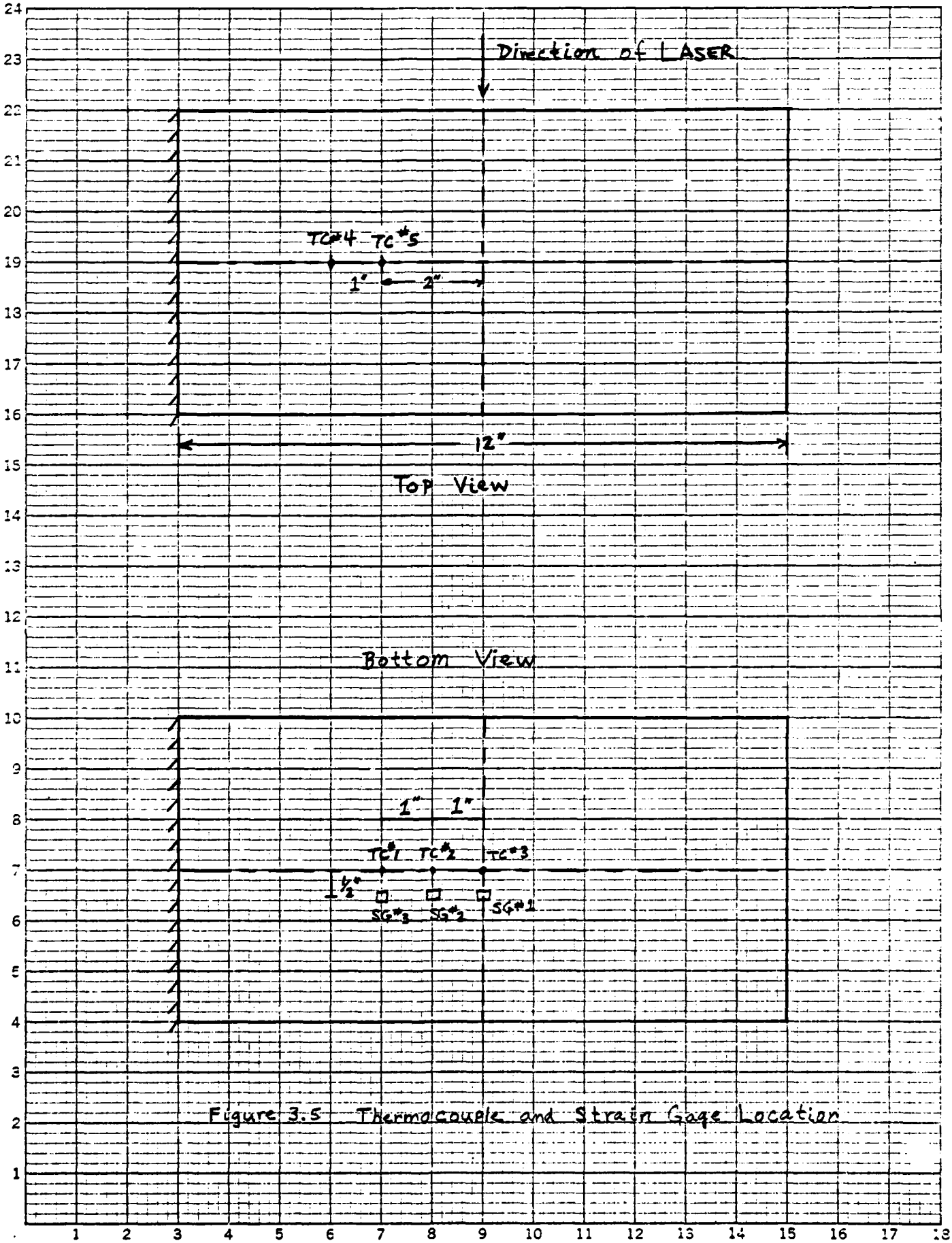

Figure 3.5 Thermocouple and Strain Gage Location

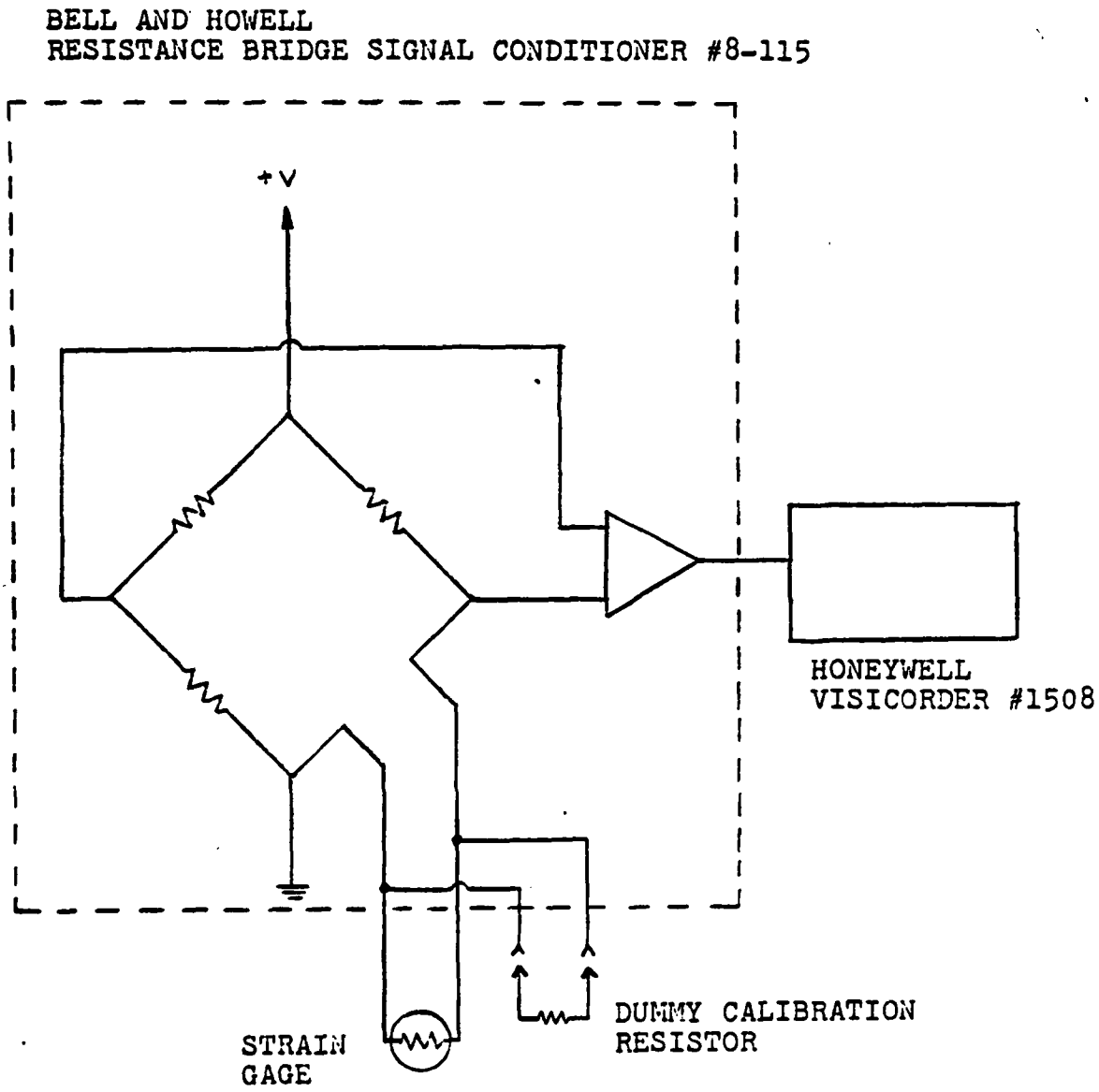

FIGURE 3.6: Strain Gage Instrumentation Circuit

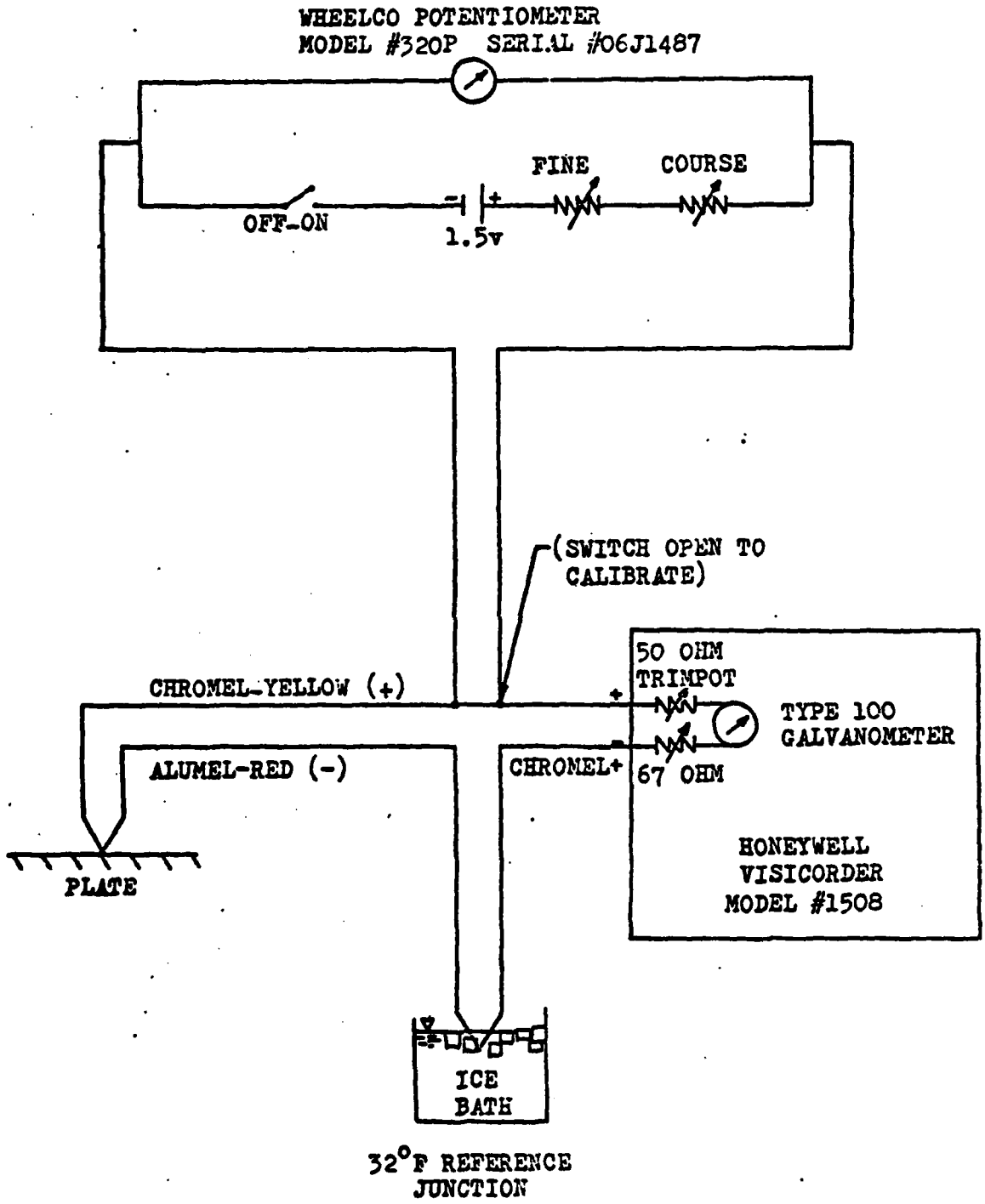

FIGURE 3.7: Thermocouple Instrumentation Circuit

FIGURE 3.8: Honeywell Visicorder

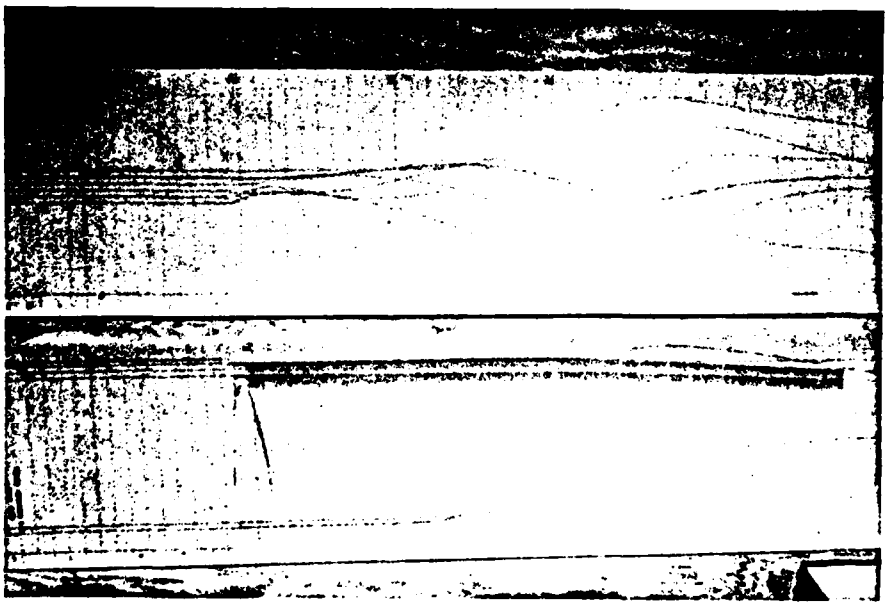

FIGURE 3.9: Stripchart Recording

CHAPTER FOUR

RESULTS

The plots presented in this chapter reflect the thermal history of each of the test plates. Each plot records the strain and temperature variations during one laser pass and subsequent cool-down. No particular time was sought between passes; the laser started another pass as soon as all preparations were complete. Some plates were cooled with compressed air if sufficient time was available. For each plate, the final readings on the last pass represent the cumulative strain state at the gage locations.

A. Distortion

The results of this investigation consist of distortion measurements, temperature data,and strain data recorded during laser passes of the test specimens. The data for distortion is presented in Table 4.1 while the remaining data is presented below in the form of plots of mechanical strain and temperature versus time.

TABLE 4.1

Measured Distortion (Degrees)

	Pass 1	Pass 2	Pass 3	Pass 4
Plate #2	0.1	0.2	0.3	0.5
Plate #3	0.9	1.6	2.2	3.6
Plate #4	0.9	2.6	3.6	4.7[1]
Plate #5	0.9	1.7	3.4	5.3[2]

	Line 1	Line 2	Line 3
Plate #6	0.9	1.4	1.9

		Pass 1	Pass 2	Pass 3
Plate #7	Line 1	0.9	2.1	3.6[3]
	Line 2	5.6	5.9	6.5[4]
	Line 3	7.5	8.1	11.0[5]

[1] 5.0° *

[2] 5.5° *

[3] 6.0° *

[4] 10.0° *

[5] 13.5° *

*Measurements were made in lab at M.I.T. Plates were at room temperature.

B. Temperature

The temperatures recorded at thermocouple number two (TC2) and thermocouple number three (TC3) have been plotted for the first pass on each plate, except Plate #5. Information for the second pass was plotted for Plate #5. The temperature data will serve as baseline data and will also be used to compare and verify existing computer programs that deal with heat transfer analysis. A comparison of the experimental results and analytical results are presented in Chapter 5.

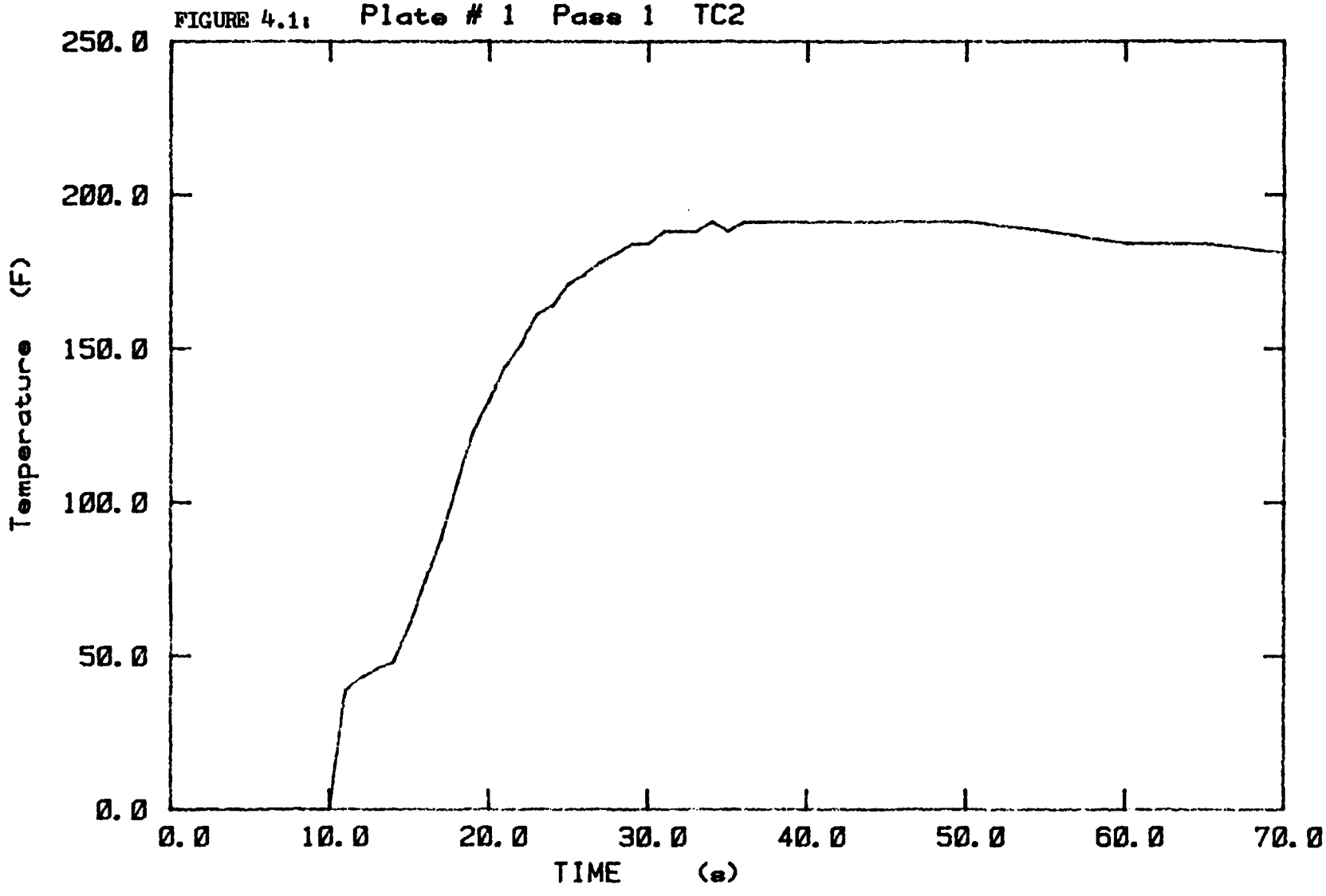
Plate # 1 Pass 1 TC2
250.0
200.0
150.0
100.0
50.0
0.0
Temperature (F)
0.0
10.0
20.0
30.0
40.0
50.0
60.0
70.0
TIME (s)

FIGURE 4.1:

FIGURE 4.2: Plate #1-Pass #1 TC3

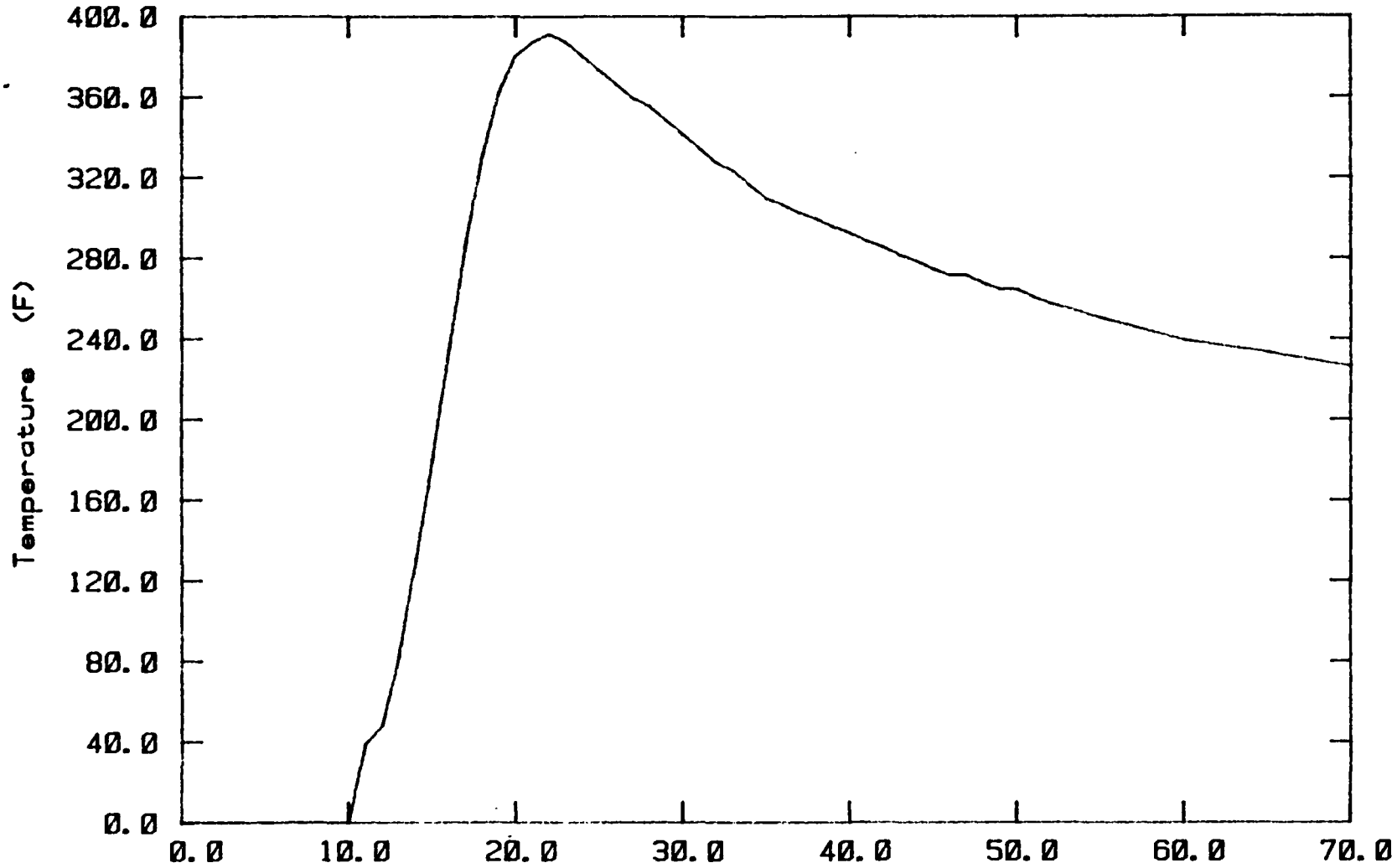

FIGURE 4.3: Plate #2 Pass #1 TC2

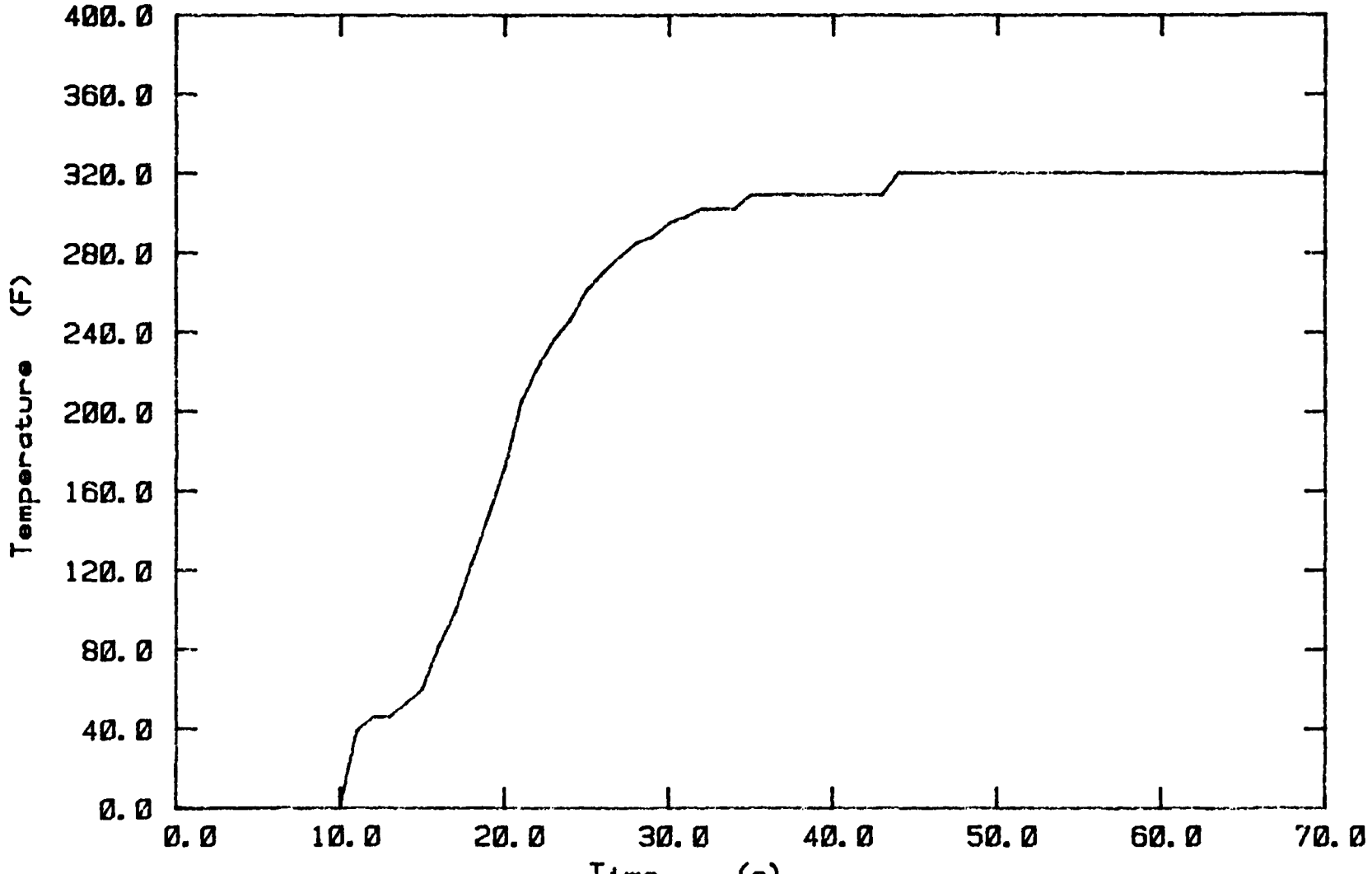

FIGURE 4.4: Plate #2 Pass #1 TC3

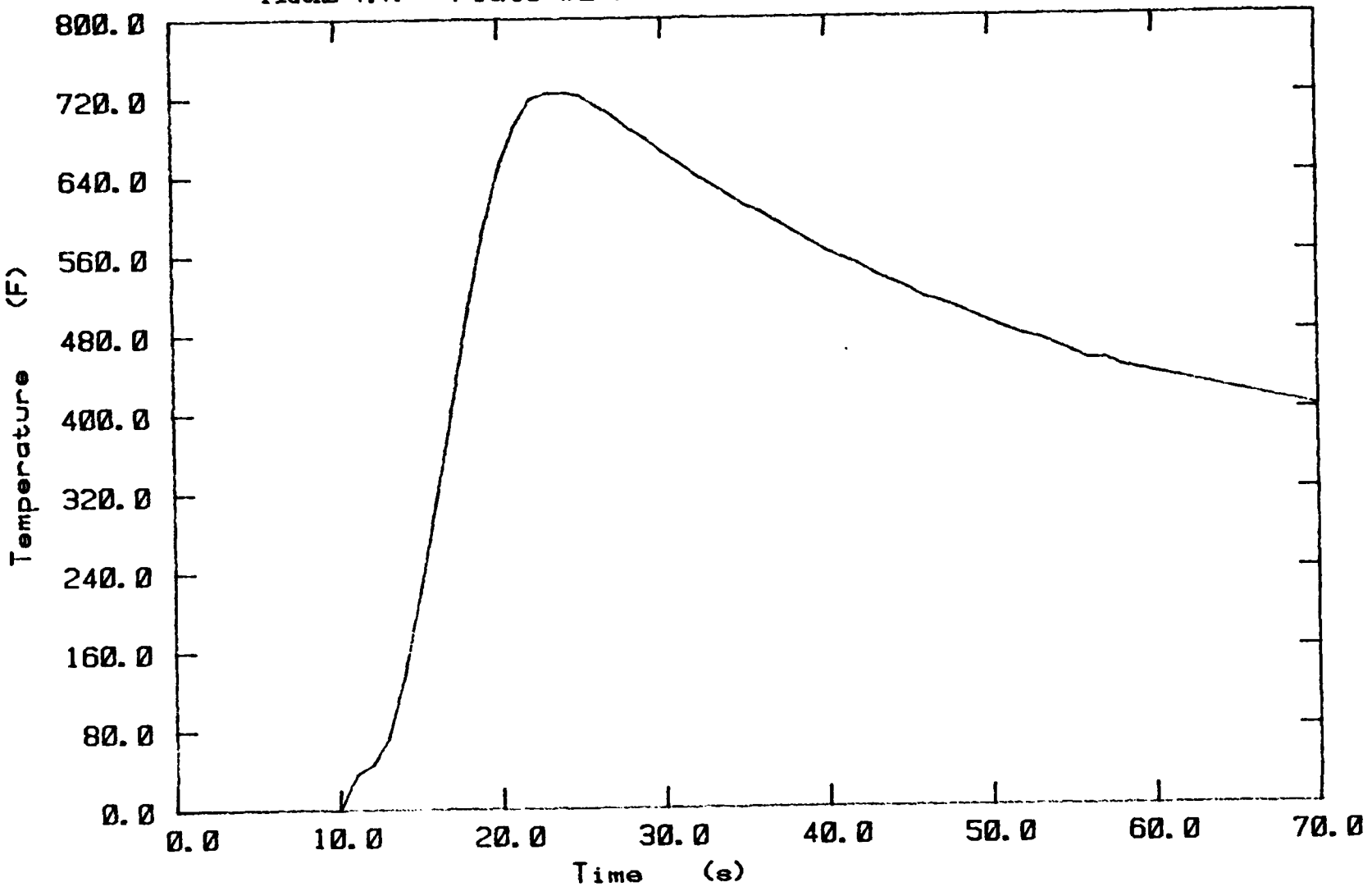

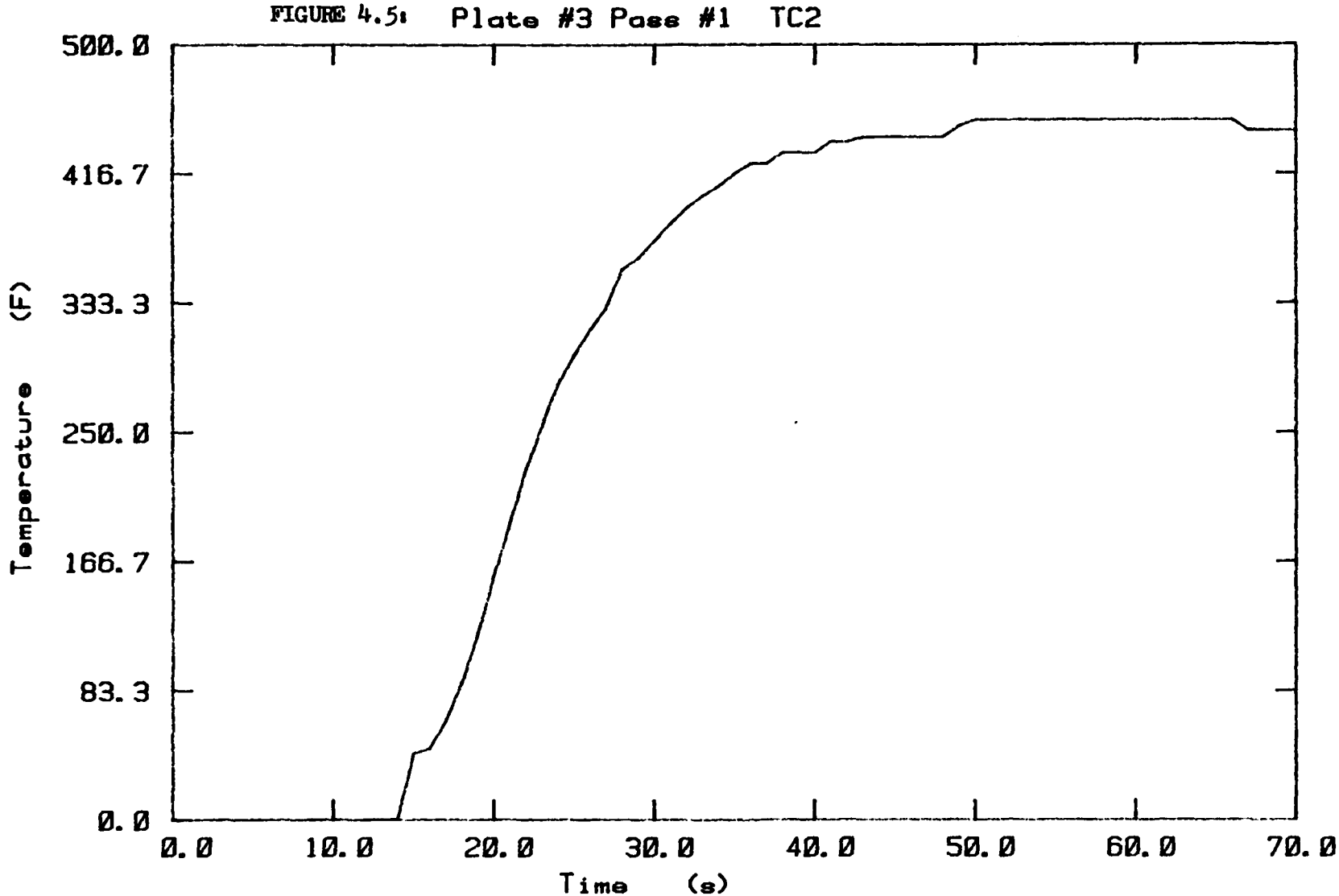
Plate #3 Pass #1 TC2
500.0
416.7
333.3
250.0
166.7
83.3
0.0
Temperature (F)
0.0
10.0
20.0
30.0
40.0
50.0
60.0
70.0
Time (s)

FIGURE 4.5:

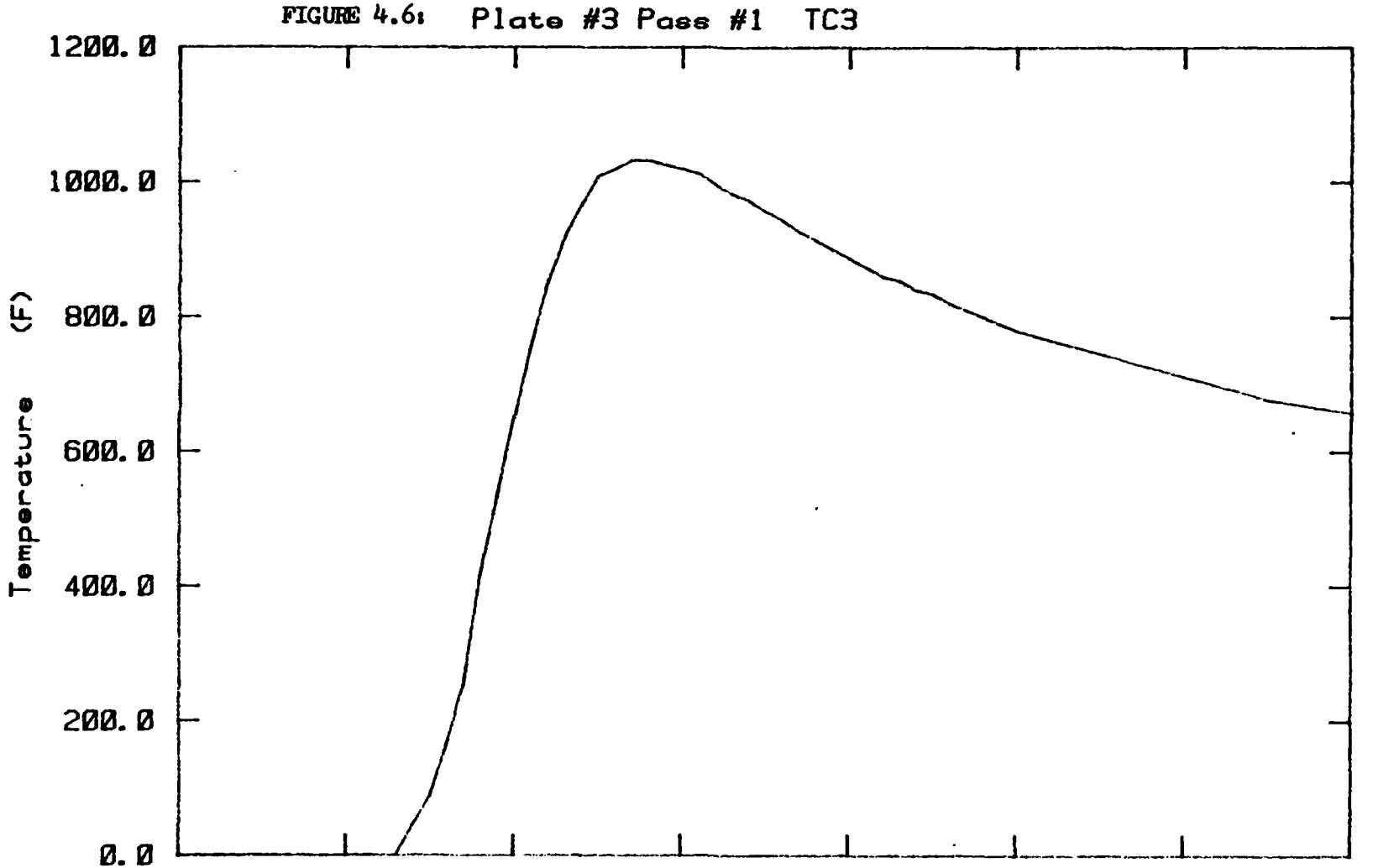
Plate #3 Pass #1 TC3
1200.0
1000.0
800.0
600.0
400.0
200.0
0.0
Temperature (F)
0.0
10.0
20.0
30.0
40.0
50.0
60.0
70.0
Time (s)

FIGURE 4.6:

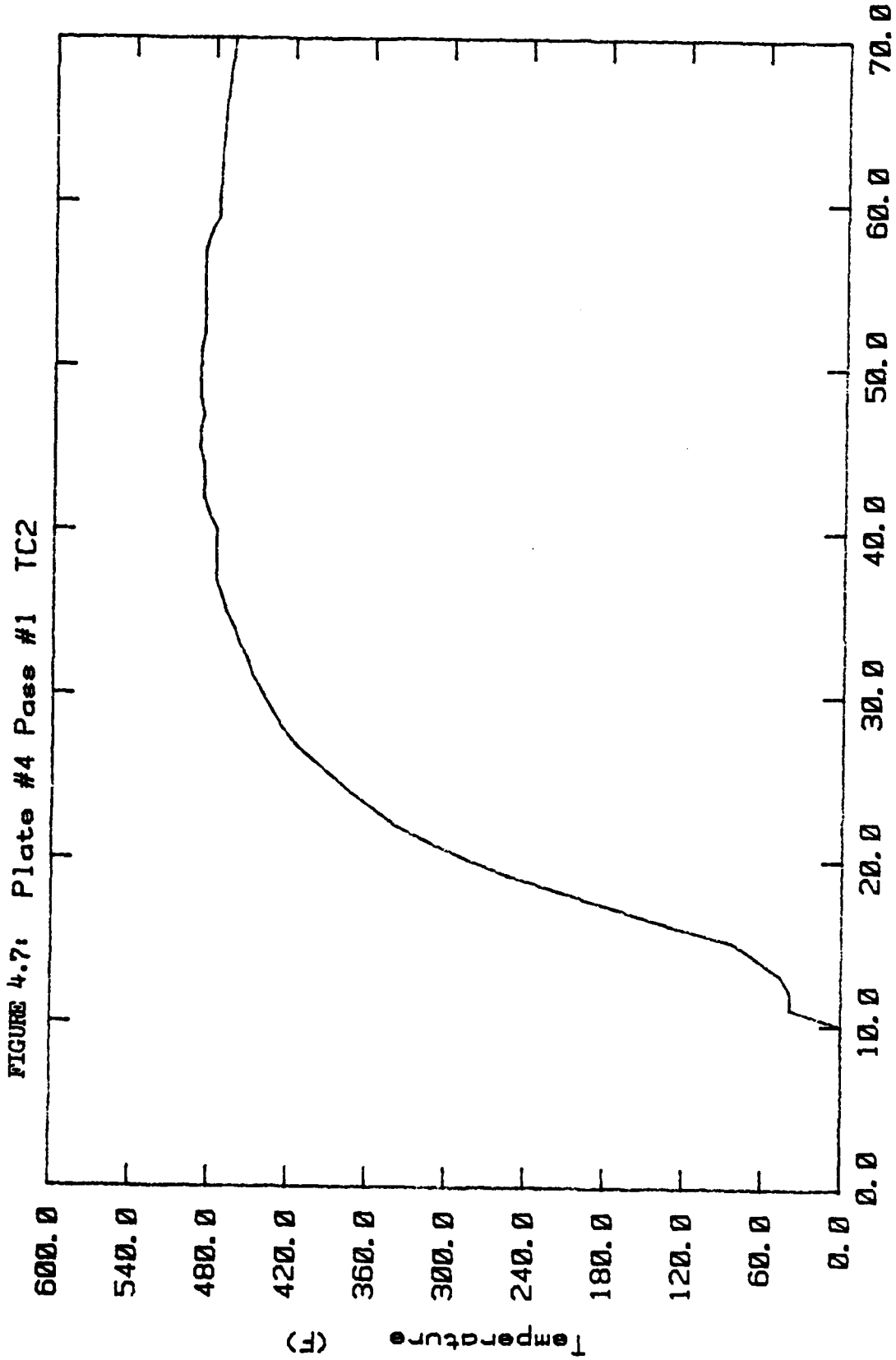

FIGURE 4.7: Plate #4 Pass #1 TC2

FIGURE 4.8: Plate #4 Pass #1 TC3

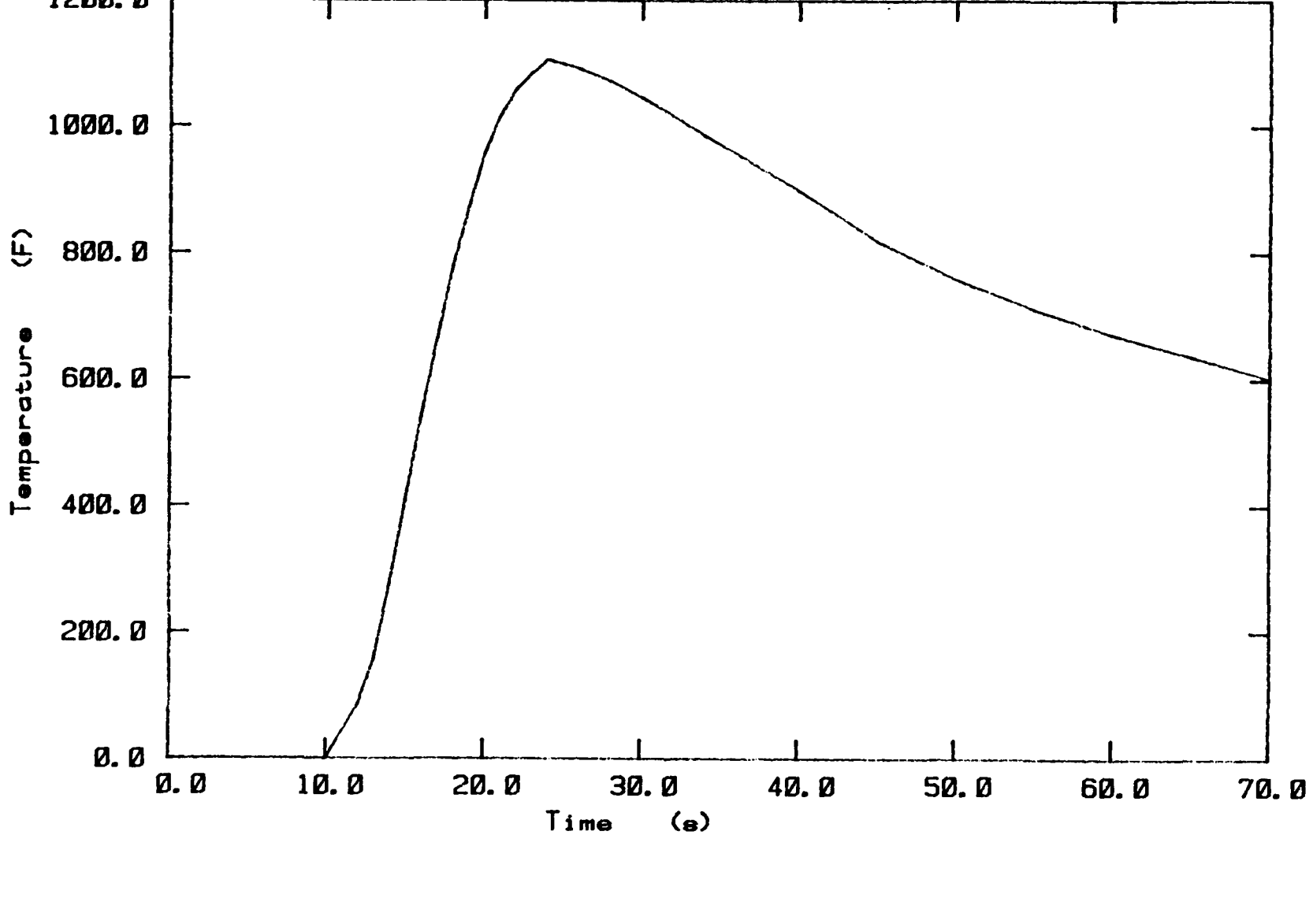

FIGURE 4.9: Plate #5 Pass #2 TC2

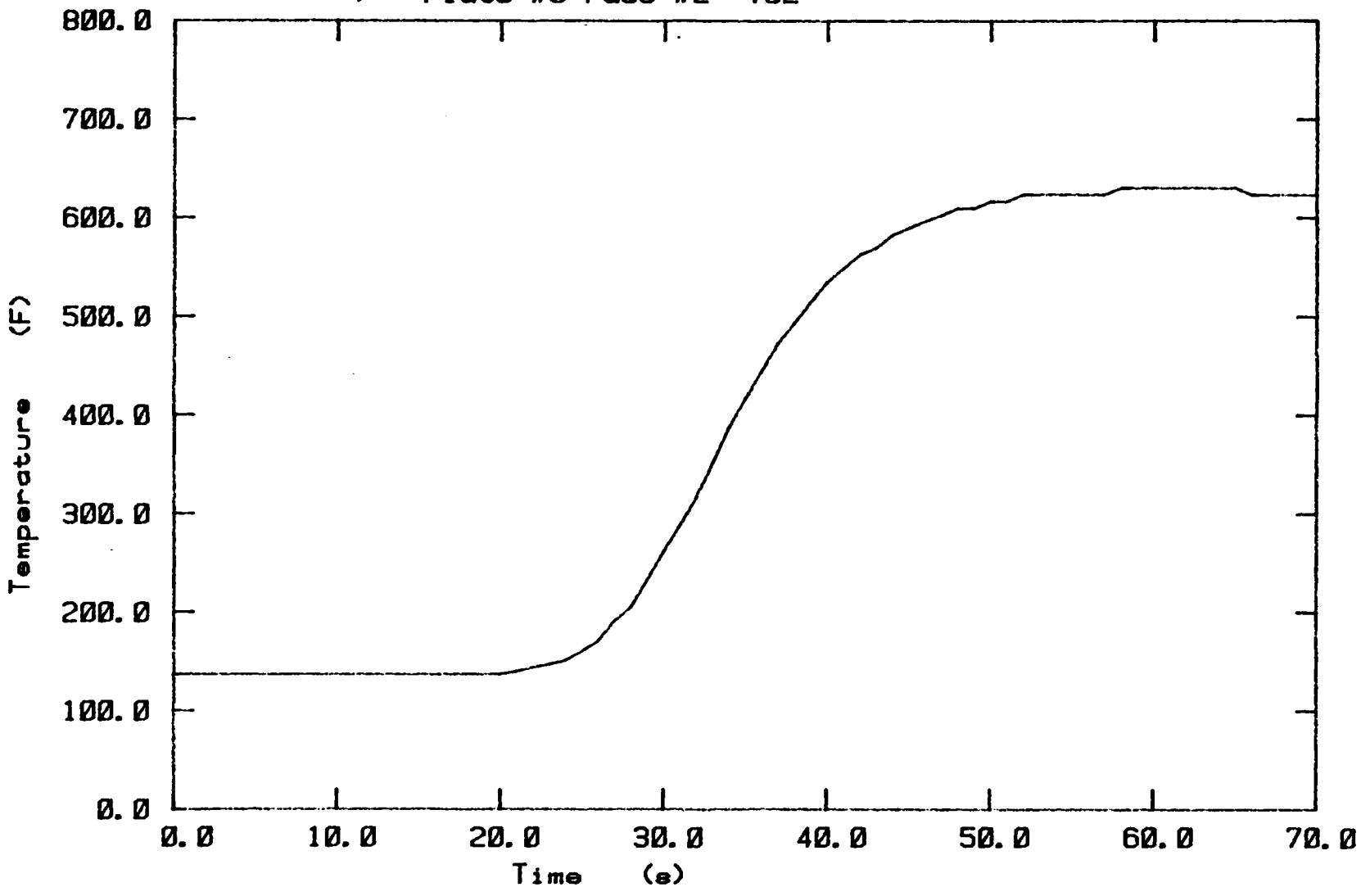

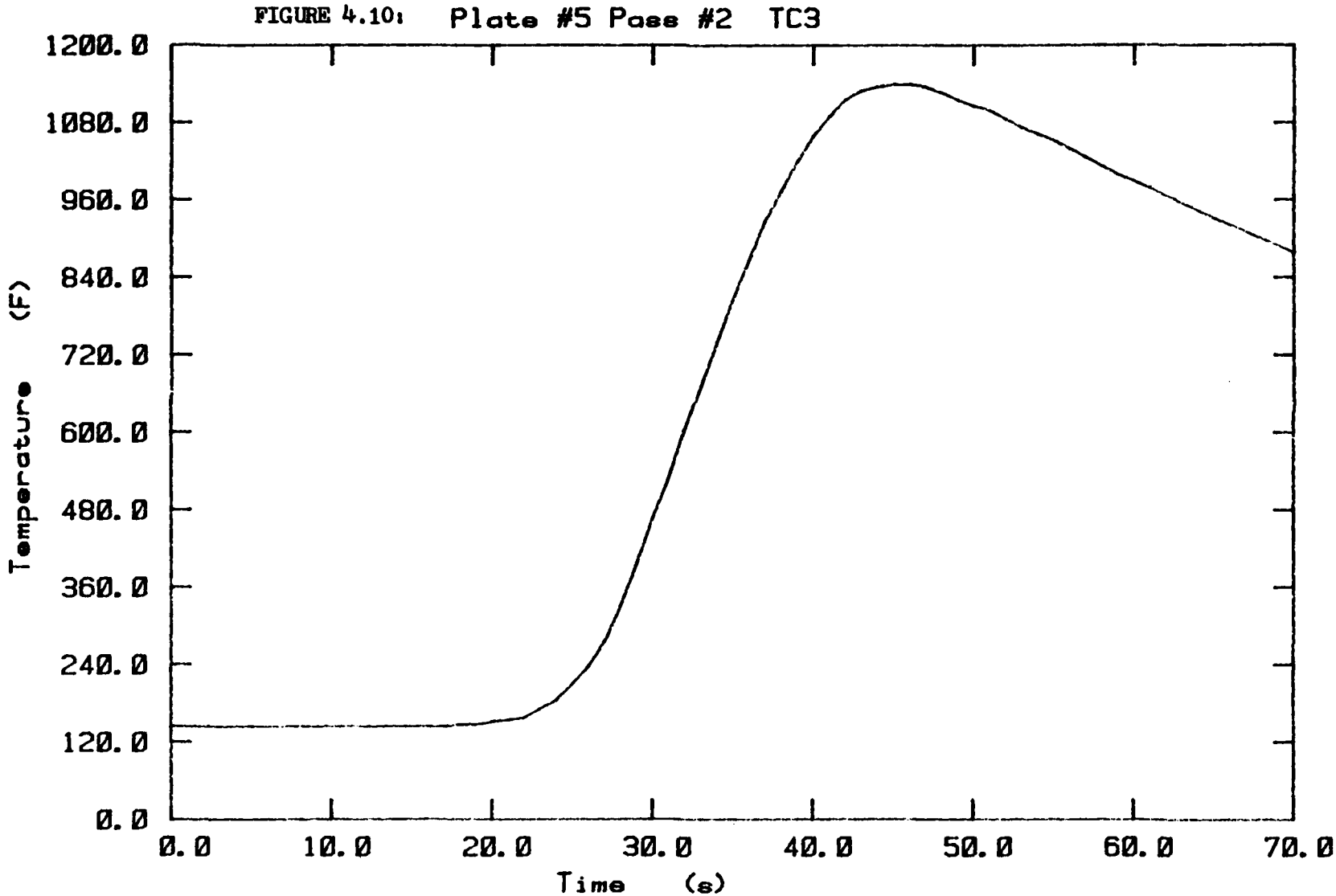
Plate #5 Pass #2 TC3
1200.0
1080.0
960.0
840.0
720.0
600.0
480.0
360.0
240.0
120.0
0.0
Temperature (F)
0.0
10.0
20.0
30.0
40.0
50.0
60.0
70.0
Time (s)

FIGURE 4.10:

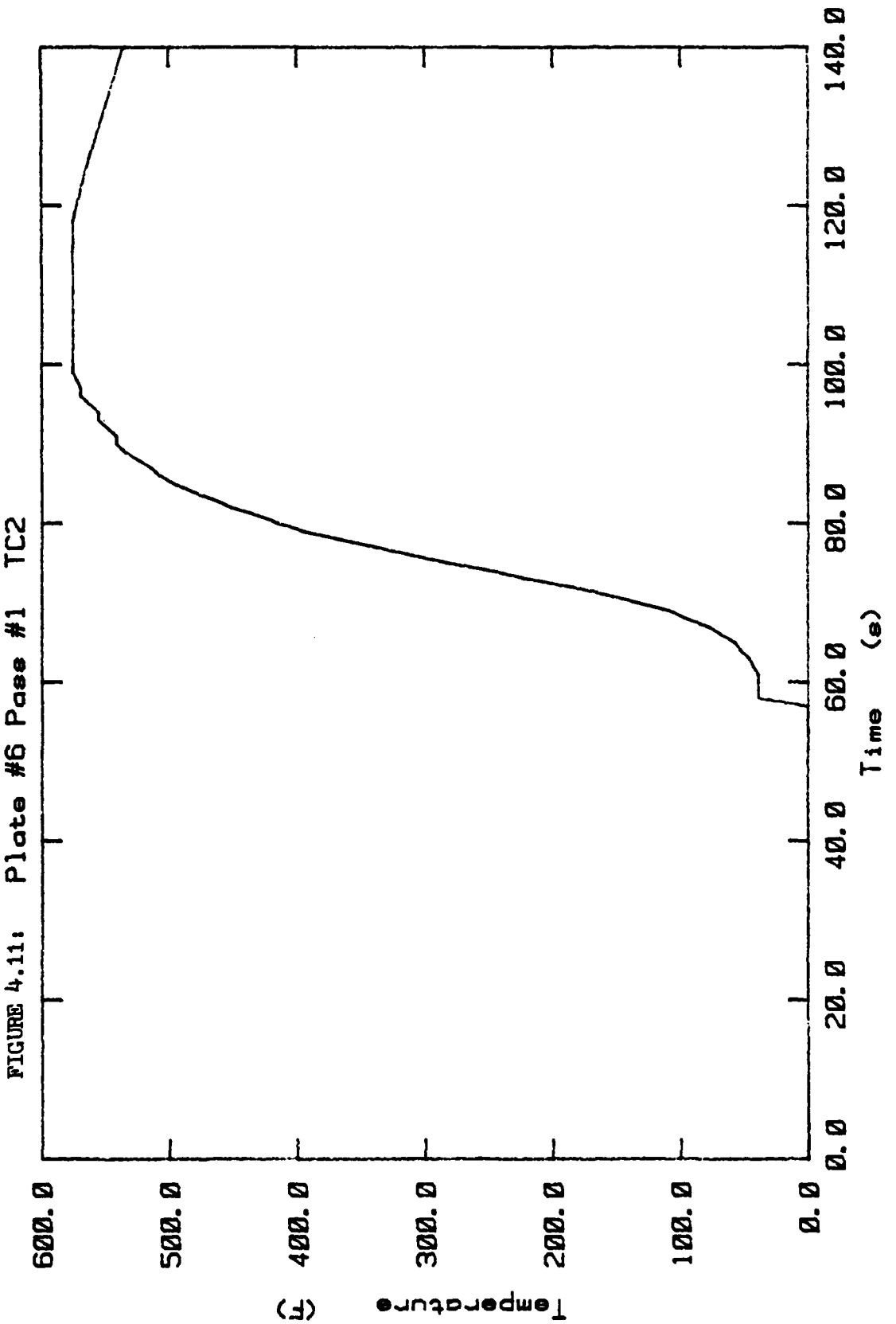

FIGURE 4.11: Plate #6 Pass #1 TC2

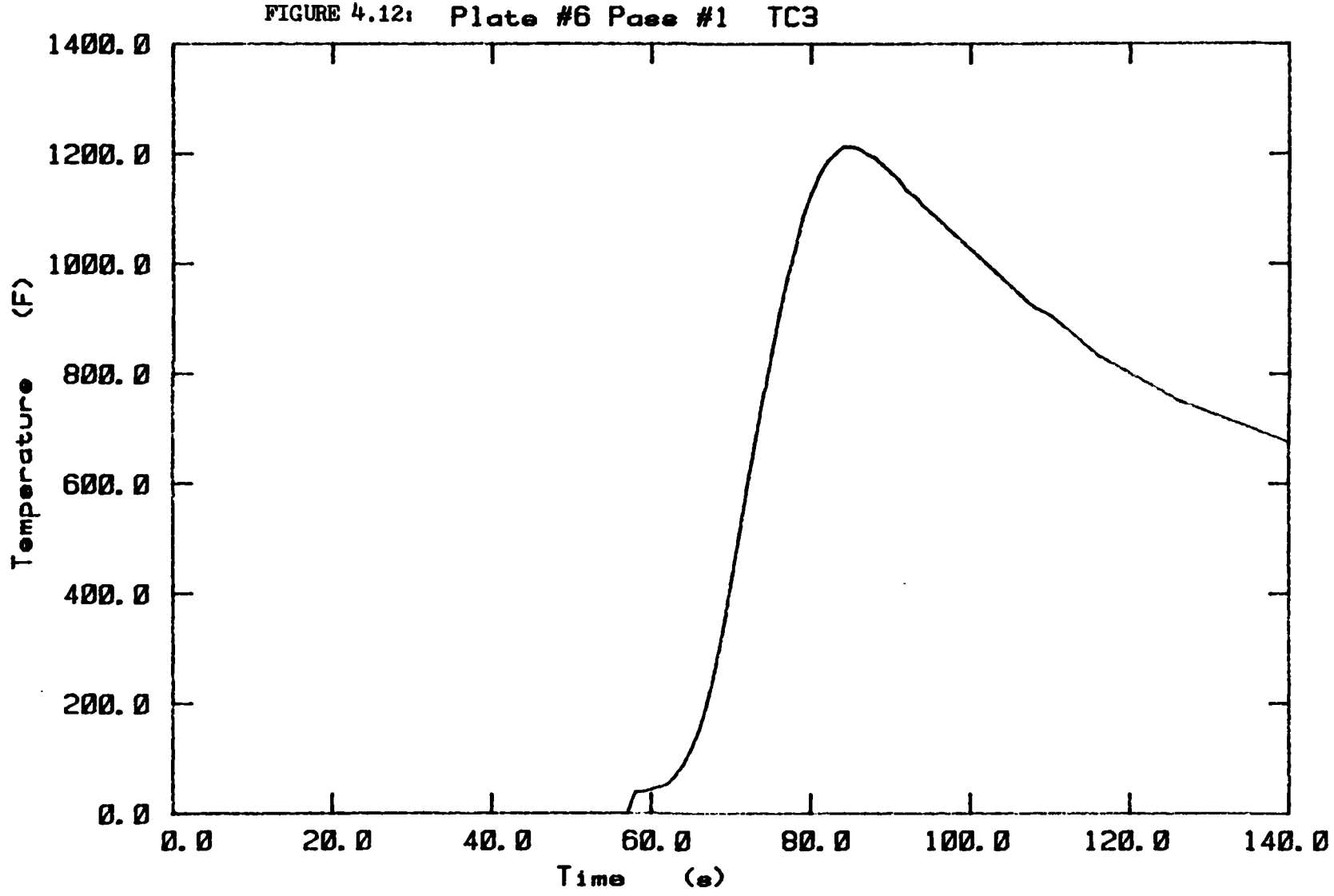
Plate #6 Pass #1 TC3
1400.0
1200.0
1000.0
800.0
600.0
400.0
200.0
0.0
Temperature (F)
0.0
20.0
40.0
60.0
80.0
100.0
120.0
140.0
Time (s)

FIGURE 4.12:

FIGURE 4.13: Plate #7 Line #1 Pass #1 TC2

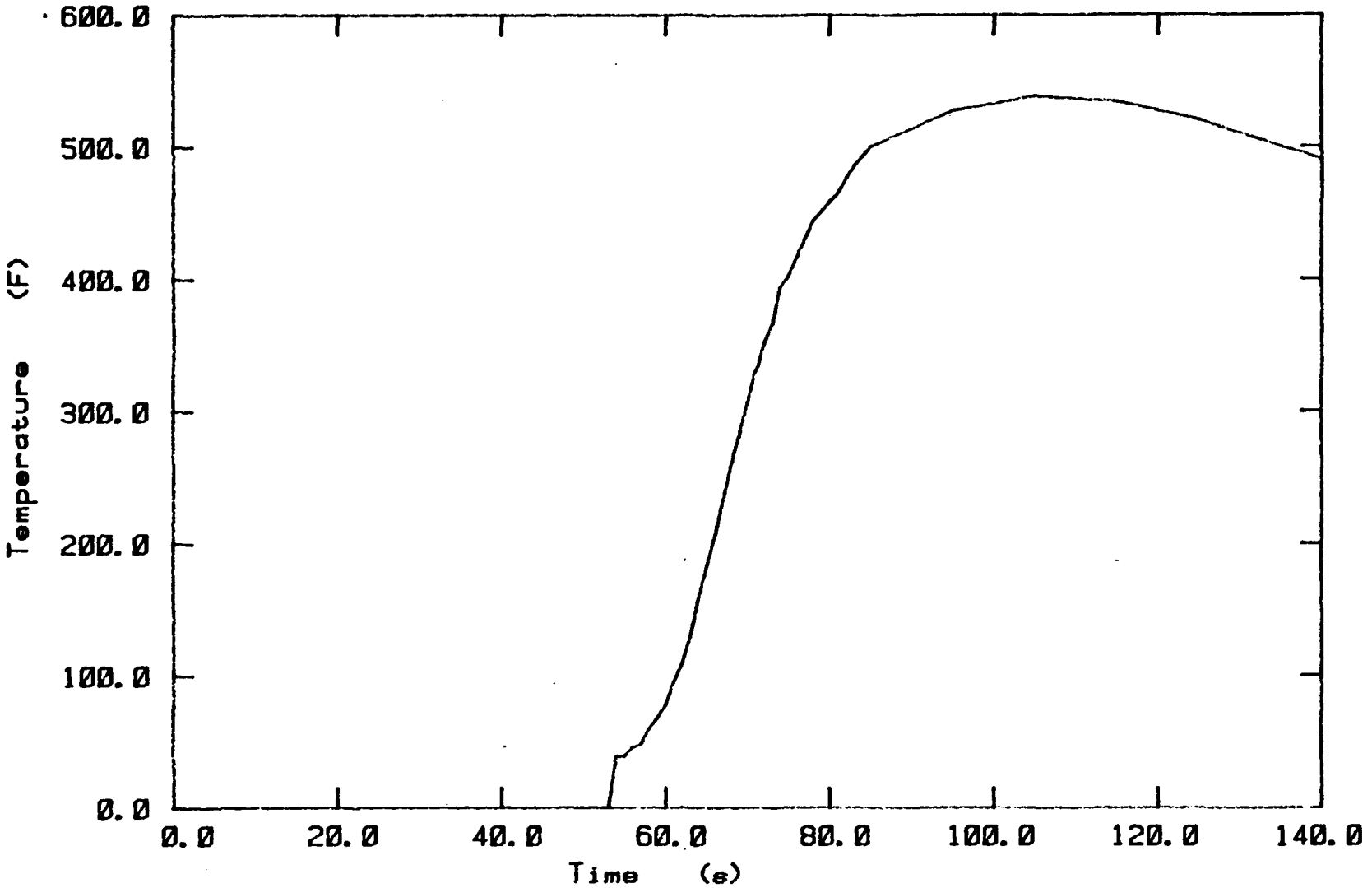

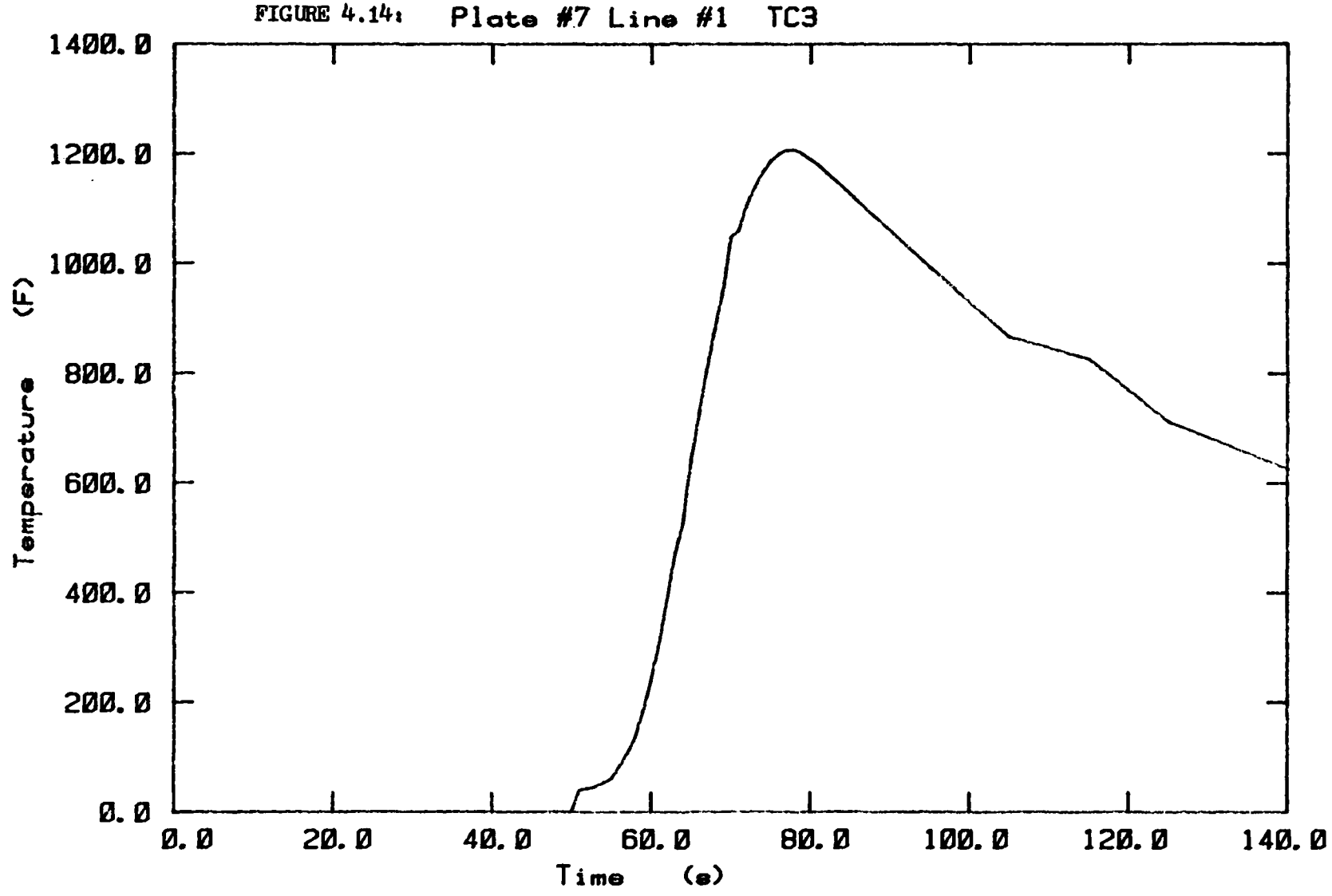
Plate #7 Line #1 TC3
1400.0
1200.0
1000.0
800.0
600.0
400.0
200.0
0.0
Temperature (F)
0.0
20.0
40.0
60.0
80.0
100.0
120.0
140.0
Time (s)

FIGURE 4.14:

C. Strains

The strains recorded at strain gage 1A (SG1A) and strain gage 1B (SG1B) have been plotted for the first pass on each plate except Plate #5. Information for the second pass was plotted for Plate #5. The strain data will serve as baseline data. No analysis has been performed on the strain data.

FIGURE 4.15: Plate #1 Pass #1 SG1A

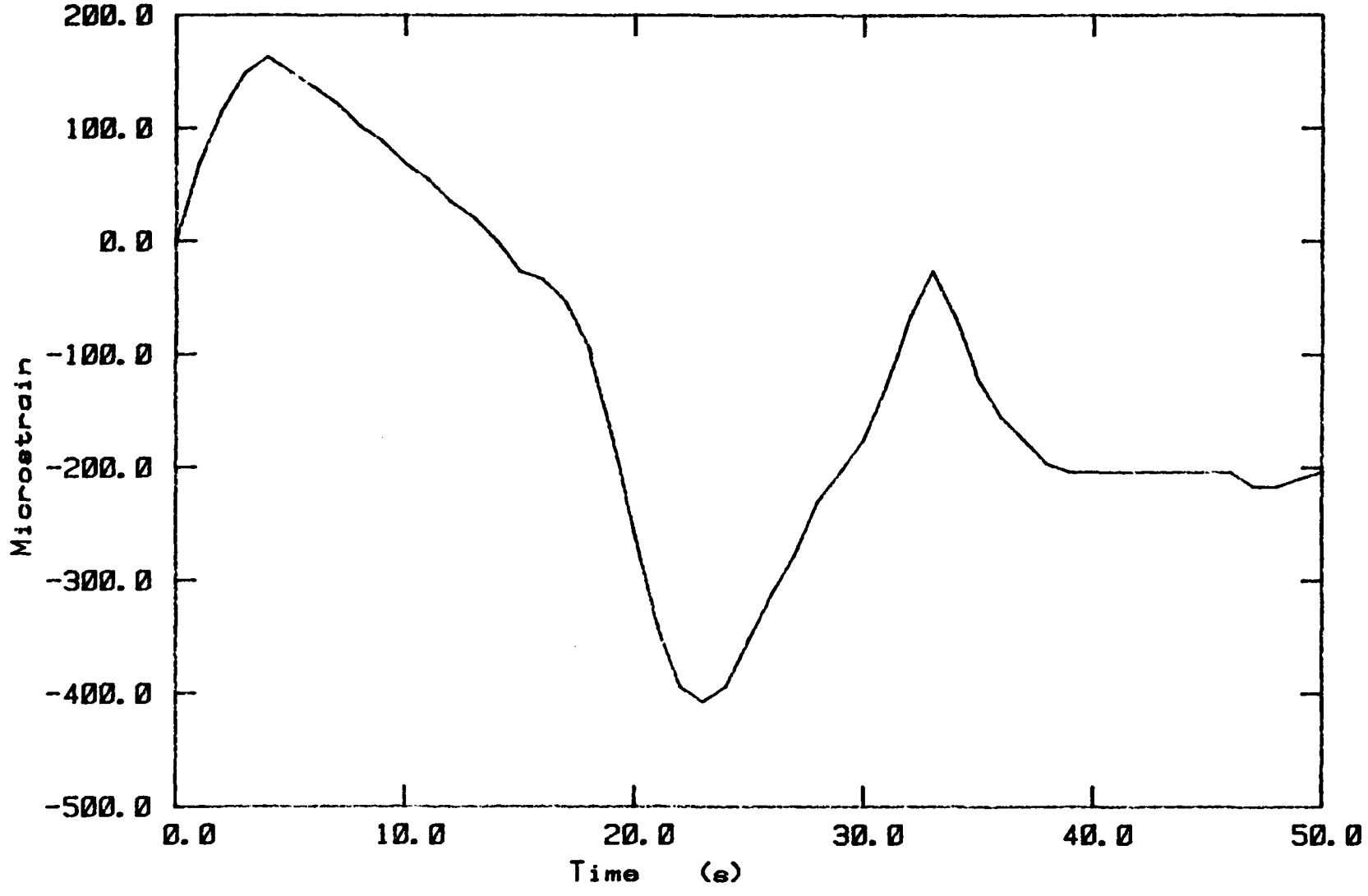

FIGURE 4.16: Plate #1 Pass #1 SG1B

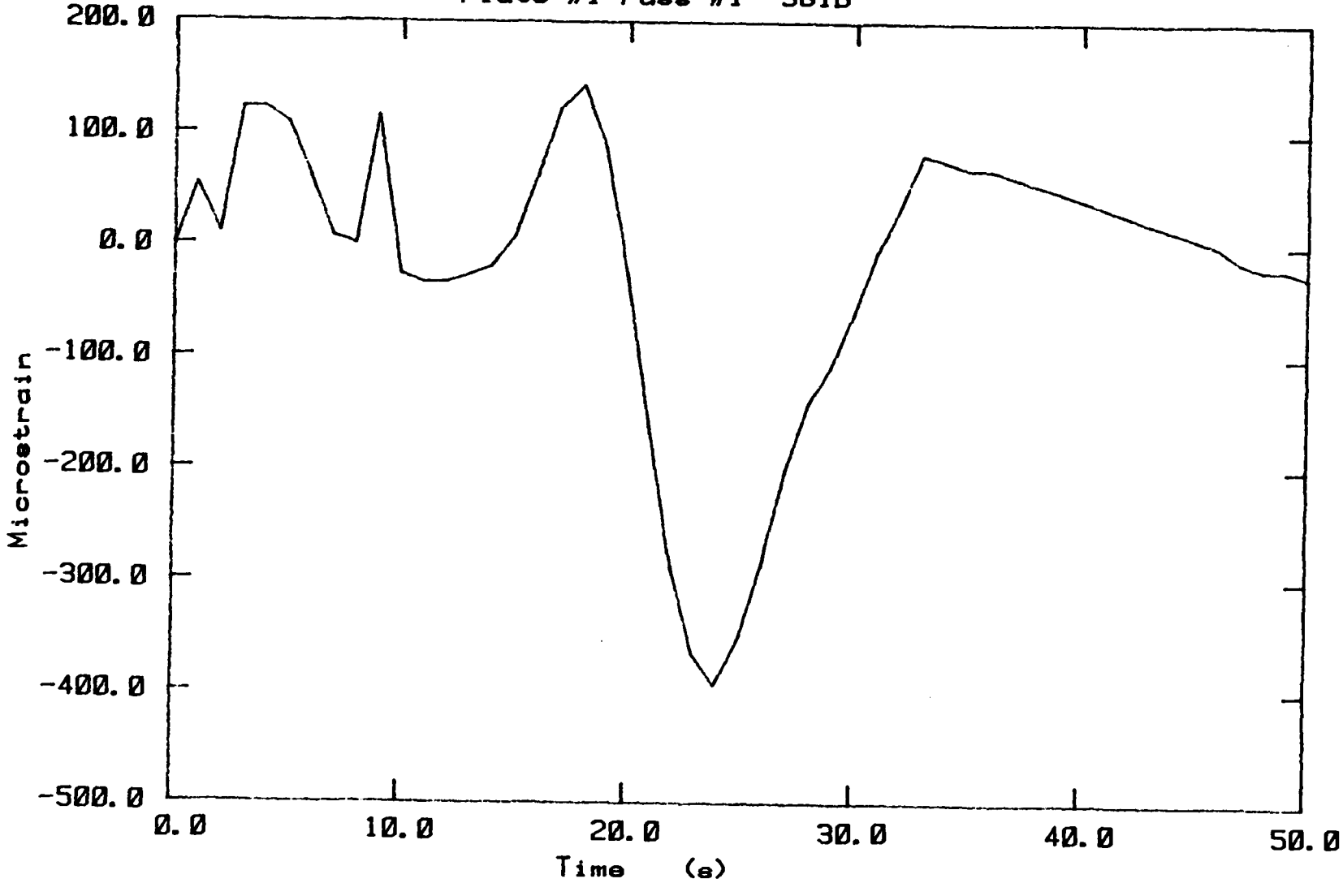

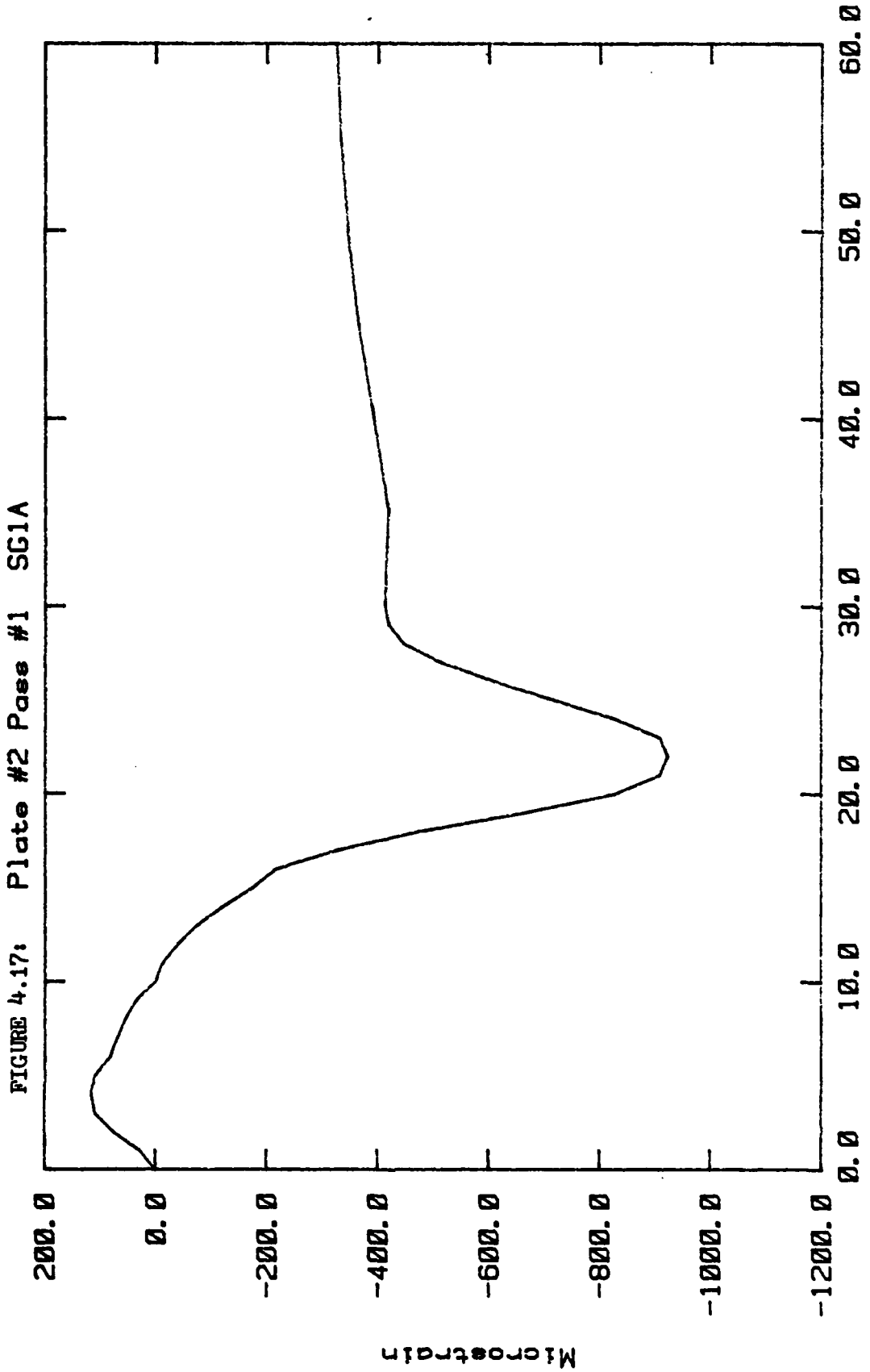
Plate #2 Pass #1 SG1A
Microstrain
200.0
0.0
-200.0
-400.0
-600.0
-800.0
-1000.0
-1200.0
0.0
10.0
20.0
30.0
40.0
50.0
60.0
Time (s)

FIGURE 4.17:

FIGURE 4.18: Plate #2 Pass #1 SG1B

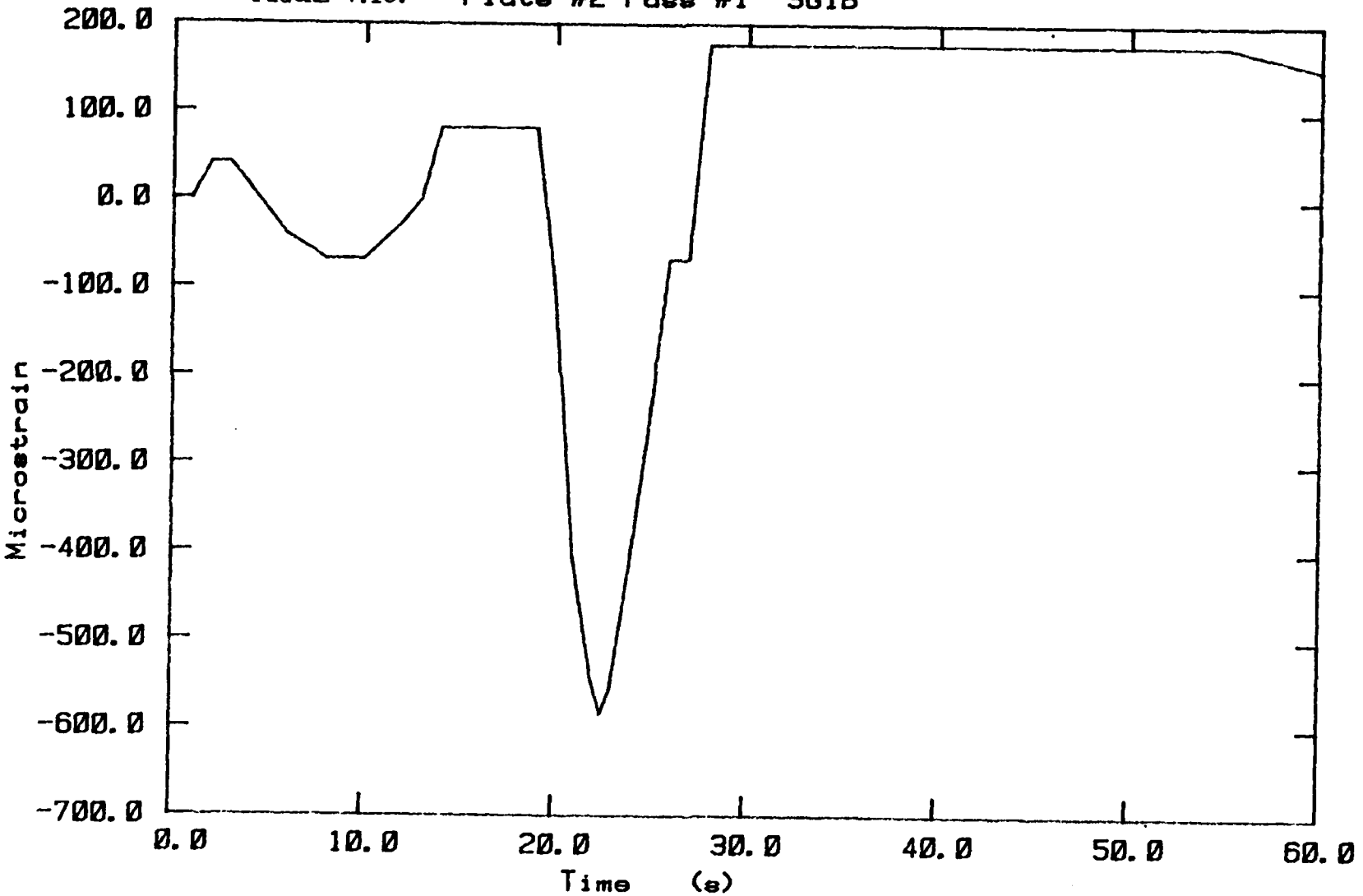

FIGURE 4.19: Plate #3 Pass #1 SG1A

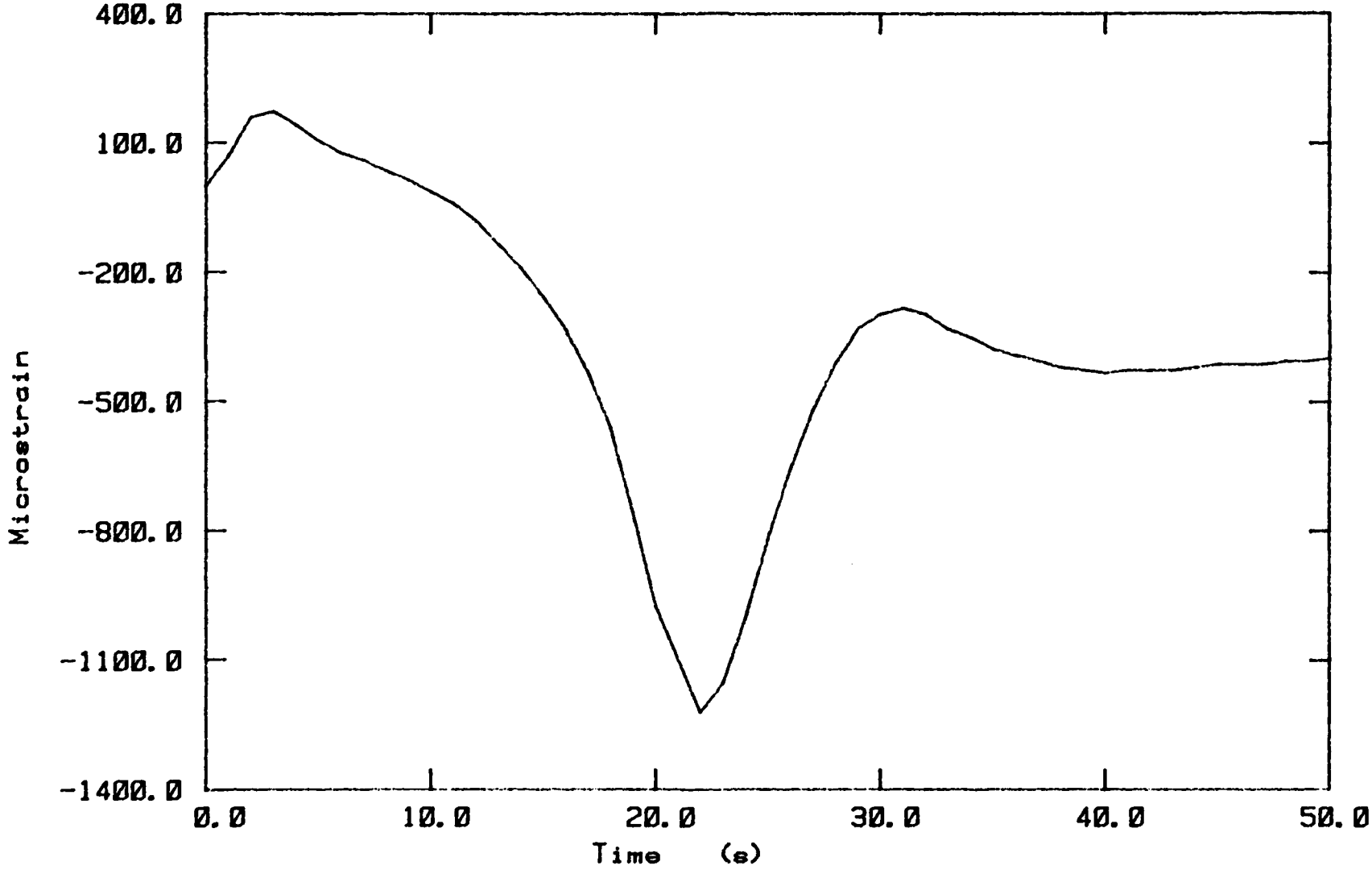

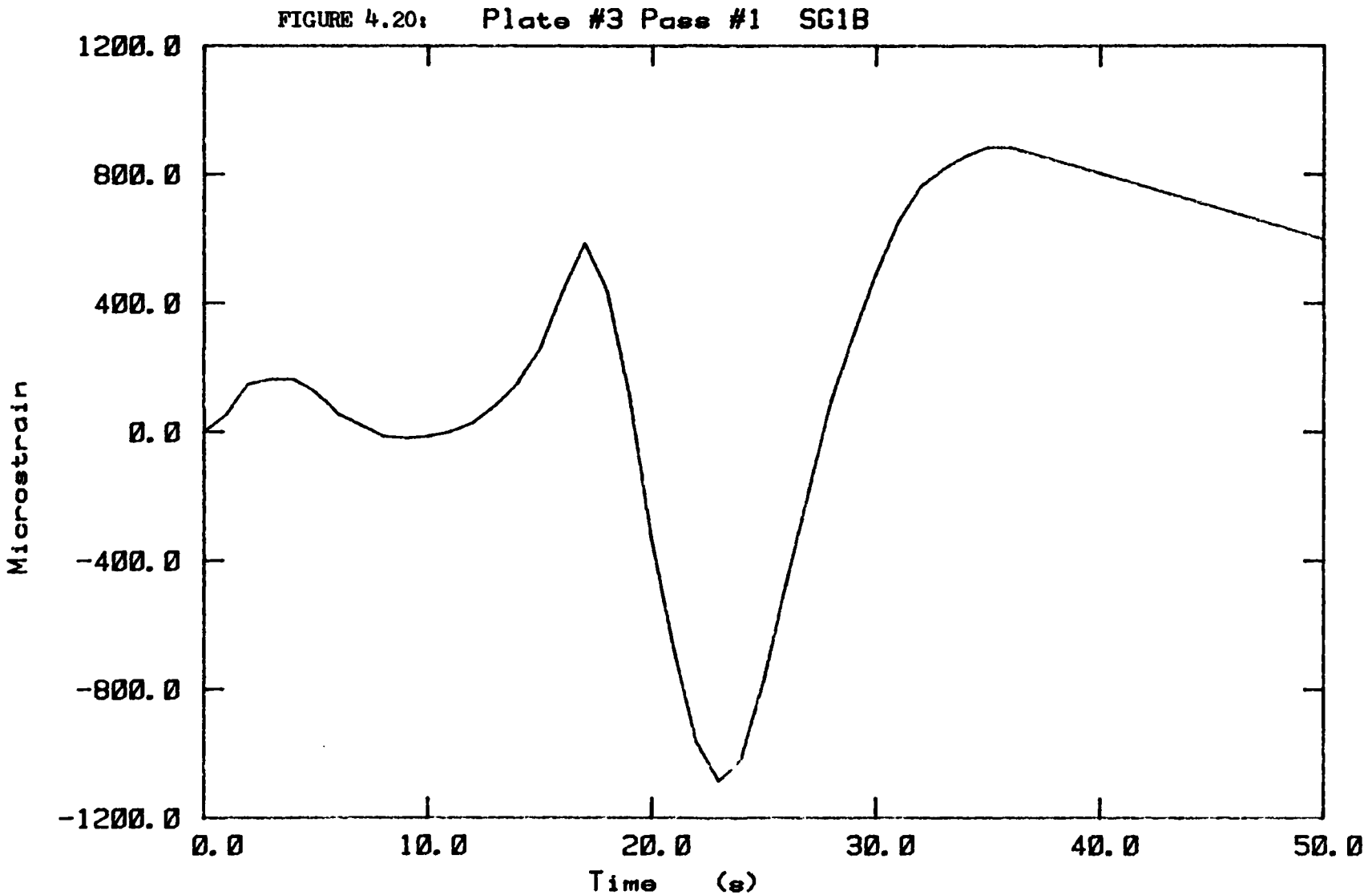
Plate #3 Pass #1 SG1B
1200.0
800.0
400.0
0.0
-400.0
-800.0
-1200.0
Microstrain
0.0
10.0
20.0
30.0
40.0
50.0
Time (s)

FIGURE 4.20:

FIGURE 4.21: Plate #4 Pass #1 SG1A

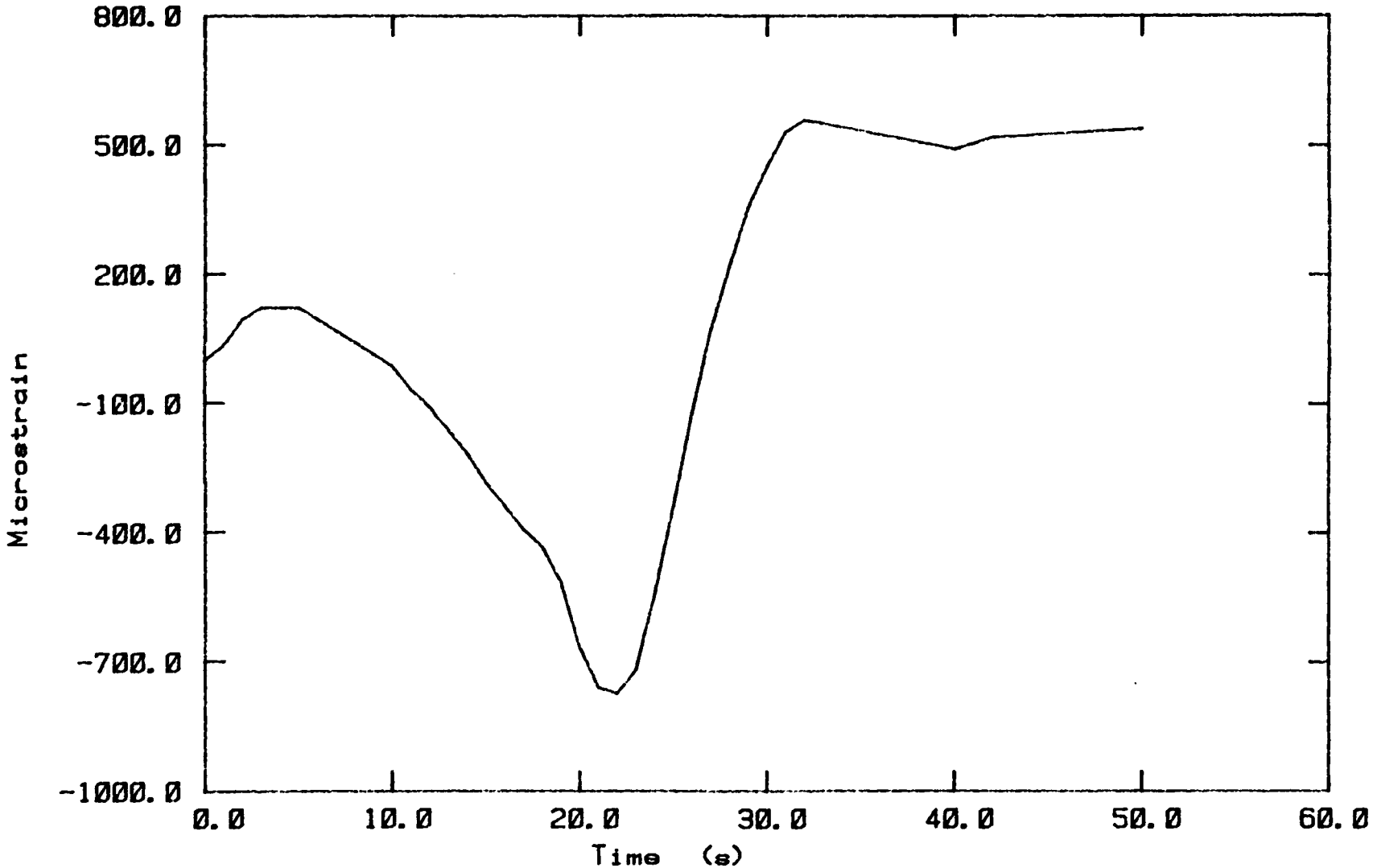

FIGURE 4.22: Plate #4 Pass #1 SG1B

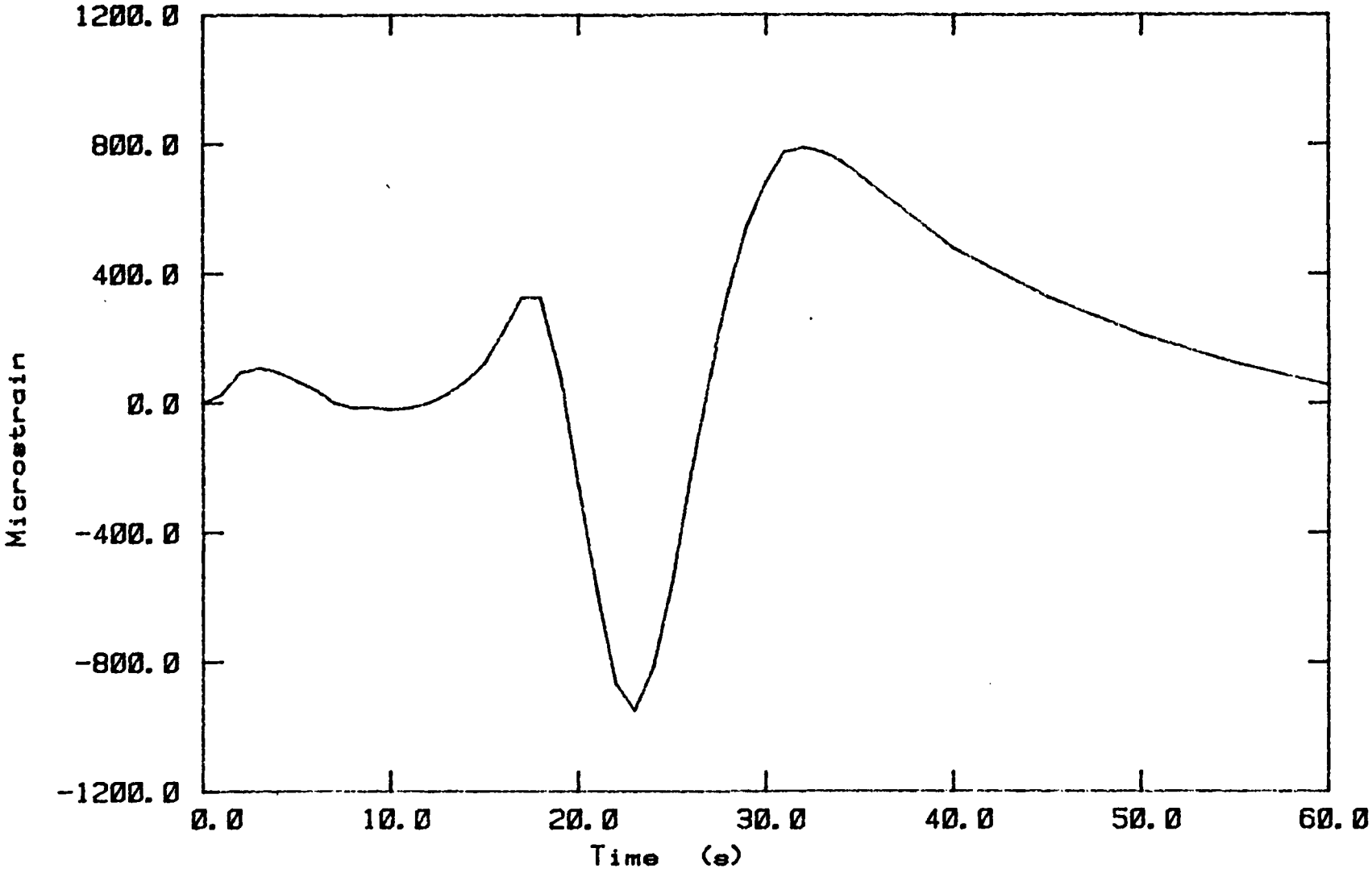

FIGURE 4.23: Plate #5 Pass #2 SG1A

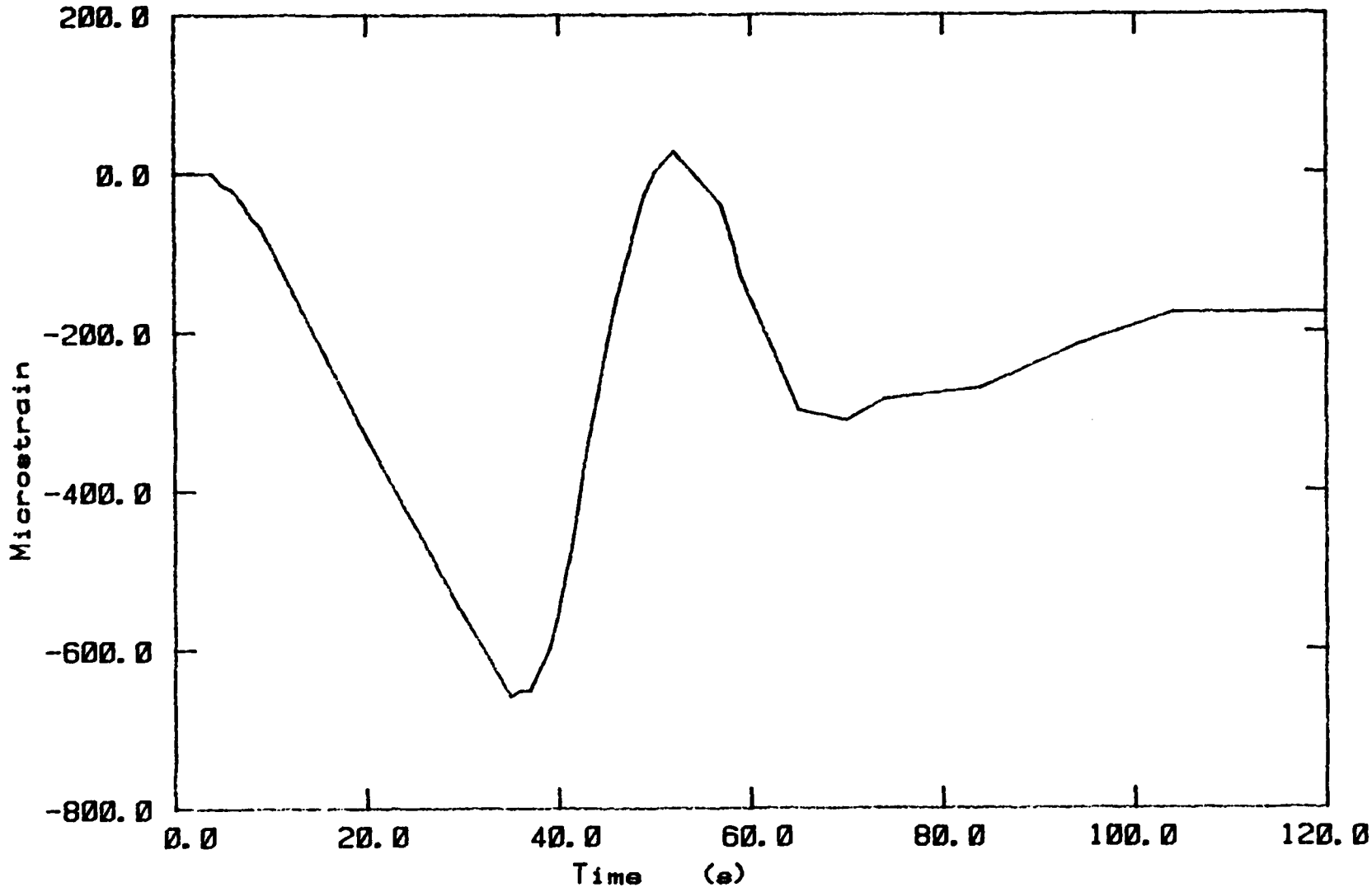

FIGURE 4.24: Plate #5 Pass #2 SG1B

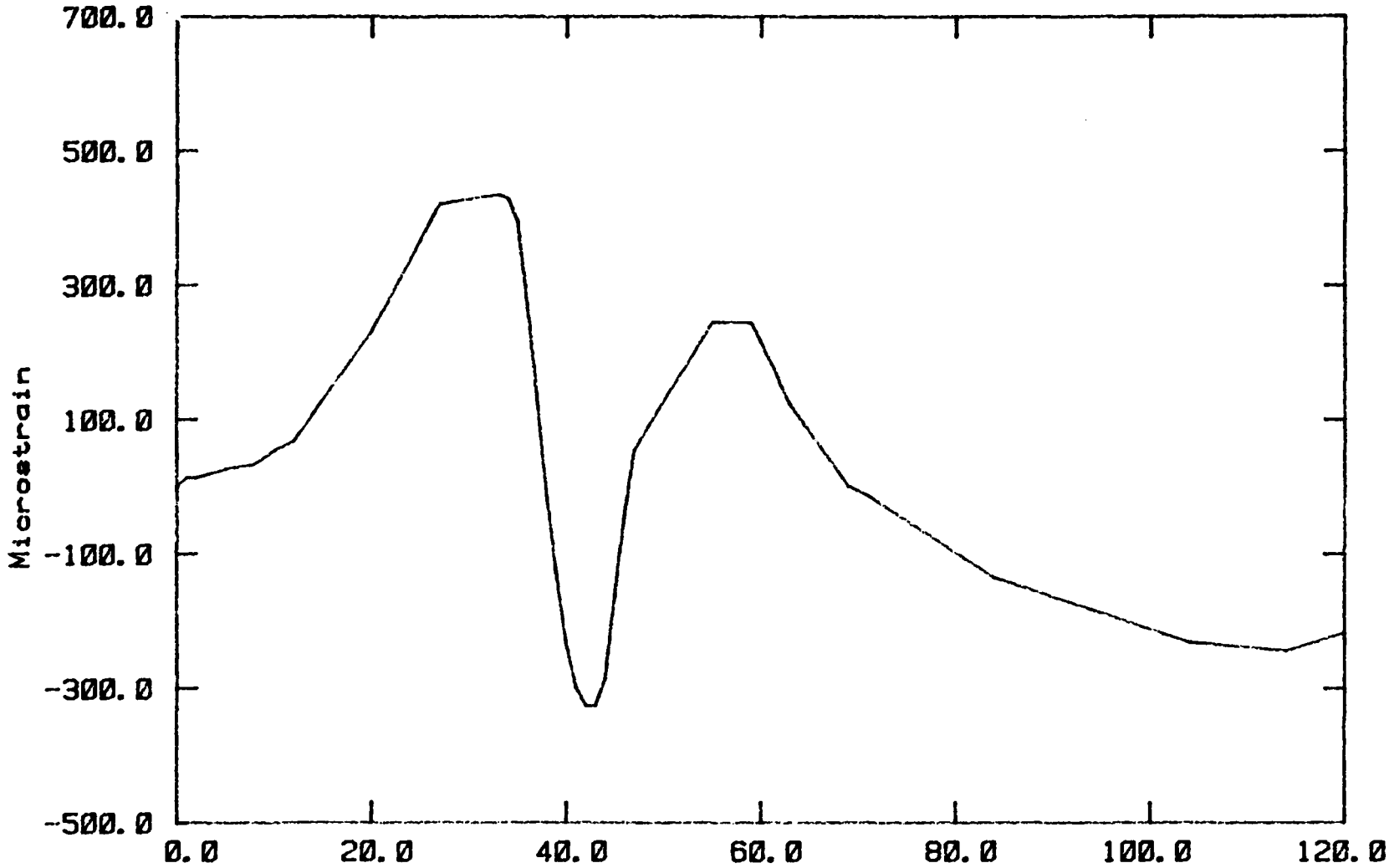

FIGURE 4.25: Plate #6 Pass #1 SG1A

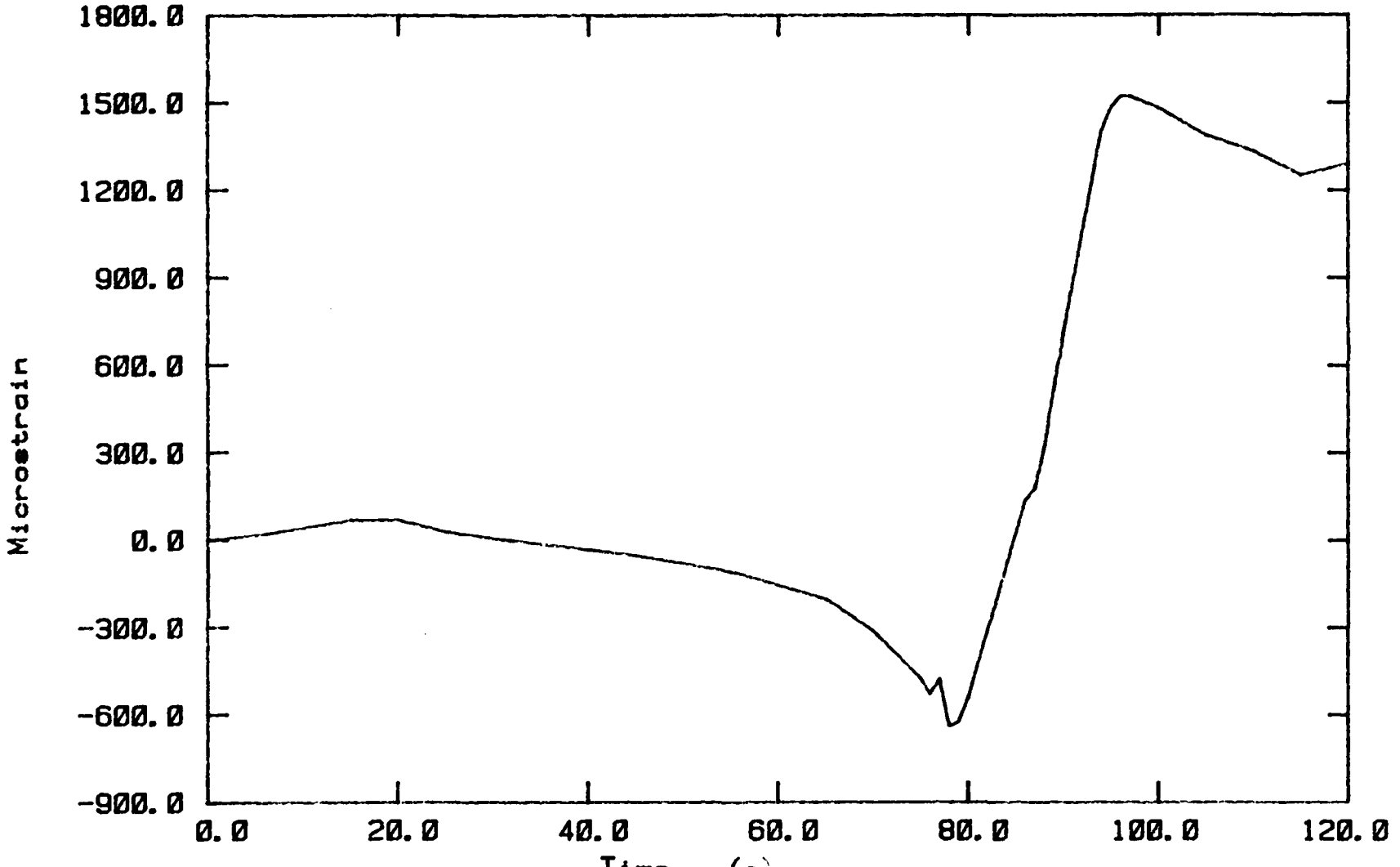

FIGURE 4.26: Plate #6 Pass #1 SG1B

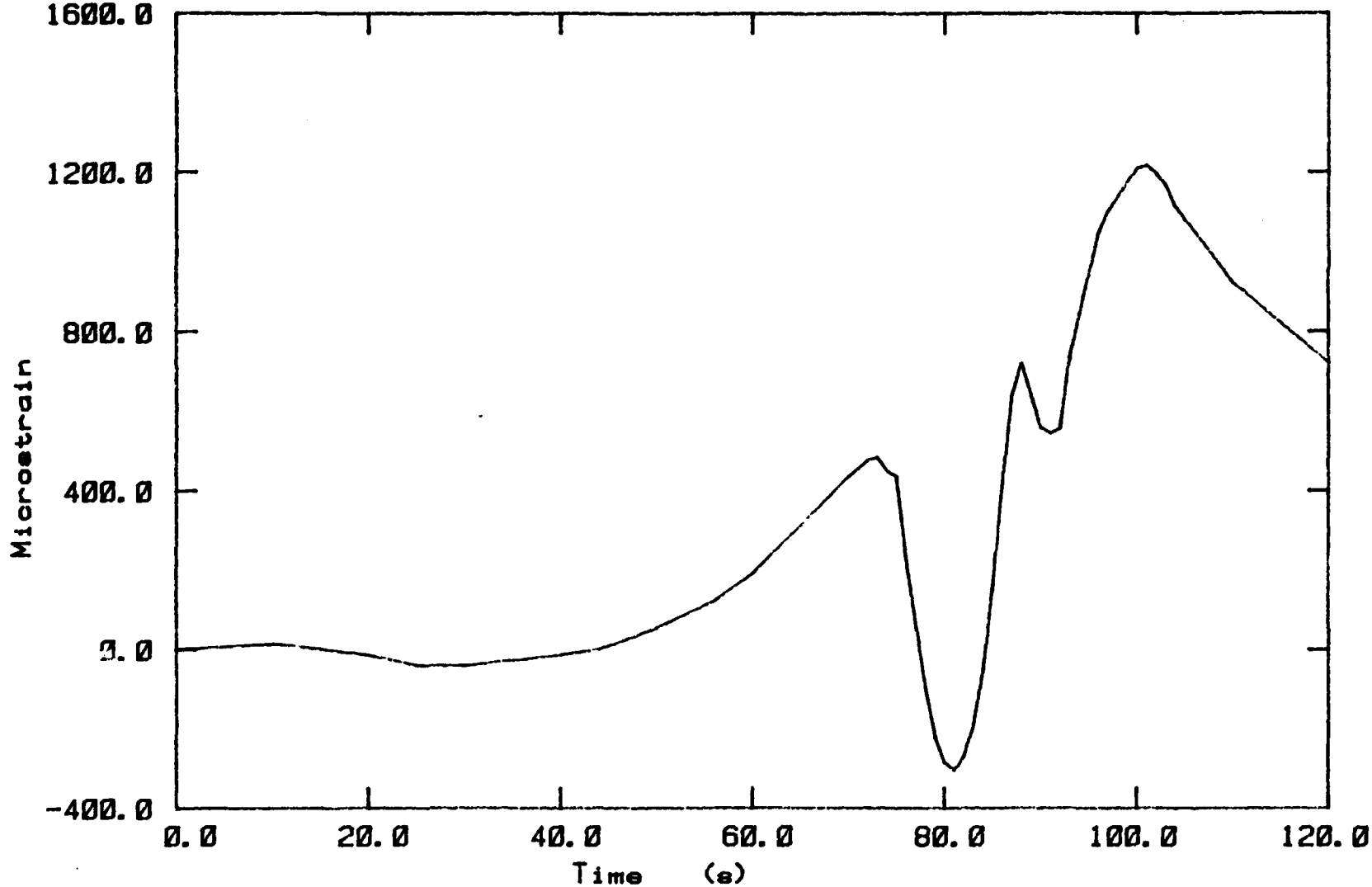

FIGURE 4.27: Plate #7 Line #1 Pass #1 SG1A

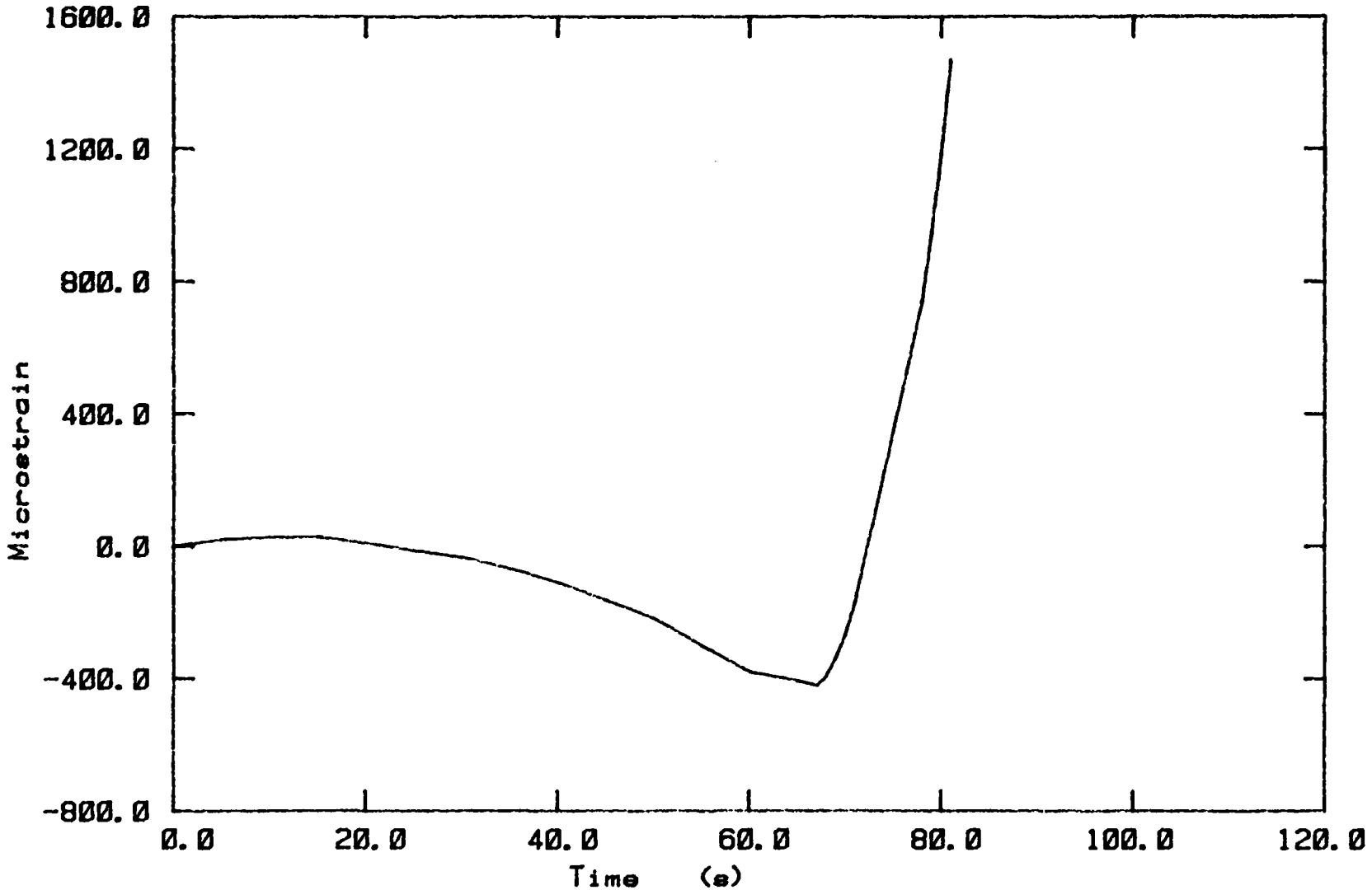

FIGURE 4.28: Plate #7 Line #1 Pass #1 SG1B

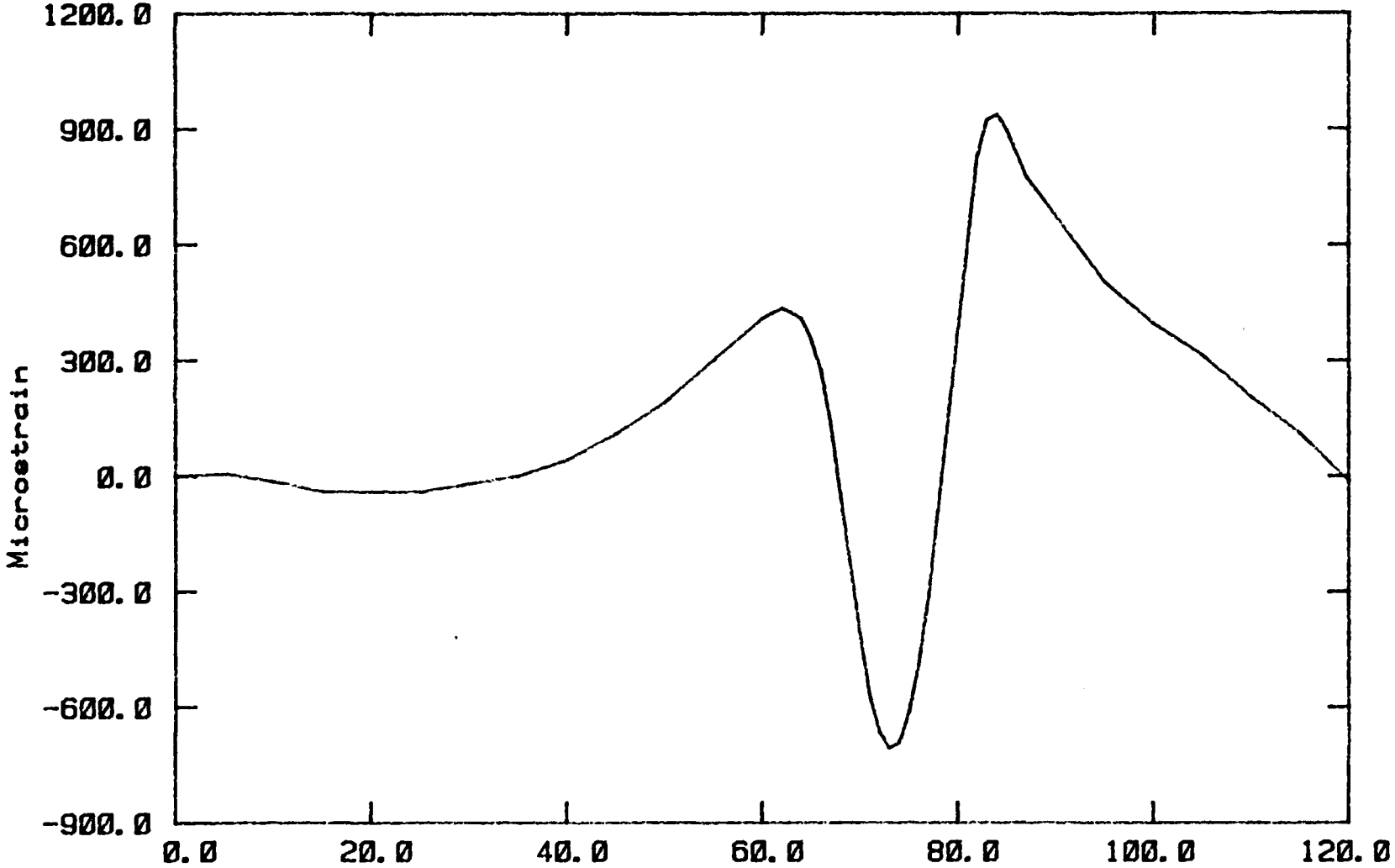

CHAPTER FIVE

DISCUSSION OF RESULTS

A. Distortion

The amount of distortion varied with the heat input and the material used. Heat input varies directly with the input laser power and inversely with the travel speed. (See Table 5.1.) When the power is low and the travel speed is high, the heat penetration is shallow and the distortion is small. This also occurs when the power is too large and the speed is too slow due to excessive heat penetration. The optimum conditions for laser forming occur when the power and travel speed are sufficient to cause good distortion without over saturating or under saturating the material with heat. Because this saturation process prohibits the needed temperature difference across the plate, the desired distortion is not achieved.

The heat input to plate #1 was small due to poor coupling, and no measurable distortion was achieved. The degree of coupling was increased on plate #2 by adding another coat of paint. The heat input therefore was increased and a distortion of 0.1° per pass was attained as shown in Figure 5.1.

TABLE 5.1

Heat Input

Plate #	Laser Power (KW)	Travel Speed (ipm)	Travel Speed (cm/min)	Heat Input* (KJ/in)	Heat Input* (KJ/cm)
1	7	12	30.5	35	13.8
2	7	12	30.5	35	13.8
3	12.7	12	30.5	63.5	25
4	12.7	12	30.5	63.5	25
5	7	6	15.2	70	27.6
6	7	6	15.2	70	27.6
7	7	6	15.2	70	27.6

$$* \text{ heat input} = \frac{\text{power}}{\text{travel speed}}$$

expected 10% loss of laser power in optics
has not been deducted

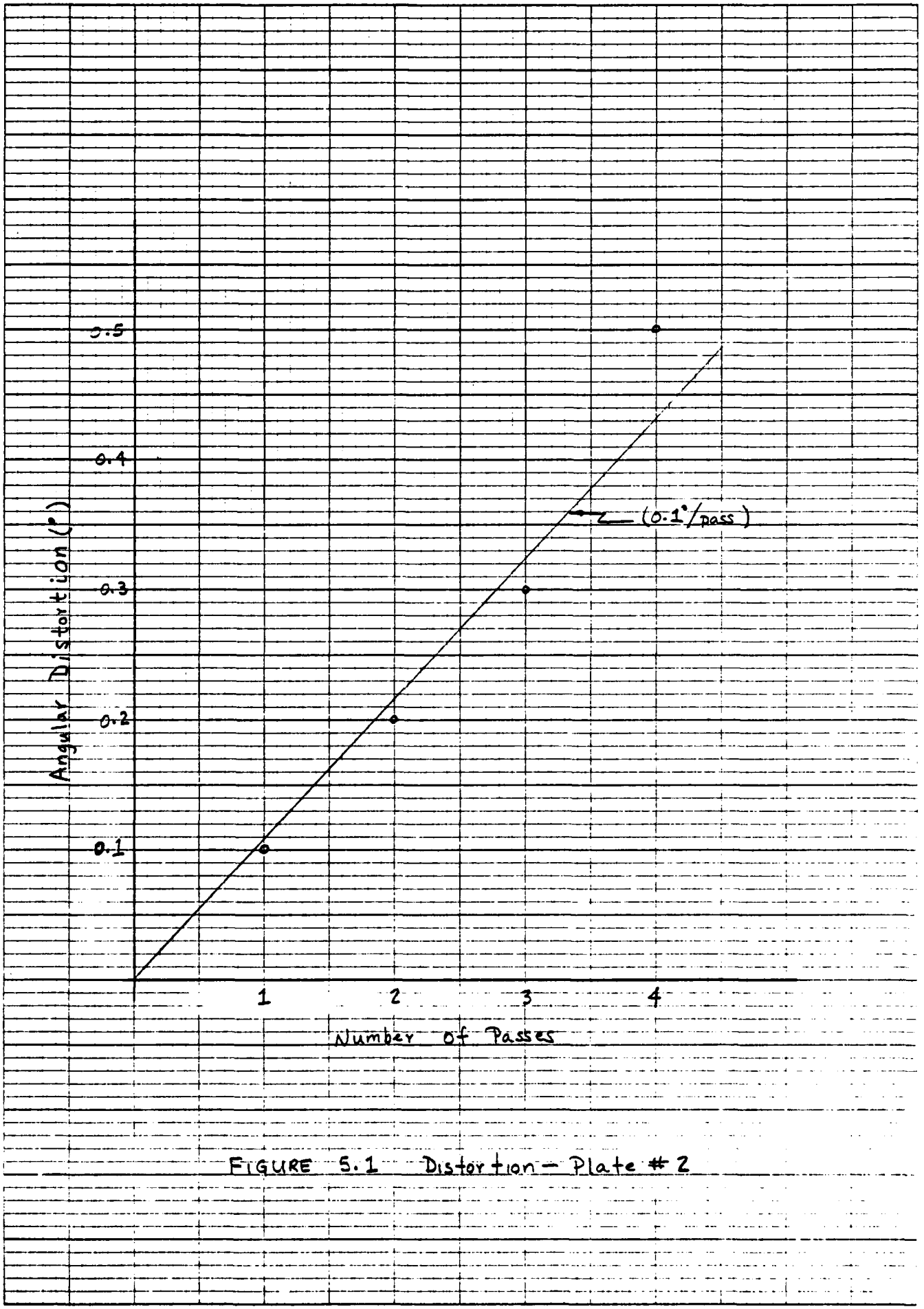

FIGURE 5.1 Distortion – Plate # 2

A comparison of distortion is shown in Figure 5.2 for plates #3 and #4. Both plates are the same size, and both have identical power input and travel speed. The 1018 steel achieved 0.3° per pass more distortion than the HY-80. This is believed due to the difference in material characteristics as evidenced by their respective stress-strain curves.

Plate #5 had a final distortion of 5.5° as compared to plate #4 which had 5.0°. Both plates are identical, although there is a slight increase in heat input for plate #5. Nonetheless, both plates achieved 1.1° per pass as shown in Figures 5.2 and 5.3.

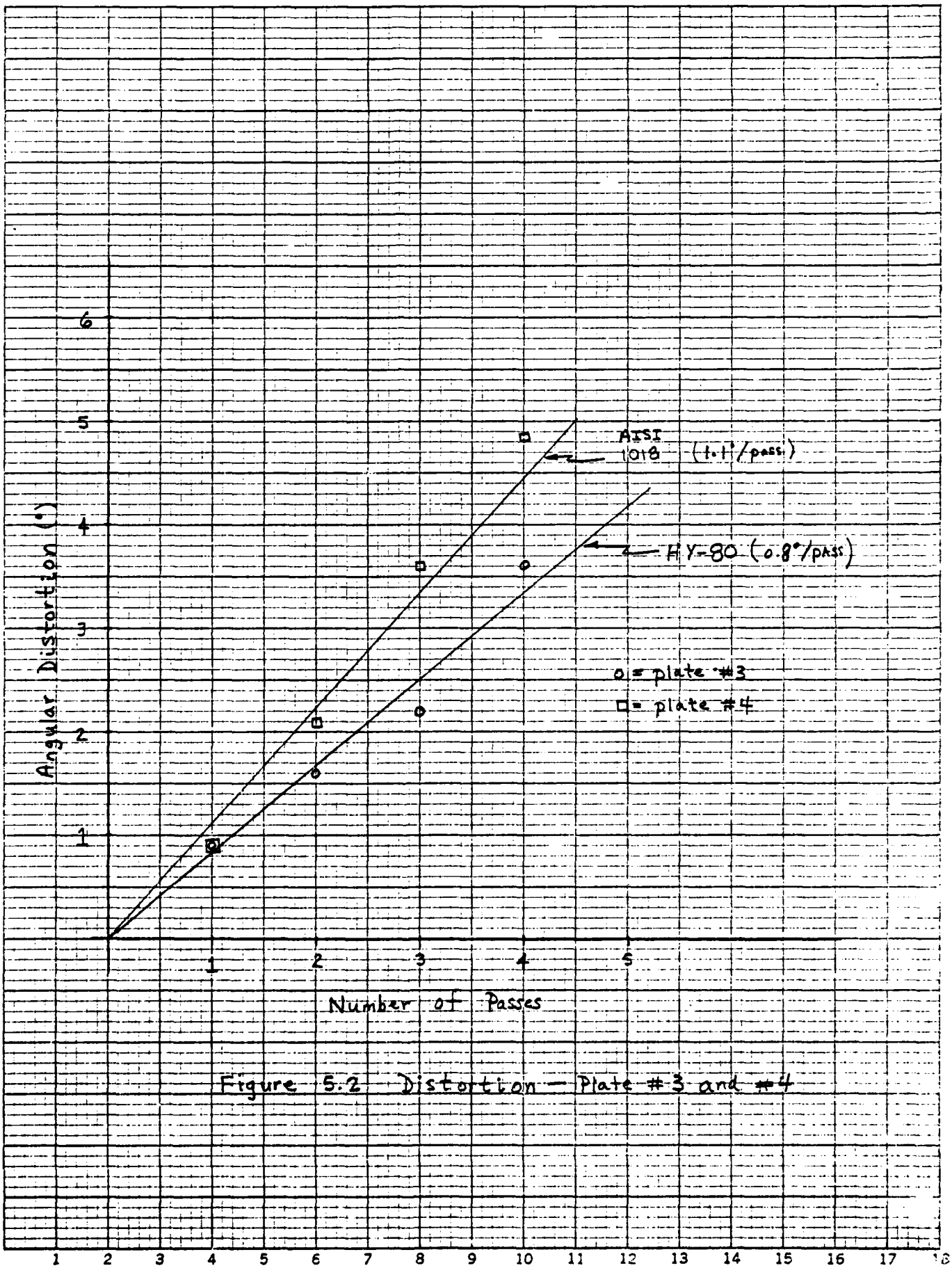

Figure 5.2 Distortion — Plate #3 and #4

AD-A144 773 REAL TIME SENSING AND CONTROL OF OUT-OF-PLANE DISTORTION DUE TO LINE HEAT..(U) MASSACHUSETTS INST OF TECH CAMBRIDGE DEPT OF OCEAN ENGINEERIN.. R C JOHNSON 2/2

UNCLASSIFIED JUN 84 N66314-78-A-0073 F/G 11/6 NL

END

FILMED

DTIC

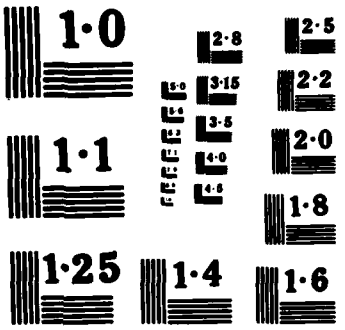
1·0
1·1
1·25
2·8
3·15
3·5
4·0
1·4
2·5
2·2
2·0
1·8
1·6

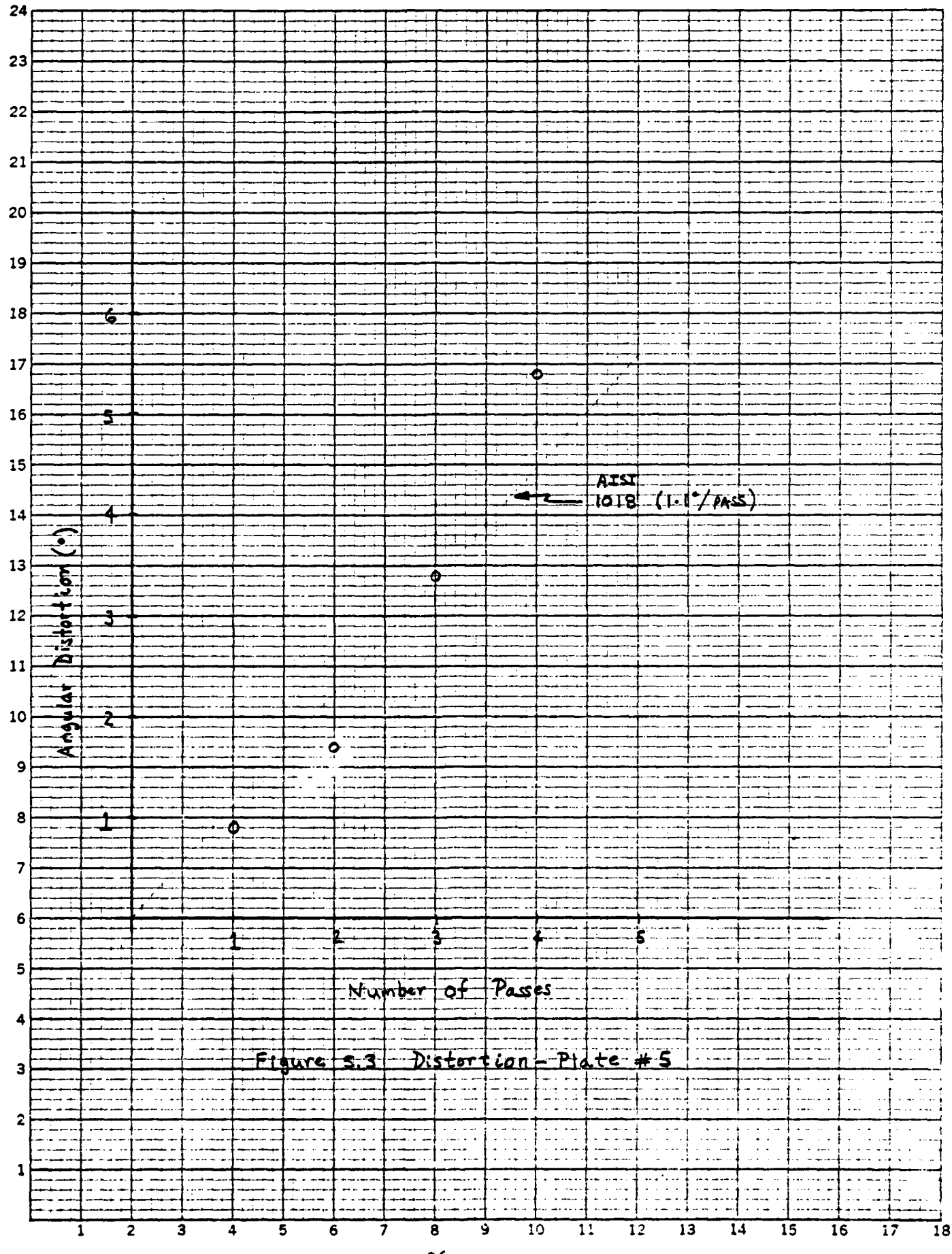

Figure 5.3 Distortion - Plate #5

5 Squares to the Centimeter

Plates #6 and #7 are the only 12" x 12" specimens. A larger specimen was desired for comparison of stress-strain data. One pass was made on each of three separate lines on plate #6 as indicated in Figure 5.4. The measured distortion, 0.7° per pass, was slightly less than in the 6" x 12" specimens of the same material. The difference can probably be attributed to the better coupling achieved on other plates on subsequent passes.

The last specimen, plate #7, had the highest amount of distortion which measured 13.5°. See Figure 5.5. The same approach as used on plate #6 was used on plate #7, although three passes were made on each line. This is believed to have increased the amount of coupling and therefore increased the final distortion.

In order to compare the amount of distortion that occured during laser line heating and welding, an attempt was made to find a suitable representation of parameter $\underline{X}$ for the laser. Three points have been plotted on Figure 5.6 which shows the same graph as Figure 2.18. Although this is only a rough comparison, the amount of distortion is less with the laser. This might be expected since melting occurs in welding; when the weld metal cools, more shrinkage will occur resulting in more angular distortion.

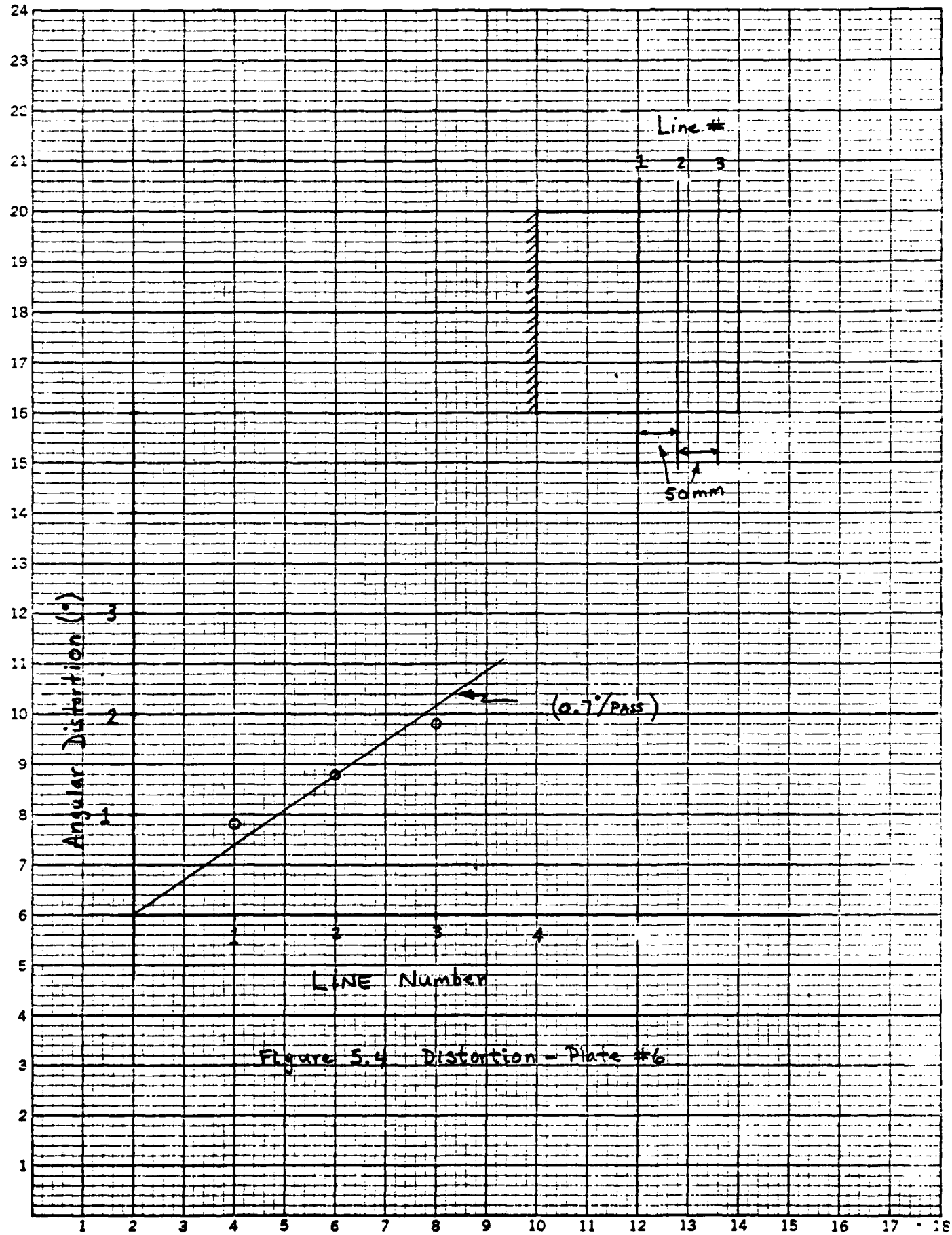

Figure 5.4 Distortion - Plate #6

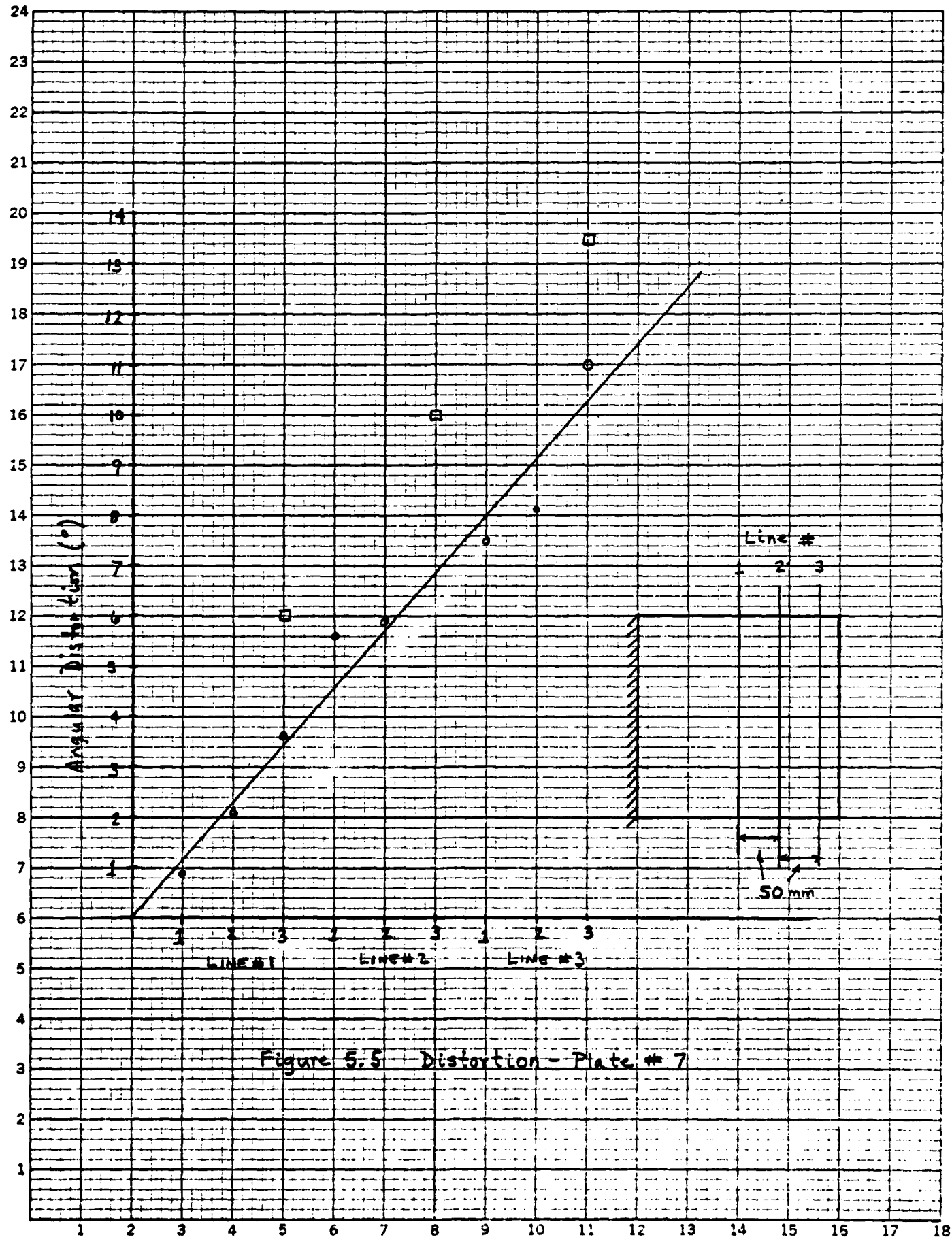

Figure 5.5 Distortion - Plate # 7

3 Squares to the Centimeter

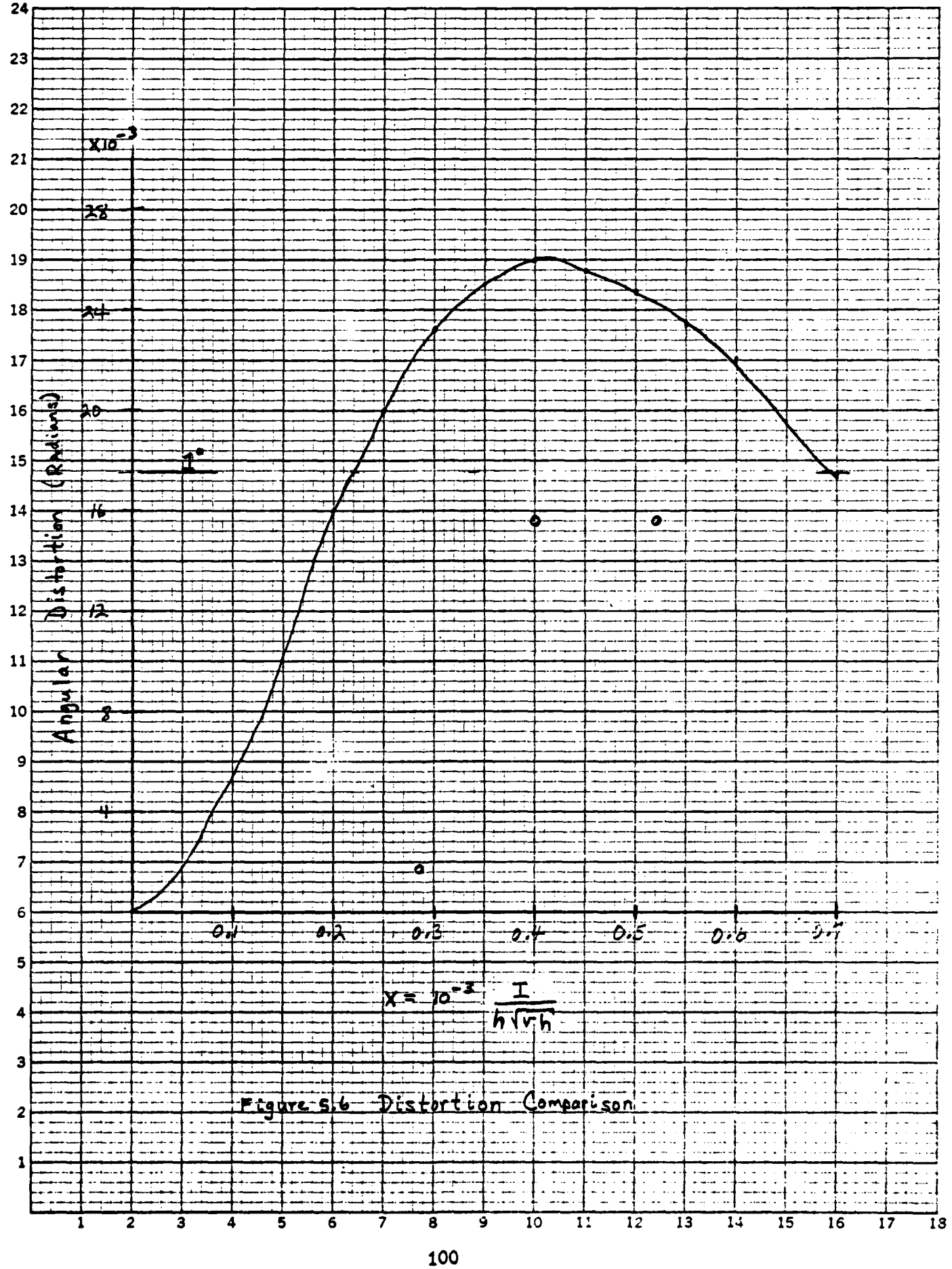

Figure 5.6 Distortion Comparison

B. Heat Transfer/Temperature Analysis

The problem of analyzing heat flow during laser forming was solved using the multipurpose finite element program, ADINAT, developed by Bathe and co-workers in the department of Mechanical Engineering [20].

Following is a discussion of the particular features of the program pertaining to the laser forming analysis.

1. Finite Element Formulation

The governing isoparametric finite element equations for the nonlinear heat transfer problem are

$$ {}^{t}\hat{\underline{K}}\,\Delta\underline{\theta}^{(i)} = {}^{t+\alpha\Delta t}\hat{\underline{Q}}^{(i-1)} \qquad (1) $$

$$ \text{with } {}^{t+\alpha\Delta t}\theta^{(i)} = {}^{t+\alpha\Delta t}\theta^{(i-1)} + \Delta\theta^{(i)} \qquad (2) $$

where,

$ {}^{t}\hat{\underline{K}} $ = the effective conductivity matrix at time t,

$ \hat{\underline{Q}} $ = heat flow vector including the effects of surface heat flow inputs.

$ \Delta\underline{\theta}^{(i)} $ = the increment of modal-point temperature in iteration i.

Equation (1) represents the heat flow equilibrium at time $t + \alpha\Delta t$, where $0 \leq \alpha \leq 1$.

All boundary conditions relevant to the laser forming problem are incorporated in the matrices of equation (1).

They include:

1. Convective heat losses from the plate's surfaces according to Newton's law.
2. Radiation heat losses, which are modeled according to the Stefan Boltzman law.
3. The heat input during laser forming is modeled using a set of time functions (linear increase as the beam approaches, uniform as it travels over the cross sections, followed by a linear decrease).

A cross section of the plate at its midlength was analyzed. The finite element mesh was applied over only half of the plate. Since the plate is symmetric, the results will be equivalent to applying the same mesh over the entire plate, but the cost will be greatly reduced. Figure 5.7 shows the finite element mesh used; it consists of a total of 84 nodes and 62 elements. The temperature obtained from the thermocouples on Plate #4, Pass 1, were used as an input to the ADINAT program. Figure 5.8 shows the temperature versus time curve calculated using ADINAT as compared to the experimental data. The correlation is much better for thermocouple #4 than for thermocouple #3 which was located on the bottom surface directly beneath the beam.

The same procedure was used to obtain Figure 5.9. As shown, the analytical analysis is in agreement with the experimental results. Figure 5.10 shows a temperature profile of the top and bottom surfaces of the specimen.

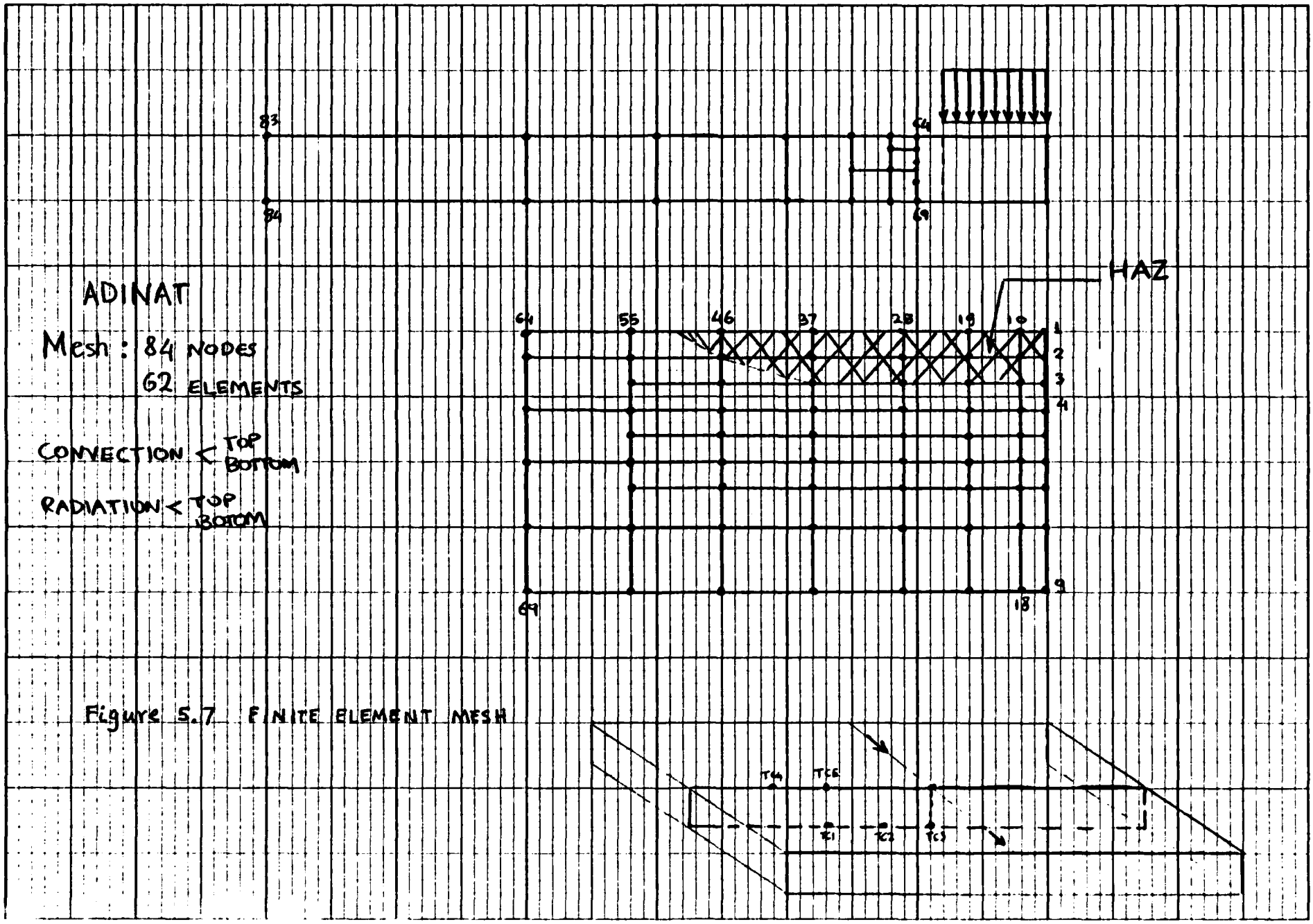

Figure 5.7 FINITE ELEMENT MESH

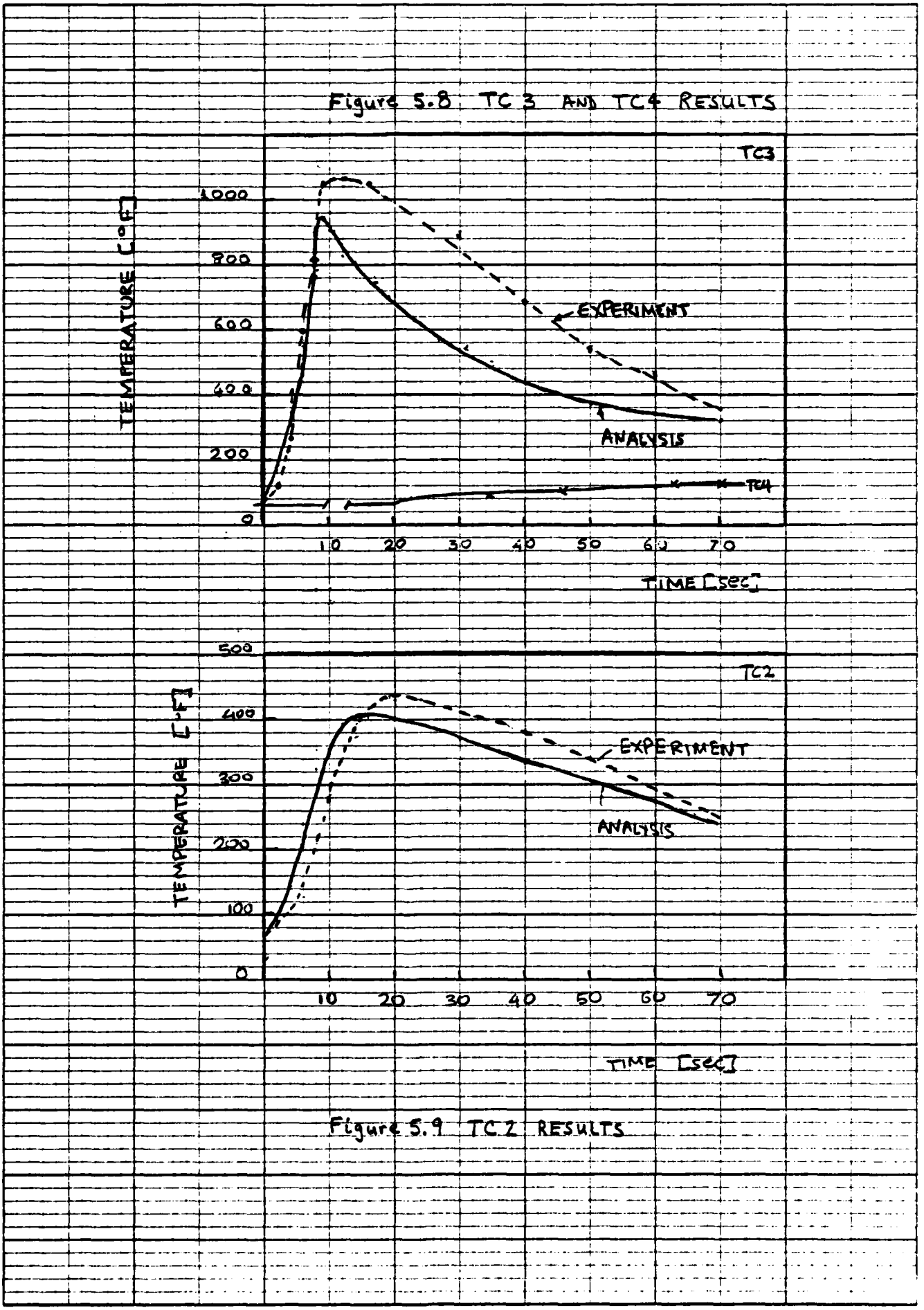

Figure 5.8 TC 3 AND TC4 RESULTS

Figure 5.9 TC 2 RESULTS

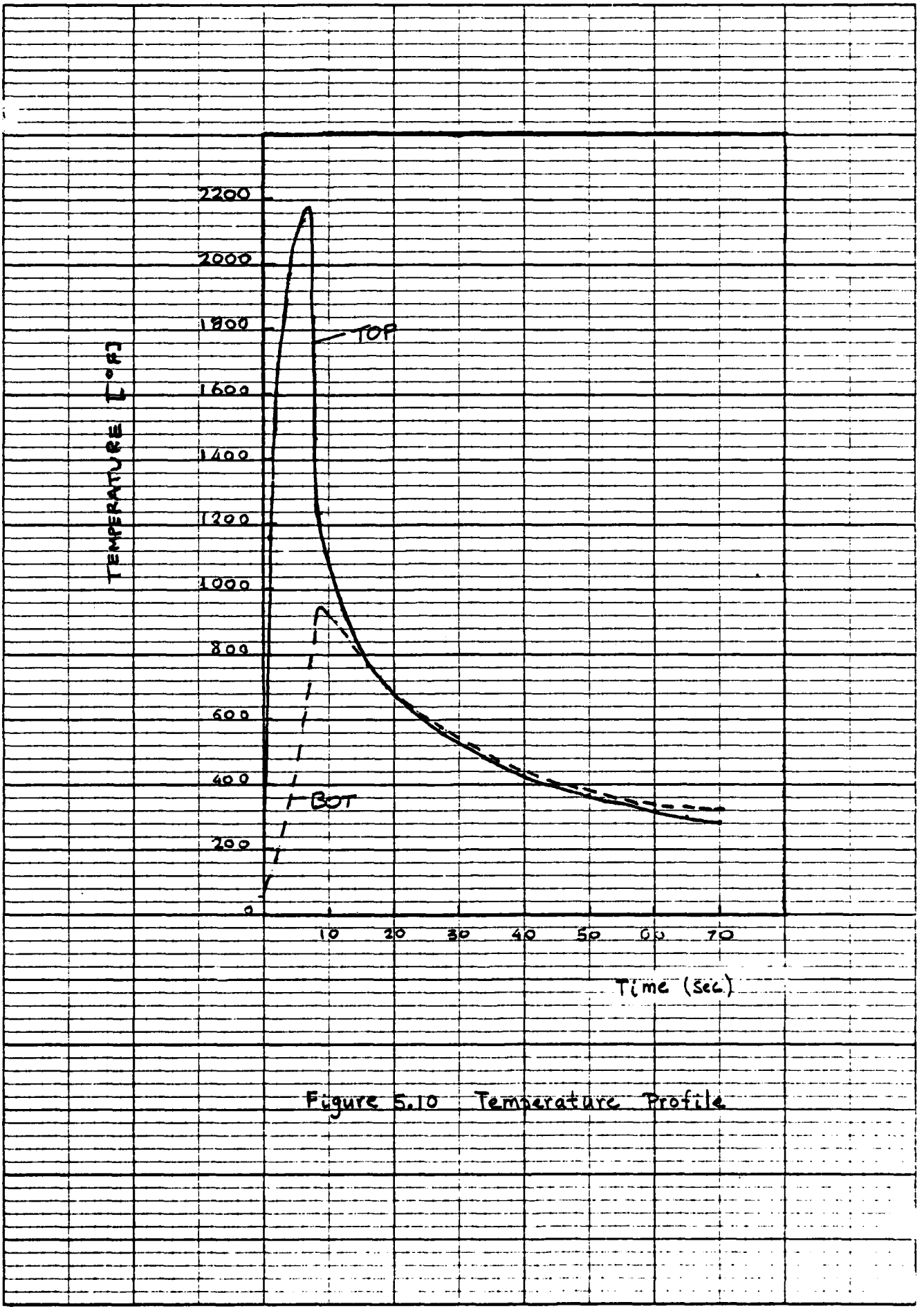

Figure 5.10 Temperature Profile

2. Material degredation Study

The temperature distribution obtained using the ADINAT program also provides information about the material degradation. Knowing the temperature history, one can predict the microstructure changes that occur during the thermal and cooling cycles by using the Continuous Cooling Transformation (CCT) diagrams.

In addition, the shape and extent of the heat-affected zone (HAZ) can be determined. The HAZ is shown in Figure 5.7 for the portion of the material that exceeded the A_1 temperature of 1330° F.

CHAPTER SIX

RECOMMENDATIONS

Due to possible problems with material degradation at higher laser output levels, it is recommended that laser power be reduced. This would reduce or eliminate much of the existing problem of material degradation. Overlapping laser beam patterns could then be used to achieve a gradual beding of the plate at lower heat input levels. It is believed that a sufficient amount of distortion can still be achieved at this lower power level.

Some type of thermal imaging system should also be acquired and used in future experiments. This would allow the determination of a more accurate temperature profile. This information could then be used to determine the temperature distribution best suited for producing a certain amount of distortion.

This investigation has demonstrated the excellent potential of a laser to form steel plates. The amount of plate distortion was satisfactory although the degree of material degradation has yet to be determined. THe interferometer has also proven itself as an excellent means of measuring very precisely the amount of distortion achieved. For these reasons, it is highly recommended that this research effort be continued.

REFERENCES

1. Masubuchi, K., Analysis of Welded Structures - Residual Stresses, Distortion, and Their Consequences, Pergamon Press, Oxford/New York, 1980.

2. Holt, R., "Primary Concepts for Flame Bending," The Welding Journal, 50(6), pp. 416-424, 1971.

3. U.S. Department of Transportation. Maritime Administration in cooperation with Todd Pacific Shipyards Corporation. Line Heating, The National Shipbuilding Research Program, November, 1982.

4. Kihara, H., Otani, M., and Fujita, Y., Recent Developments in Shipbuilding Practice in Japan, Volume 5 of the 60th Anniversary Series of the Society of Naval Architects of Japan, Tokyo, 1961.

5. Engel, S.L., "Basics of Laser Heat Treating," Lasers in Manufacturing Conference, November, 1976.

6. E.V. Lock, "High Power Carbon Dioxide Lasers and Their Applications," Optical Engineering, Vol. 17, No. 3, May/June 1978, pp. 192-197.

7. R.A. Hella, "Material Processing with High Power Lasers," Optical Engineering, Vol. 17, No. 3, May/June 1978, pp. 198-201.

8. J. Benedek, A. Shachrai, L. Levin, "Case Hardening of Steel by a Carbon Dioxide Laser Beam," Optics and Laser Technology, Vol. 12, No. 5, Oct. 1980, pp. 247-253.

9. M.J. Yessik, "Laser Material Processing," Optical Engineer, Vol. 17, No. 3, May-June 1978, pp. 202-209.

10. D.S. Gnanamuthu, "Laser Surface Treatment," Optical Engineering, Vol. 19, No. 5, Sept/Oct 1980, pp. 783-792.

11. S.S. Charschan, "The Evolution of Laser Machining and Welding," Electro-Optical Systems Design, Vol. 13, No. 8, August 1981, pp. 63-73.

12. Cook, W. "Laser Interferometer for Weld Deformation Measurement." Instrumentation project in Ocean Engineering 13.713. Mimeographed. Cambridge: M.I.T., December, 1982.

13. Satoh, K., Matsui, S., Terai, K., and Iwamura, Y., "Water-Cooling Effect an Angular Distortion Caused by the Process of Line Heating in Steel Plates," Journal of the Society of Naval Architects of Japan, Vol. 126, pp. 445-458, 1969.

14. Johnson, E.K., "Study of Flame Heating of Steel Plate," M.S. Thesis, M.I.T., May 1971.

15. Walsh, R.A., "Investigation of Distortion Removal in Welded Structures," M.S. Thesis, M.I.T., May 1969.

16. Duffy, D.K., "Distortion Removal in Structural Weldments," M.S. Thesis, M.I.T., May 1970.

17. Iwamura, Y., and Rybicki, E.F., "A Transient Elastic-Plastic Thermal Stress Analysis of Flame Forming," Transactions of ASME, Journal of Engineering for Industry, February 1973, pp. 163-171.

18. Watanabe, M., and Satoh, K., "Effect of Welding Conditions on the Shrinkage and Distortion in Welded Structures," The Welding Journal, 40(8), Research Supplement, 377s - 384s, 1961.

19. High Power Laser Committee of the Japan Welding Engineering Society. Technical Report on Research on Metal Working by High Power Laser. Japan: High Power Laser Committee of the Japan Welding Engineering Society, 1983.

20. Bathe, K.J., "ADINAT - A Finite Element Program for Automatic Dynamic Incremental Nonlinear Analysis of Temperature." AVL Report 82448-5, Mechanical Engineering Department, M.I.T., May 1977.